7/25/68

FERROELECTRICITY OF THE NUCLEIC ACIDS

AND SELECTED

NUCLEOTIDES AND POLYRIBONUCLEOTIDES

A THESIS

Presented to

The Faculty of the Graduate Division

by

Richard Anthony Lorey

In Partial Fulfillment

of the Requirements for the Degree

Doctor of Philosophy in the School of Physics

Georgia Institute of Technology

August, 1969

FERROELECTRICITY OF THE NUCLEIC ACIDS

AND SELECTED

NUCLEOTIDES AND POLYRIBONUCLEOTIDES

Approved:

Chairman

Date approved by Chairman *8-22-69*

ACKNOWLEDGMENTS

TABLE OF CONTENTS

         History of Ferroelectricity
         Physical Properties of Ferroelectric Materials
         Chemical Structure of the Nucleic Acids
         Crystal Nature of the Chemicals Used in
         this Research
         Purpose of this Research
         Review of the Literature

         Precision
         Interpretation

LIST OF TABLES

LIST OF ILLUSTRATIONS

LIST OF ILLUSTRATIONS (Continued)

LIST OF ILLUSTRATIONS (Continued)

SUMMARY

The nucleic acids are known to be involved in the metabolism, reproduction and growth of living systems. Recent experiments have implied that ribonucleic acid (RNA) is intimately associated with the memory process. The present work was initiated as a search for a physical property of RNA that could relate RNA to this process.

A physical property which can readily account for information storage, and hence memory, is hysteresis. Ferromagnetic hysteresis is the mechanism responsible for information storage in such devices as tape recorders and computers. Since ferromagnetic materials exist in only trace amounts in neural tissue it is unreasonable to assume this mechanism could relate RNA and the memory process. Another type of hysteresis which can lead to an explanation of information storage is ferroelectric hysteresis. Hence, it is of interest to determine if RNA is ferroelectric.

A previous report indicated that deoxyribonucleic acid (DNA) may be ferroelectric. Therefore, for the present work it was considered desirable to study the dielectric properties and ferroelectric character of RNA and DNA, the several ribonucleotides and two synthetically produced polyribonucleotides.

The equipment used in this research consisted of apparatus used for hysteresis observation and apparatus used for

measuring dielectric constants as functions of temperature. The circuit of Sawyer and Tower was used to display the ferroelectric hysteresis loops on an oscilloscope. Heating the samples permitted observation over the temperature range of 25°C to approximately 100°C. The dielectric constant measurements consisted of measuring capacitances dynamically by plotting capacitances on an X-Y recorder as a function of temperature.

The salts of the various acids were mixed with water and allowed to harden into relatively flat specimens. Electrodes were then painted on these samples and leads were attached to the electrodes. The material thus became the dielectric medium inside parallel plate capacitors. These capacitors were used in both the hysteresis observations and dielectric constant measurements.

The dielectric constants of the nucleic acids and other related materials exhibit the characteristic behavior of many ferroelectric materials as the temperature nears their Curie points. No high temperature Curie point was observed for any of the materials studied here. A low temperature irregularity in the dielectric constant of RNA may be a ferroelectric transition or simply a change in the value of the coercive field strength. No saturation of the hysteresis loops was observed for any of the materials studied here. Indications are that the nucleic acids and the associated biological molecules are ferroelectric in a

temperature region between approximately $30^{\circ}C$ and $80^{\circ}C$. The existence of ferroelectricity in the nucleic acids appears to be independent of the type of pentose sugar present, the types of bases present, the sequence of bases and the length of the molecule. Finally, it is suggested that the origin of the ferroelectricity of these materials may be in the phosphate group of the molecules.

Recommendations are made for ferroelectric, pyroelectric and crystallographic studies on the nucleic acids and several other related chemicals.

CHAPTER I

INTRODUCTION

Investigations of the chemical and physical properties of the nucleic acids have largely been concerned with the relationships of these properties to the role of the nucleic acids in the life processes. For example, it is known that the nucleic acids are of prime importance in controlling metabolism, reproduction and growth of living systems (1). Recently however, experiments have implied that ribonucleic acid (RNA) is intimately associated with the memory process of platyhelminths and mammals (2,3,4). It is therefore of interest to determine any relationship between the various properties of RNA and the memory process.

Any scientific correlation between the properties of RNA and the memory process must ultimately be based on chemical or physical principles. Furthermore, this corre-lation must take into account the distinction between long and short term memory. The two types of memory are defined here as follows: (1) long term memory is the reception and storage of information and the availability for recall long after the reception of the information, and (2) short term memory is the reception and storage of information, the immediate availability for recall after reception and the

possible short term retention of the information. As a mechanism to explain long term memory, it is quite reasonable to assume a chemical coding of the RNA. A chemical coding of genetic information is already known to exist in RNA and in deoxyribonucleic acid (DNA). The use of this mechanism to explain short term memory is not feasible since the chemical reaction of macromolecular synthesis, required by chemical coding, is too slow to account for the immediate recall required by the definition of short term memory. One is thus led to search for some other information storage mechanism to explain short term memory. From a physical standpoint an information storage mechanism based on hysteresis permits a ready explanation of the immediate recall of short term memory. Two common types of materials exhibiting hysteresis are ferromagnetic and ferroelectric materials. Ferromagnetic hysteresis accounts for the storage and recall of information of such mechanical devices as computers and tape recorders. However, an explanation based on a ferromagnetic hysteresis mechanism is unacceptable since ferromagnetic materials exist in only trace amounts in neural tissue. Hence, it is of interest to determine the existence of ferroelectricity in RNA.

History of Ferroelectricity

It is possible to divide all crystal types into 32 crystal classes, according to their rotational symmetries. Of these 32 crystal classes, or point groups as they are

often called, 11 have a center of symmetry (inversion center) and are called centrosymmetric. The remaining 21 classes lack an inversion center and are called noncentrosymmetric.

Crystals in 20 of the 21 noncentrosymmetric crystal classes exhibit the phenomenon of piezoelectricity (5). This is the ability of certain materials to polarize, producing an electric field, when subjected to a compression or tension. Conversely, when placed in an electric field, these materials expand or contract. It is possible then to predict piezo-electricity on the basis of crystallographic information alone, although the effect is not always large enough to detect.

Of those crystal classes which exhibit piezoelectri-city, ten classes possess a polar axis (5). A polar axis is an axis along which exists a possible permanent (spontaneous) polarization. This spontaneous polarization is usually masked by surface charge. Heating these crystals will permit obser-vation of the polarization by producing a change in the polar-ization. These crystals are thus said to be pyroelectric. The existence of pyroelectricity, like piezoelectricity, may be deduced once the point group symmetry of a crystal is known.

If the direction of the spontaneous polarization of a pyroelectric material can be reversed by application of an electric field without causing dielectric breakdown, the crystal is said to be ferroelectric. Ferroelectricity is a dielectric property and can be determined only from dielectric measurements, not from crystallographic measurements. The

name is derived strictly from analogy between the dielectric behavior of these crystals and the magnetic properties of ferromagnetic materials. For example, it is found that ferroelectric materials exhibit a domain structure analogous to the magnetic domain structure of ferromagnetic crystals and exhibit electric hysteresis similar to ferromagnetic hysteresis. Furthermore, quite a few ferroelectric materials exhibit a transition temperature beyond which they are no longer polar and where their dielectric constants obey, again in analogy to ferromagnatism, a Curie-Weiss law

$$\epsilon = C/(T - T_0), \tag{1}$$

where ϵ is the dielectric constant, C is the Curie constant, T is the temperature and T_0 is a characteristic temperature (6).

Ferroelectricity was discovered in Rochelle salt by Valasek in 1921 (7). For some time thereafter the effect was not observed in any material except Rochelle salt. It is now known however, that ferroelectricity exists in many materials and an impressive list of known ferroelectric materials could be cited. It is possible to divide some well studied ferro-electric materials into four families: (1) the ferroelectric tartrate family represented by Rochelle salt, (2) the alkali metal dihydrogen phosphates and arsenates of which KH_2PO_4 is a typical representative, (3) the oxygen-octahedra family

which includes the subgroup with the perovskite (CaTiO$_3$) structure, represented by BaTiO$_3$ and (4) the family represented by guanidine aluminum sulfate hexahydrate.

Several theories are known which attempt to explain the ferroelectricity, in large measure, of that class of ferroelectric materials represented by barium titanate. Barium titanate has a cubic structure in its nonpolar phase, which makes it a convenient structure for relatively simple theoretical treatment. Two of the theories which have been successful are those of Devonshire (1949) and Cochran (1960) (8,9,10). Devonshire's work is a thermodynamic, phenomenological theory, while Cochran's theory is based on lattice dynamics.

Physical Properties of Ferroelectric Materials

As mentioned above, ferroelectric materials exhibit a domain structure analogous to that in ferromagnetic materials. Since polarization is defined as the electric dipole moment per unit volume it is possible to associate with each domain a region in which the electric dipoles are all aligned. However, the association of these dipoles with specific pairs of opposite charges may not always be possible (see Appendix A).

The hysteresis exhibited by a ferroelectric material can easily be understood on the basis of domain structure. Figure 1 represents a hysteresis loop for a typical single crystal ferroelectric material. The exact shape of the
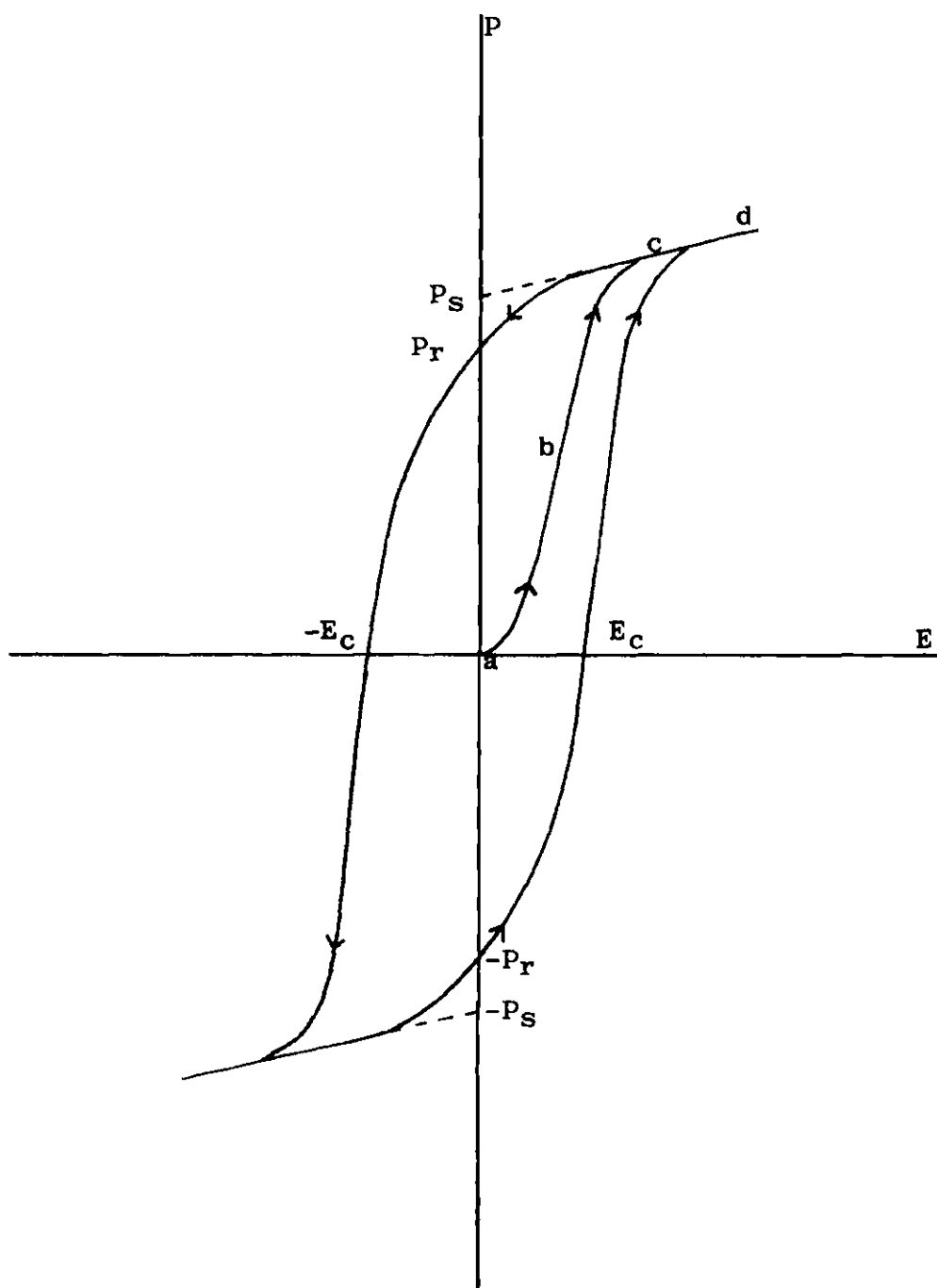
Figure 1. Ferroelectric Hysteresis Loop

hysteresis loop obtained for a given specimen will depend upon a number of factors. If the specimen is not a single crystal, one obtains a superposition of loops due to crystallites. A number of other factors which may affect the shape of the hysteresis loop are the temperature, humidity, strength and frequency of the switching field, conductivity of the specimen, physical dimensions and prior thermal and electrical history (7,11). Referring again to Figure 1, at point a the specimen has no net polarization, i.e., all the domains are randomly oriented. As the electric field is increased from zero (a to b) the polarization increases rapidly, this means that there is a net alignment of domains in the direction of the applied field. Upon further increase of the electric field (b to c) saturation is reached (c to d). At this point no new alignment takes place. The intersection of the polarization axis and the extrapolated portion of the linear part of this curve is referred to as the spontaneous polarization P_s. As the electric field is reduced to zero, a few of the domains aligned with the applied field switch back to random orientations and consequently at zero field a residual or remnant polarization P_r remains. As the electric field is increased in the opposite direction, switching of domains occurs until an equal number of domains are aligned in both directions and there is no net polarization. The value of the electric field at this point is called the coercive field strength E_c. This last value is

not a well-defined quantity but rather depends on temperature, measuring frequency and waveform of the applied voltage (12). Upon further increase of the electric field in the negative direction, saturation is again reached and the remaining portion of the loop is analogous to that previously discussed. As already noted many ferroelectric materials exhibit a temperature at which the hysteresis loop disappears, in which case the loop degenerates to a straight line, i.e., the polarization is then a linear function of the applied field.

It is possible to define the dielectric constant or permittivity ϵ of a ferroelectric material when in the polar phase in several ways (7). The susceptibility X is defined by

$$X = P/E \tag{2}$$

and is related to ϵ , in the cgs system, by

$$\epsilon = 1 + 4\pi X , \tag{3}$$

and in the MKS system, by

$$\epsilon = X + 1. \tag{4}$$

Here, four distinct susceptibilities, and therefore four permittivities, may be defined: (1) the overall susceptibility P/E with values of P and E from point c of Figure 1, (2) the differential susceptibility $\partial P/\partial E$ at any point,

(3) the saturation susceptibility, which is the slope at point c of Figure 1, and (4) the initial or "small signal" susceptibility, which is the slope $\partial P/\partial E$ at zero external field. In this thesis the dielectric constant will be taken to mean the initial or "small signal" dielectric constant.

The dielectric constants of ferroelectric materials are normally quite high. More accurately, one or more of the components of the dielectric constant tensor may be quite high. As the temperature is raised (or lowered in the case of a lower transition point) the dielectric constant increases, and at or near the transition point (or Curie point) may become exceedingly large. Above the Curie point in the nonferroelectric phase, the dielectric constant obeys a Curie-Weiss law (Equation 1).

Chemical Structure of the Nucleic Acids

The nucleic acids are composed of pentose sugars, phosphoric acid, purines and pyrimidines. The pentose sugars involved are ribose in RNA and deoxyribose in DNA (1,13,14). The purines and pyrimidines are commonly referred to as bases. The purines adenine and guanine, and the pyrimidine cytosine, occur in both RNA and DNA. The pyrimidine uracil occurs only in RNA and the pyrimidine thymine (5-methyluracil) occurs only in DNA. The chemical structures of these purines and pyrimidines are illustrated in Figure 2. Figure 3 shows the chemical structure of the pentose sugars and phosphoric acid.

A purine or a pyrimidine base is bonded to a pentose

Cytosine   Uracil   Thymine
(5-methyluracil)

Pyrimidines

Adenine   Guanine
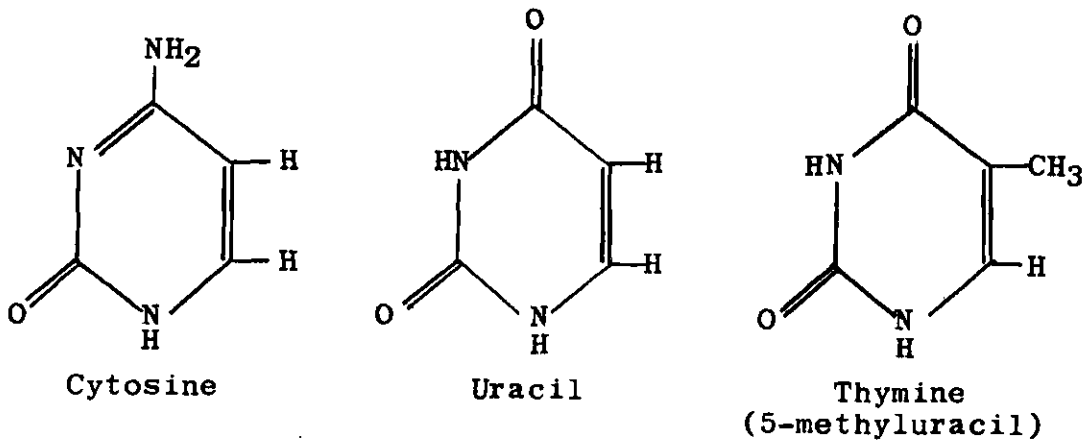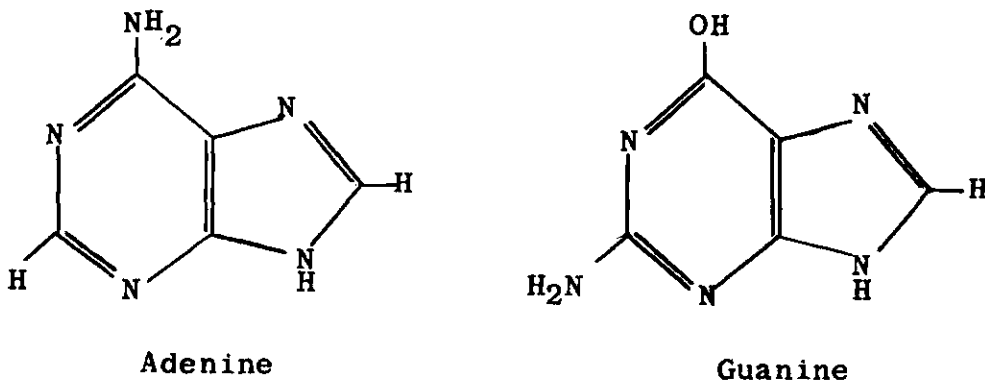
Purines

Figure 2. Purines and Pyrimidines of the Nucleic Acids
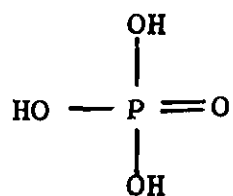
Phosphoric Acid
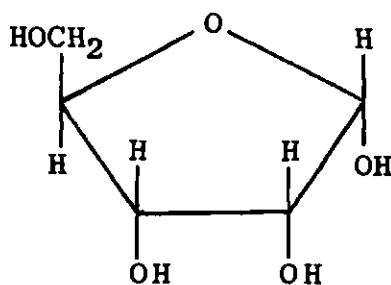
Ribose
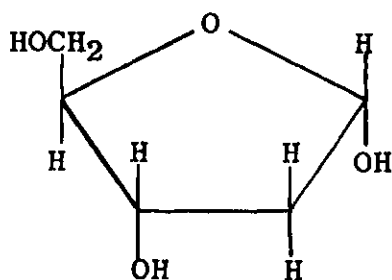
Deoxyribose

Figure 3. Phosphoric Acid, Ribose Sugar and Deoxyribose Sugar

sugar and the combination is known as a nucleoside. Figure 4 illustrates the nucleoside of adenine, known as adenosine or adenine riboside, and of cytosine, known as cytidine or cytosine riboside. If the nucleoside is formed with deoxyribose sugar the combination is referred to as a deoxyriboside. The chemical structures of ribosides and deoxyribosides are identical insofar as bond positions are concerned and hence the illustration does not show any deoxyriboside.

The phosphoric ester of a nucleoside is known as a nucleotide. The phosphoric acid is attached to the pentose sugar as illustrated in Figure 5, where again only the case for ribose sugar is shown. The nucleotides illustrated are adenylic acid or adenosine-5'-monophosphate and cytidylic acid or cytidine-5'-monophosphate. The 5' refers to the particular sugar carbon atom bonded to the phosphate group. Other nucleotides are possible with the attachment of the phosphate group to a different position on the pentose sugar but these will not be considered here.

The nucleic acids are formed by the bonding of nucleotides into long chains. The nucleotides formed with adenine, guanine, cytosine and uracil make up RNA with bonding occurring between the phosphate group of one nucleotide and the pentose sugar of another nucleotide as shown in Figure 6. In DNA the uracil nucleotide is replaced by the thymine nucleotide. Furthermore, DNA consists of two of these nucleotide chains linked by hydrogen bonds between the purines

Adenine Riboside (adenosine)

Cytosine Riboside (cytidine)
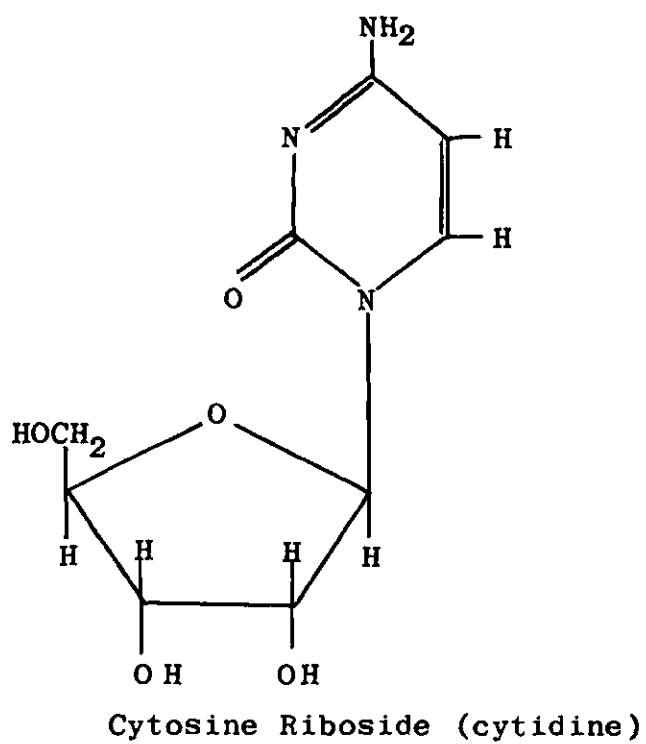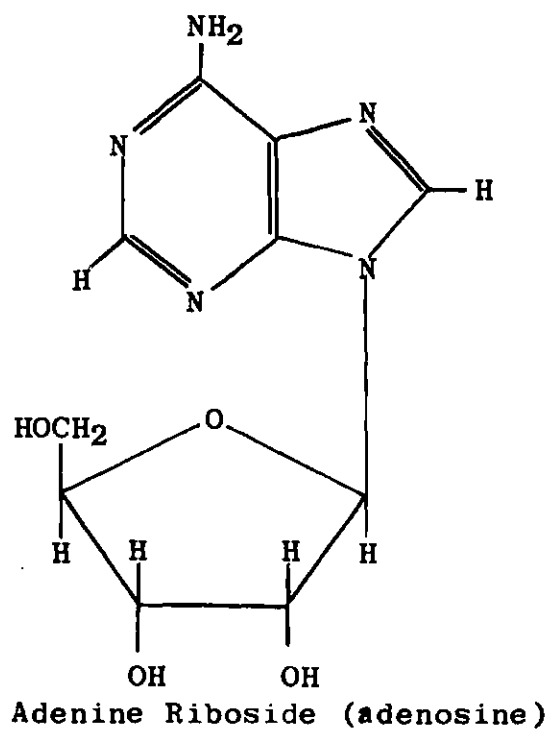
Figure 4. Adenine Riboside and Cytosine Riboside
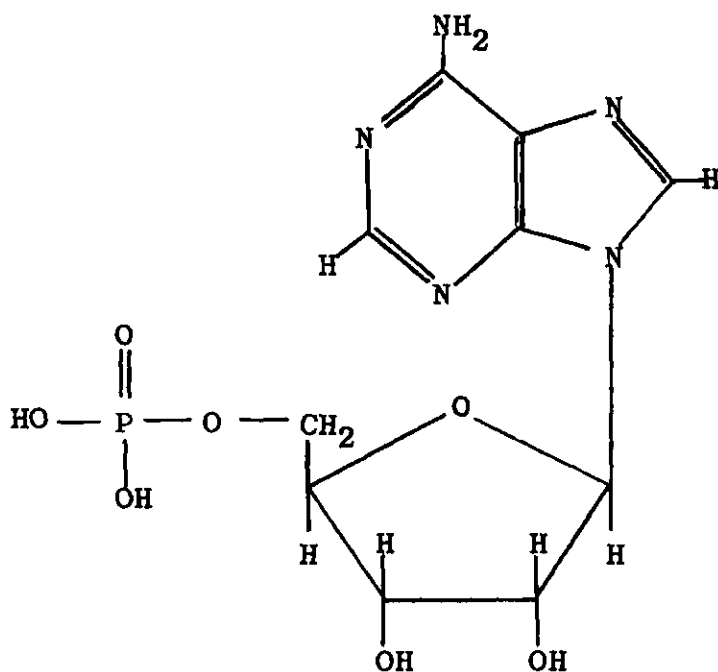
Adenylic Acid (adenosine-5'-monophosphate)
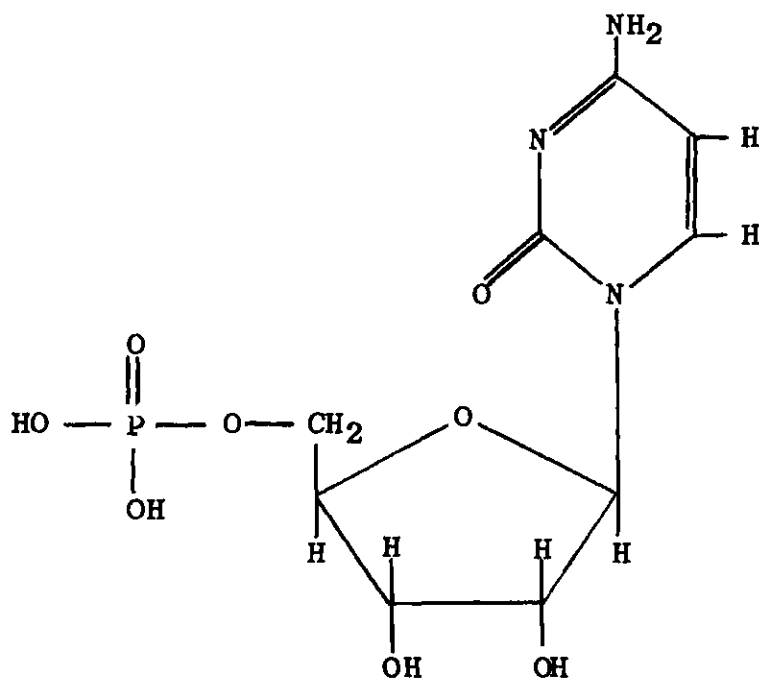
Cytidylic Acid (cytosine-5'-monophosphate)

Figure 5. Adenylic Acid and Cytidylic Acid
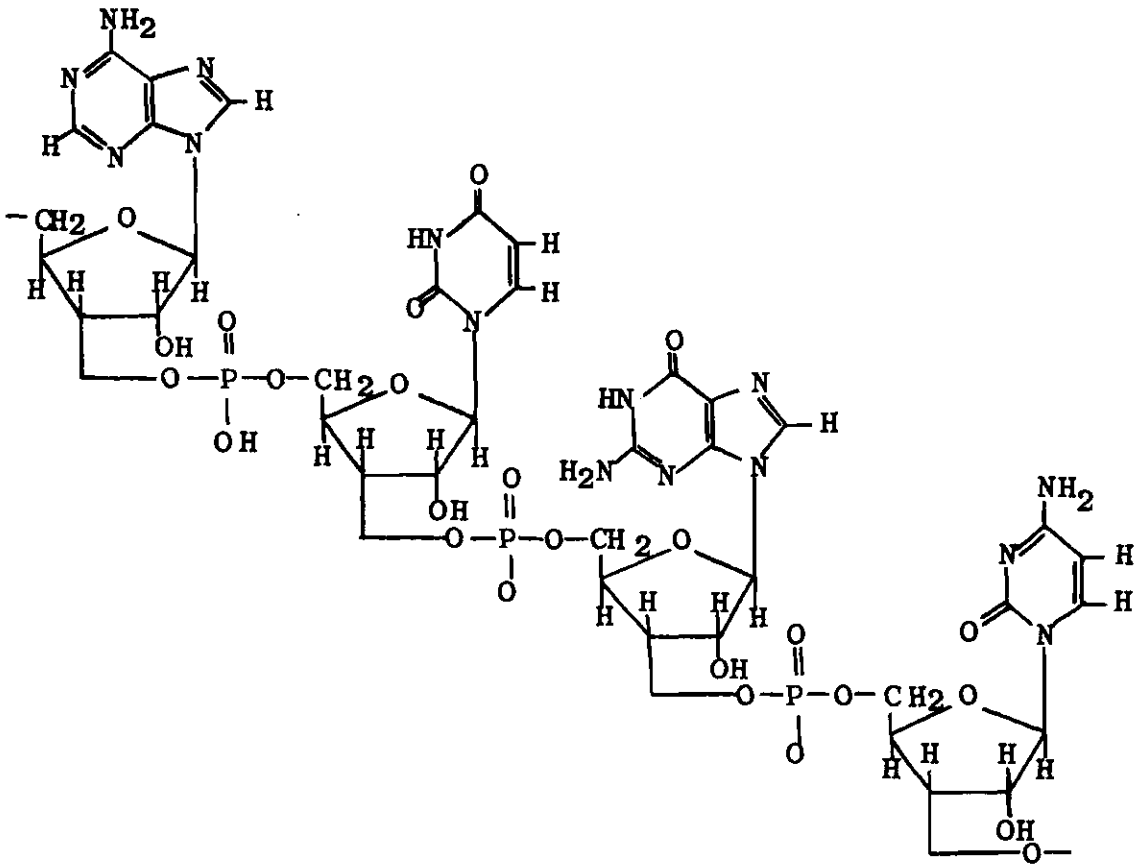
Figure 6.   Ribose Nucleic Acid

and pyrimidines. In this connection adenine bonds with thymine, and guanine bonds with cytosine as shown in Figure 7.

It is possible to synthetically produce polyribonucleotides with only one particular type of base. The names given to the adenine and cytosine polyribonucleotides are polyadenylic acid and polycytidylic acid respectively.

The chemicals with which this thesis is concerned are listed in Table 1. As indicated in this table the salts of the various acids were used rather than the actual acids themselves. All these chemicals were obtained commercially.

Crystal Nature of the Chemicals Used in this Research

X-ray pictures (Laue photographs) were obtained of the four macromolecular materials used here, and of guanylic acid disodium and cytidylic acid disodium. Attempts to obtain Laue photographs of adenylic acid sodium and thymidylic acid sodium were unsuccessful. The necessarily long exposure times, of the order of seven or eight hours, permitted the absorbtion of water and subsequent dissolution of the latter two materials. The X-ray information indicated that the samples of guanylic acid disodium and cytidylic acid disodium were polycrystalline in nature. The photographs of the cytidylic acid disodium sample most clearly showed this crystal nature. It will be assumed by analogy that the adenylic acid sodium and thymidylic acid sodium samples were also polycrystalline. This analogy is reasonable because adenine and guanine are both purines and thymine and cytosine are both pyrimidines.
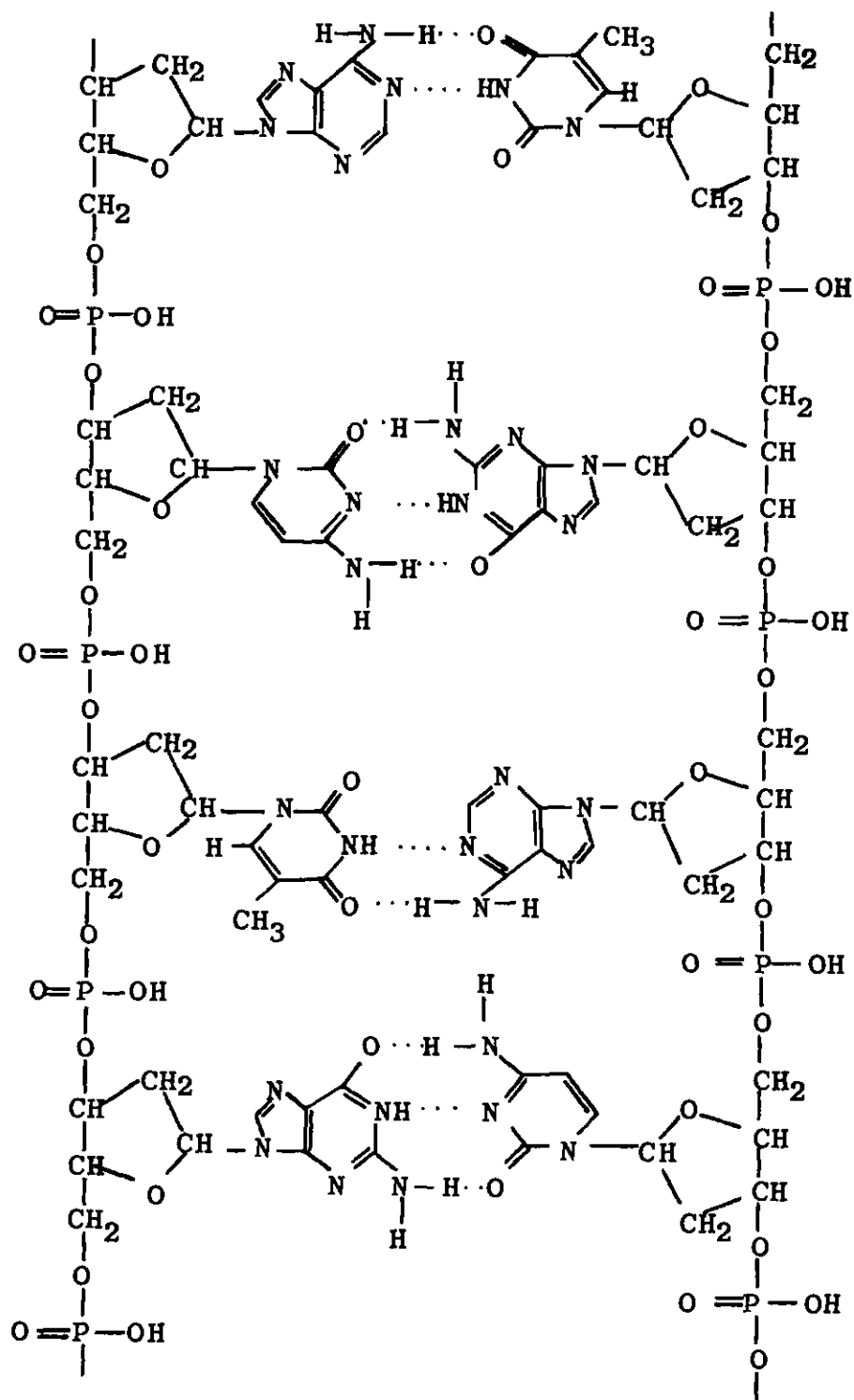
Figure 7.   Deoxyribose Nucleic Acid

Table 1.   The Chemicals Used in this Research

1. Adenine

2. Adenosine

3. Adenylic Acid (Adenosine-5'-Monophosphate) Sodium

4. Cytidylic Acid (Cytidine-5'-Monophosphate) Disodium

5. Guanylic Acid (Guanosine-5'-Monophosphate) Disodium

6. Thymidylic Acid (Thymidine-5'-Monophosphate) Sodium

7. Uridylic Acid (Uridine-5'-Monophosphate) Disodium

8. Sodium Deoxyribonucleate

9. Sodium Ribonucleate

10. Polyadenylic Acid Potassium

11. Polycytidylic Acid Potassium

The photographs of the four macromolecular materials did not indicate crystalline structures. However, it is quite probable there exist some degree of intramolecular order with intermolecular disorder. Fibers of these materials drawn from solution with the macromolecules lying generally along the fiber axis are usually employed in X-ray work (15,16,17). The bulk form used here could be expected to yield little information concerning the crystal nature of these materials. All X-ray work here was done at room temperature.

In connection with the macromolecular structure it should be noted that DNA can exist both in a crystalline and in a paracrystalline form (15,16,18,19). The exact structure is determined by the relative humidity and the most crystalline form occurs at approximately 70 per cent relative humidity (18). At higher humidities the paracrystalline form results and at lower humidities the loss of water distorts the structure, causes irregularities, but leaves the basic structure intact (15). Figure 7 illustrates the chemical structure of DNA. The basic physical structure of DNA is a double helix with the sugar-phosphate chains forming the backbones and the hydrogen bonded purines and pyrimidines connecting these chains (1,13,14,18). The crystalline form of DNA has a face-centered monoclinic lattice, has a repeat distance along the helix axis of 28 Å, contains approximately 30 per cent water by weight and the bases are tilted about 25° from the helix axis (18,19). The paracrystalline form

of DNA contains more water, has a repeat distance of 34 Å
and has all the bases parallel to each other and perpendicu-
lar to the helix axis but with random rotation about their
own molecular axes (18,19). The structural changes which
occur with changes in humidity are not part of the helix-
coil transitions associated with heat denaturation which
occurs in the range of 70°C to 80°C (1,20). In contrast to
DNA and most of the other polyribonucleotides, the structure
of polyadenylic acid is independent of humidity (17). Poly-
adenylic acid may form a double helix with the sugar-phos-
phate backbone chains held together by purine-purine hydro-
gen bonds and purine-phosphate hydrogen bonds (17). The
bases are inclined about 10° from the perpendicular to the
helix axis and the resulting structure is quite compact.
Denaturation, helix-coil transition, occurs over a tempera-
ture range centered at 90°C (17).

Purpose of this Research

This work was stimulated by the search for a physical
property of RNA which could relate RNA to the memory process.
It is interesting to note that the results of this investiga-
tion are particularly pertinent to the search for possible
mechanisms for information storage in neural tissue. However,
the purpose of this research is the experimental investigation
of the dielectric properties and ferroelectric character of
the nucleic acids, RNA and DNA, and several other related
compounds.

Review of the Literature

A report on the dielectric properties and ferroelectric character of DNA was made in 1960 (21). The material used was the lyophilized sodium salt of DNA which was pressed into a wafer. Neither the lyophilized nor the wafer form of sodium DNA is used in this research. The only other known experimental work reported concerning the ferroelectricity of the nucleic acids was done on the sodium salt of RNA in 1968 and coauthored by the present investigator (22).

CHAPTER II

INSTRUMENTATION AND EQUIPMENT

The equipment used in this investigation consisted mainly of that designed to observe the dielectric hysteresis and that designed to measure dielectric constants. All of the measurement techniques used in this work are of standard nature and none of the equipment has been uniquely designed for this experiment.

The "classical" method of Sawyer-Tower was used to observe dielectric hysteresis (23). The actual circuit used is shown schematically in Figure 8, where C_0 is a standard capacitor and C_x is the sample capacitor. Figure 9 shows a typical hysteresis loop obtained using this circuit with a sample crystal of barium titanate. The picture was taken with a polaroid camera and then reproduced from the photograph.

It is of value here to consider the Sawyer-Tower circuit in more detail. The capacitors C_0 and C_x are related by the inequality

$$C_0 \gg C_x .$$ (5)

With this condition it is readily seen that the horizontal
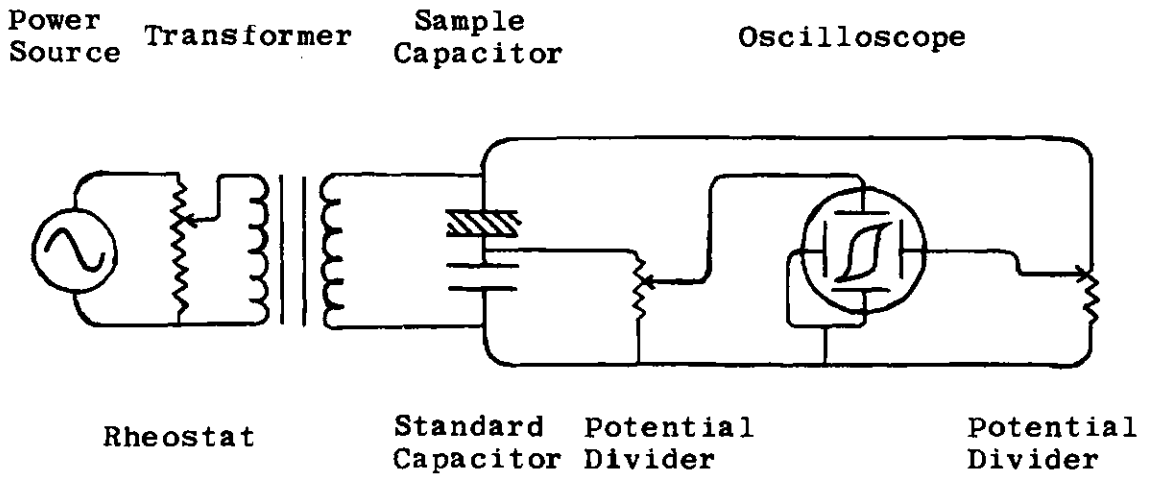
Figure 8. Sawyer-Tower Circuit
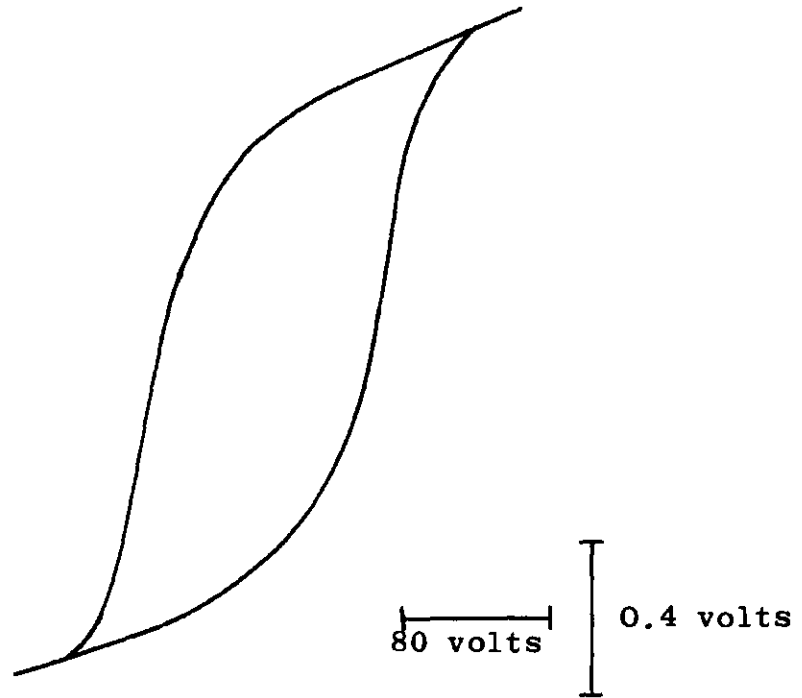
Figure 9. Hysteresis Loop of Barium Titanate

input voltage is given by

$$V = E_x + E_o \cong E_x \; , \tag{6}$$

where V is the input voltage, E_x is the voltage across the sample and E_o is the voltage across C_o. This approximation follows from consideration of the equation relating E_o to the charge on either capacitor,

$$E_o = Q/C_o \; . \tag{7}$$

Since the applied electric field is equal to the sample voltage divided by the thickness of the sample which is a constant, the horizontal displacement on the oscilloscope is proportional to the electric field. Furthermore, since the polarization is equal to the charge on the sample divided by the area of the sample which is a constant, and the charge is related to the voltage as shown in Equation 7, the vertical displacement on the oscilloscope is proportional to the polarization.

If the sample C_x is replaced by a linear element such as a resistor, capacitor or a parallel combination of these two, the oscilloscope will display an ellipse or its degenerate case, a straight line. It may be shown (see Appendix B) that the coordinates of the oscilloscope trace are related by an equation of the following type

$$Ax^2 + Bxy + Cy^2 + Dx + Ey + F = 0 , \qquad (8)$$

where the constants are functions of the capacitance, resistance and frequency of the circuit and where not all constants necessarily differ from zero. This equation represents an ellipse or its degenerate case provided that the inequality

$$B^2 - 4AC < 0 \qquad (9)$$

is satisfied. Thus, ideal linear elements will yield either an ellipse, a circle or a straight line.

Considering again the nonlinear element, in most cases the ferroelectric sample has a finite conductivity. The resulting hysteresis loop may be regarded as consisting of three contributions as seen in the equation

$$Q(V) = P(V) + C \cdot V + (1/R) \int V dt . \qquad (10)$$

The first term in Equation 10 represents the spontaneous polarization contribution, the second term represents the capacitance contribution and third term represents the conductivity contribution (11). If the input voltage is sinusoidal and given by

$$V = V_0 \sin \omega t , \qquad (11)$$

Q may be expressed as

$$Q = P(V) + V_o(C \cdot \sin \omega t - 1/\omega R \cdot \cos \omega t) , \qquad (12)$$

or

$$Q = P(V) + C/\cos \phi \cdot V_o \sin(\omega t - \phi) , \qquad (13)$$

where ϕ is related to C by the equation

$$\tan \phi = 1/\omega RC . \qquad (14)$$

Thus the horizontal deflection voltage phase is shifted and the resulting hysteresis loop shows rounded ends.

The circuit used to measure the dielectric constant as a function of temperature is shown schematically in Figure 10. The thermocouple was made of chromel alumel and was used to drive the X-axis of an X-Y recorder. Figure 11 shows the calibration curve for the thermocouple using solid CO_2, ice and boiling water as reference points. The signal across C_o is amplified, rectified and made to drive the Y-axis of the X-Y recorder. The curve obtained on the X-Y recorder is then a measure of the capacitance (dielectric constant) as a function of temperature. Figure 12 shows a plot of peak input voltage versus rectified voltage showing a linear relation in the range utilized. To obtain a
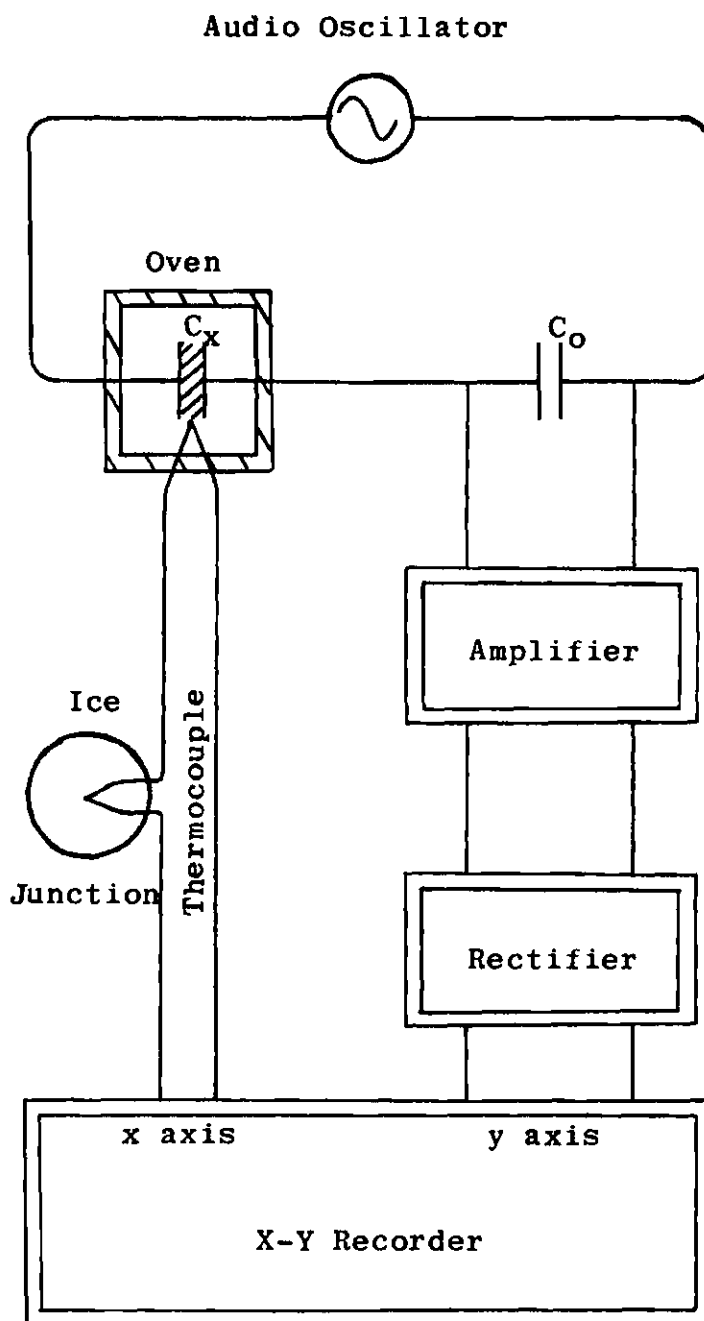
Figure 10. Capacitance Measuring Circuit
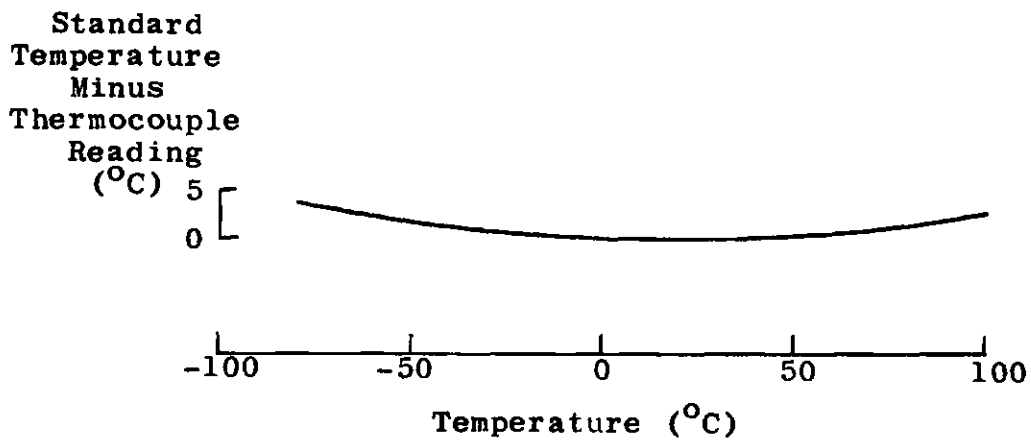
Figure 11. Thermocouple Calibration
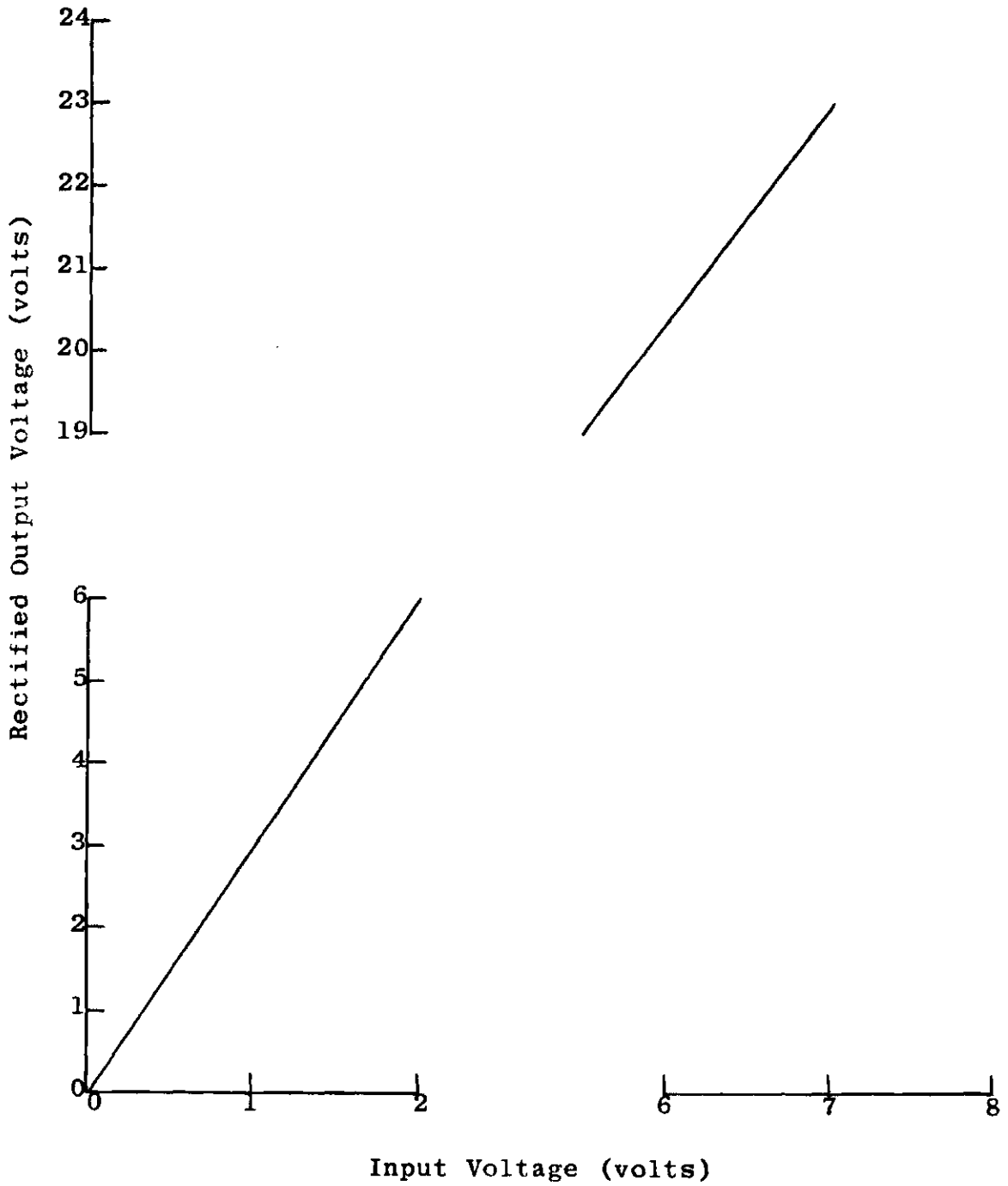
Figure 12.   Input Voltage Versus Rectified Output Voltage

capacitance scale on the X-Y recorder, standard capacitances were measured on a General Radio impedance bridge and then placed in the circuit in the position of C_x. This procedure was carried out with each sample measured.

The oven used to heat the samples was made by wrapping 18 loops of nichrome wire around a 100 ml pyrex beaker and surrounding this with aluminum oxide refractory brick. Access to the oven was provided by a teflon door through which leads to the sample and thermocouple were placed. A port was provided for observation of the sample with a microscope. Figure 13 shows a schematic diagram of the oven.

Aluminum cups were made on a lathe to the dimensions shown in Figure 13. These cups were used in the preparation of samples.

Other miscellaneous equipment used included a microscope used to measure the thickness of samples, a refrigerator used in drying samples and a hydraulic press used to make wafers of some of the materials.
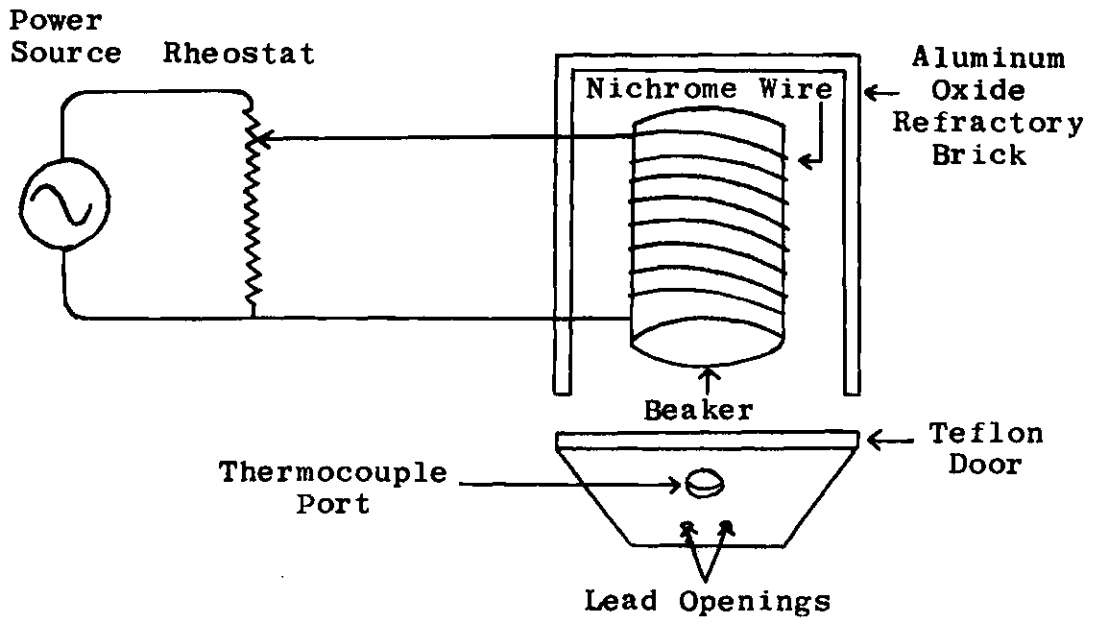
Sample Oven
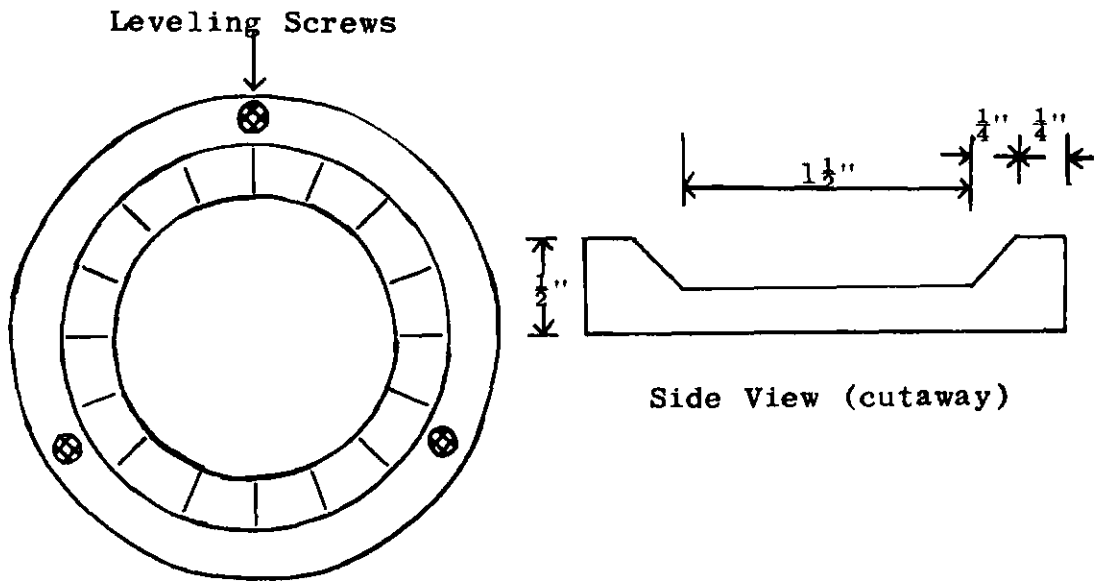
Top View

Side View (cutaway)

Sample Cups

Figure 13. Sample Cups and Sample Oven

CHAPTER III

EXPERIMENTAL PROCEDURE

The experimental procedure in these experiments con-
sisted of three phases; sample preparation, hysteresis ob-
servation and dielectric constant measurement.

Sample Preparation

Two procedures were used to obtain specimens suitable
for measurements. The first method involved dissolution of
the sodium or potassium salt of the various acids in dis-
tilled water. The amount of each chemical used, with the cor-
responding amount of water, is listed in Appendix C. These
do not necessarily correspond to saturated solutions but
rather to amounts of solute and solvent which would readily
result in dissolution. These solutions were then poured into
the aluminum cups described in Chapter II. The cups were
then placed in a refrigerator at approximately 5°C, to pro-
vide slow evaporation of the water. The evaporation of the
water yielded generally flat samples whose physical appear-
ance, size and shape are described briefly in Appendix C.
In the case of cytidylic acid disodium it was necessary to
allow evaporation to proceed at room temperature because the
material obtained from the refrigerator redissolved when
brought to room temperature. This dissolution procedure did

not yield usable samples of adenine, adenosine or uridylic acid disodium. To obtain samples of these materials a second procedure was used. Wafers were made of the powdered material using a hydraulic press. The amount of each material used and the pressure applied are listed in Appendix C. For comparison purposes, wafers were also made of adenylic acid sodium.

Electrodes were painted on the samples using DuPont Silver Preparation-Electronic Grade 4929. Leads 0.010 inch in diameter were placed on the silver electrodes and became attached upon drying and hardening of the electrodes. The samples thus became the dielectric medium inside parallel plate capacitors. To insure complete hardening of the electrode material, the coated samples were allowed to remain in the refrigerator at approximately 5°C for 24 hours.

The thickness of each sample was measured using a stereomicroscope equipped with a reticle whose smallest division is 0.001 inch. The area of the electrodes were determined from the stencils used for painting the electrodes. Electrodes were painted on glass slides using the stencils and these areas were determined by using the stereomicroscope reticle.

In both the hysteresis observation and the dielectric constant measurement, the sample was placed in the oven described in Chapter II. Figure 14 shows the heating curves for this oven for a few settings of the Variac oven control.
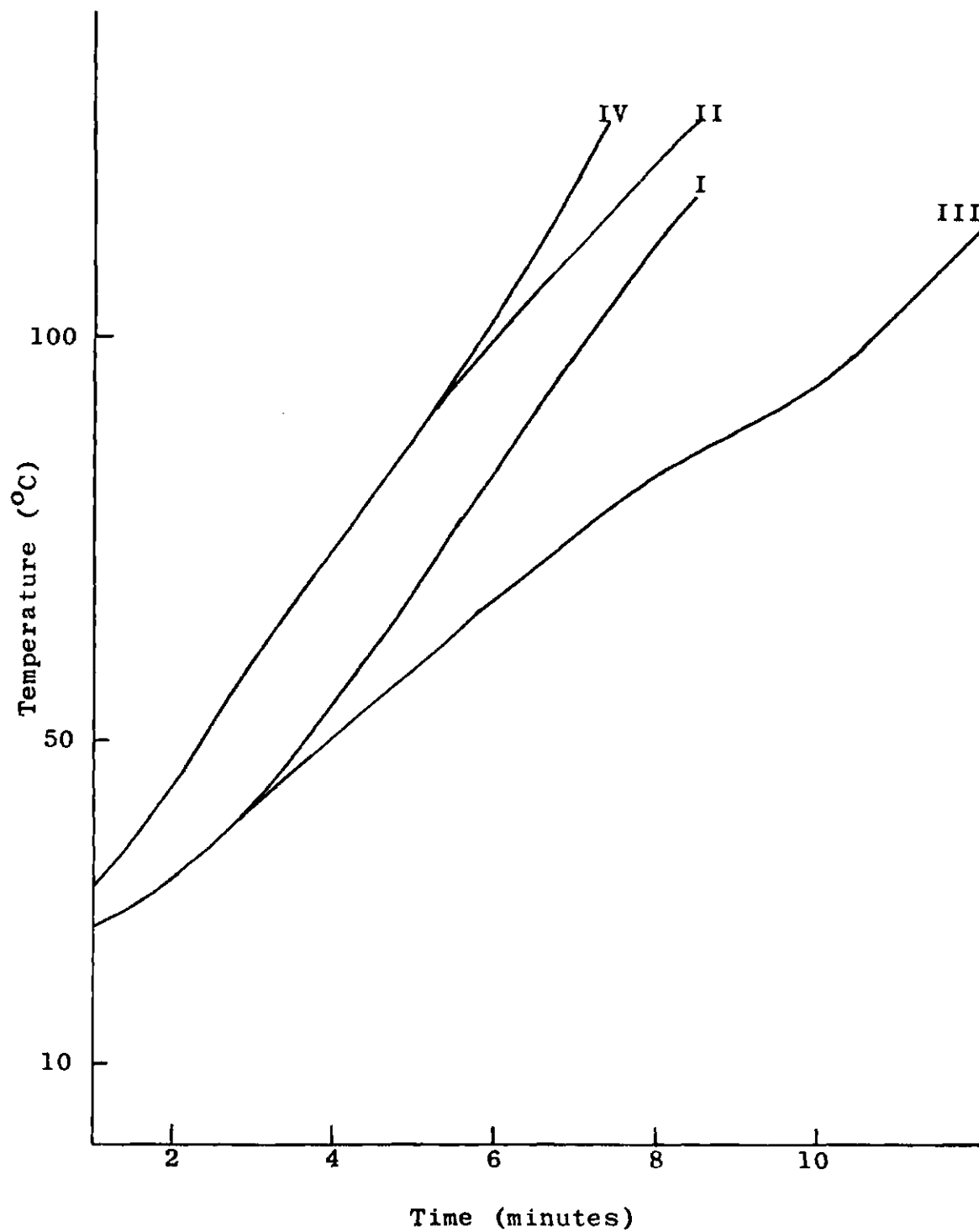
Figure 14. Oven Heating Curves

The rate at which the samples were heated appears in the
compilation in Appendix D.

Hysteresis Observation

Attempts to observe hysteresis were made on all
materials, some of which were in the dissolved and hardened
form and some in wafer form. However, no hysteresis loops
were observed for any of the wafers. The samples were placed
in the Sawyer-Tower circuit and the loops observed on an
oscilloscope.

In order not to cause excessive heating of the sample
due to the applied alternating voltage, only small signals
were used. In this way the heating of the sample was due
almost entirely to the oven. In order to test whether the
thermocouple reading represented the actual sample tempera-
ture, the following procedure was utilized. Several layers
of the sodium RNA solution were applied to one junction of
a thermocouple and allowed to harden. This junction was
placed in the oven adjacent to another thermocouple and the
oven heated at twice the fastest rate used in the experiment.
Over the temperature range used, room temperature to approx-
imately $100^{\circ}C$, the lag was never greater than three degrees.

The observed hysteresis loops were photographed with
a Polaroid camera and subsequently were reproduced from the
photographs.

Dielectric Constant Measurement

The capacitances of each sample was measured as a

function of temperature using the apparatus described in Chapter II. Small signals were used to measure the capacitances and their values are listed in the compilations in Appendix D.

In all cases it was assumed that the samples were ideal parallel plate capacitors. The ratios of the thicknesses of the samples to the diameters of the circular electrodes are listed in Appendix D. With this assumption, computation of the dielectric constant from the value of the capacitance is quite straightforward. Tables and Graphs of these measurements are also in Appendix D.

CHAPTER IV

RESULTS

Precision

It is of interest to examine the errors associated with the measurements in this research prior to discussing the results; this will hopefully provide a better understanding of the results and their interpretation. The quantities which are involved in the measurement of the dielectric constant that contribute to the error are: (1) the temperature, (2) the capacitance, (3) the sample electrode area, and (4) the sample thickness.

Figure 11, which is the calibration curve for the thermocouple used here, shows that the error in the temperature is less than three degrees between $25^{O}C$ and $100^{O}C$. Furthermore, the greatest error occurs at the high temperature end of this region. As explained in Chapter III, the sample temperature lagged the oven temperature less than three degrees when the oven was heated at twice the fastest rate used during the actual experiment. Since the heating rate decreases during heating, the temperature lag is greatest at the lower portion of the above temperature scale. Hence, it is reasonable to assume that the temperature error is less than four or five degrees over the entire temperature scale utilized.

The values of the capacitances obtained from the impedance bridge and used for calibration of the X-Y recorder are accurate to within one percent. However, a large error results due to the method used for measuring the sample capacitance. The finite width of the recorder pen point and the resulting trace contribute significantly to this error. When measuring small capacitances the trace width may represent a large percentage of the capacitance scale. A more sensitive scale might decrease this percentage provided any resulting increase in noise level did not broaden the trace sufficiently to negate the advantage of any scale change. Thus some optimum scale must be established in order to minimize the error when measuring small capacitances. Even when measuring larger capacitances, the error introduced by the trace width usually can not be neglected.

The electrode area was determined by the method described in Chapter III. Sufficient numbers of electrodes of each size used were measured in order to determine the reproducibility and spread in the values of the areas. This procedure was used to determine the error due to area in each sample.

The thickness of each sample was measured a minimum of four times by the method described in Chapter III. The average value of these measurements was taken to be the sample thickness. Any sample whose faces were nonparallel by two or more degrees was not used for measurement.

Using the parallel plate capacitance approximation, the dielectric constant ϵ is obtained by using the equation

$$\epsilon = Cd/ \epsilon_o A \ , \tag{15}$$

where C is the sample capacitance, d is the sample thickness, ϵ_o is the permittivity of free space and A is the electrode area. Thus the error in the dielectric constant is just the sum of the errors of the sample capacitance, thickness and area. This cumulative error is listed along with its associated dielectric constant in Appendix D.

Additionally, the water content of the samples leads to an error in the dielectric constant. This error becomes appreciable at higher temperatures where presumably the water molecules are more mobile and are able to contribute to the sample conductivity. Higher temperature is assumed here to be above 70°C or 80°C. Since an ideal conductor has an infinite dielectric constant, one would expect the exceedingly large dielectric constants that occur at high temperatures. The values of these dielectric constants are listed in Appendix D. In particular it is to be noted that the dielectric constant for thymidylic acid sodium is quite large even at room temperature. The water concentration in this chemical may have been extremely high and thus contributed to the conductivity at lower temperatures. Therefore, particular care must be exercised when evaluating these high temperature

constants.

Finally, expansion of the samples at the high temperatures defined here may lead to an appreciable error. This expansion is generally not uniform since the electrodes add local stresses to the surfaces and the departure of the shape of the samples from parallel plate capacitors may be significant.

Interpretation

The interpretation of the hysteresis loops and the dielectric constants for each chemical is discussed separately. The hysteresis loops and at least one dielectric constant curve for each material are included in this chapter. These serve to illustrate many of the items to be discussed and the reader may refer to Appendix D for the remaining dielectric constant curves. All hysteresis loops shown were obtained at a frequency of 60 cps and unless otherwise stated the dielectric constants were obtained at a frequency of 1000 cps. On the hysteresis loop illustrations D is the electrode diameter in centimeters, d is the sample thickness in centimeters, HC is the rate of heating and refers to Figure 14 and the voltage scales shown are uncalibrated voltages from the measuring oscilloscope.

Sodium RNA. The most striking feature of the dielectric constant versus temperature curve for sodium RNA, shown in Figure 15, is the irregularity which occurs at approximately $53^{O}C$. Reference to Figures 37, 38, 39 and 40 in Appendix D shows
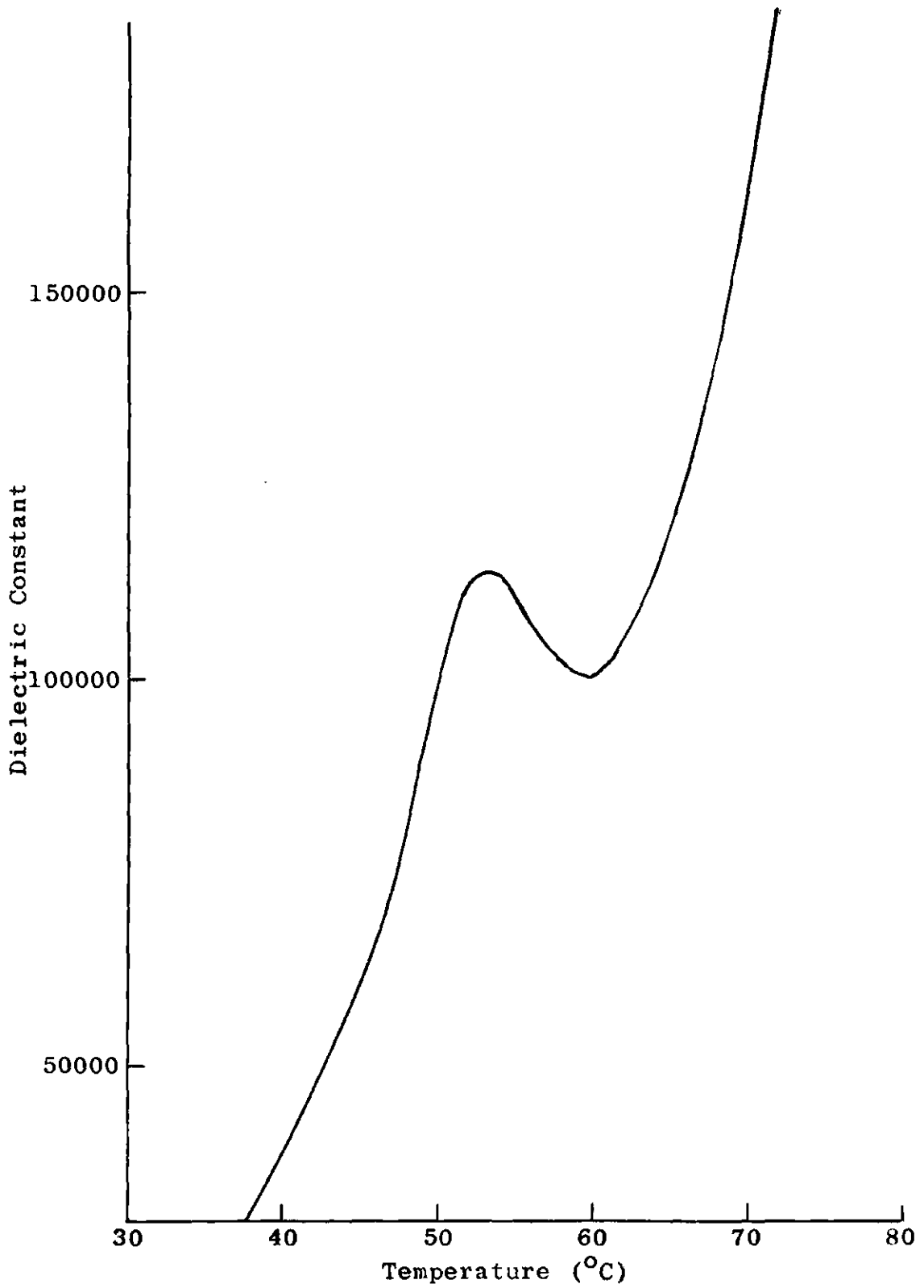
Figure 15. Dielectric Constant of Sodium RNA

that although the shape of this irregularity is not always the same, it does occur within a five degree temperature range between $52^{\circ}C$ and $57^{\circ}C$. Figures 41 and 42 in Appendix D show respectively the dielectric constant versus temperature at 100 cps and at 500 cps. It is clear that the irregularity is decreased, less pronounced, at the lower frequencies. This set of seven curves was obtained from two separate sample preparations with measurements made at different times and with different ambient conditions. Figures 15, 37 and 38 refer to samples from one preparation, and Figures 39, 40, 41 and 42 refer to samples from another preparation. For later reference the dielectric constant curve may be divided into three temperature regions: (1) up to $45^{\circ}C$ or $50^{\circ}C$, (2) from $45^{\circ}C$ or $50^{\circ}C$ to $60^{\circ}C$, and (3) above $60^{\circ}C$.

Figure 16 illustrates the hysteresis loops obtained for sodium RNA. As stated previously the samples used were not single crystals and were conducting, and a combination of these two factors is probably responsible for the general roundness and lack of saturation of the hysteresis loops. The loops below $40^{\circ}C$ actually show very little evidence of hysteresis, those above $58^{\circ}C$ show what is considered here to be quite good hysteresis and those loops between $40^{\circ}C$ and $58^{\circ}C$ show a gradual change between these two extremes. At temperatures above $75^{\circ}C$ or $80^{\circ}C$ the loops gradually disappeared as the sample denatured. All the loops appear to be very slightly asymmetric which may be indicative of an internal alignment

D = 0.487   d = 0.0406   HC = III

29 °C
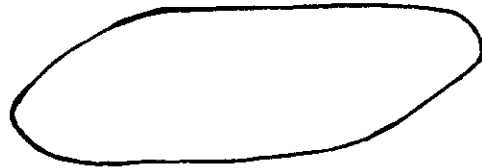
37 °C

47 °C

53 °C

58 °C

66 °C
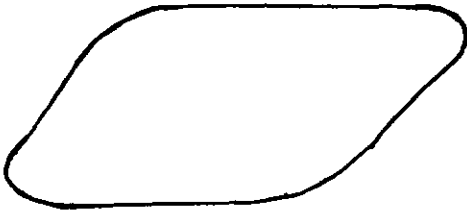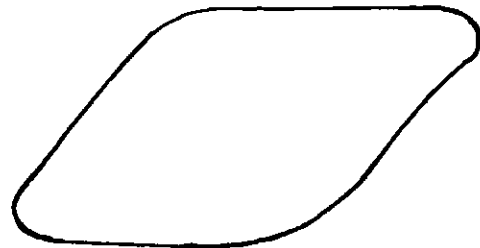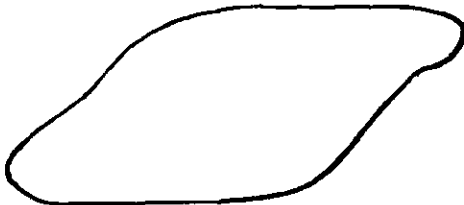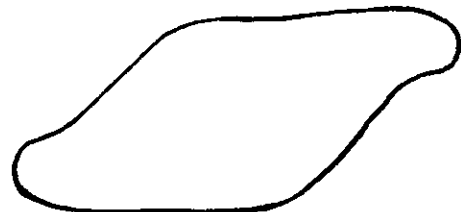
Figure 16. Hysteresis Loops of Sodium RNA

of dipoles during solidification.

It is quite evident that the three regions of the sodium RNA dielectric constant curve can be correlated with the three temperature divisions of the hysteresis loops. The gradual changes in the hysteresis loops correspond to the rather broad regions of the dielectric constant curve of 100 cps. The sharper regions of the dielectric constant curve of 1000 cps can not be correlated with hysteresis loops since it was not possible to obtain loops at a frequency of 1000 cps.

The five dielectric constant curves of 1000 cps were averaged and the result is plotted in Figure 17 for the temperature region of 35°C to 50°C. A Curie-Weiss law has been fitted to this curve and the result is also plotted in Figure 17. In the region between 35°C and 50°C the dielectric constant ϵ obeys the following

$$\epsilon = 4.55 \times 10^5/(55.25-T). \tag{16}$$

Similar curves were obtained for the dielectric constant at 500 cps and 100 cps and are shown in Figures 18 and 19 respectively. In the temperature range between 35°C and 55°C the dielectric constant at 500 cps obeys

$$\epsilon = 5.15 \times 10^5/(61.2-T), \tag{17}$$

and in the same temperature range the dielectric constant at
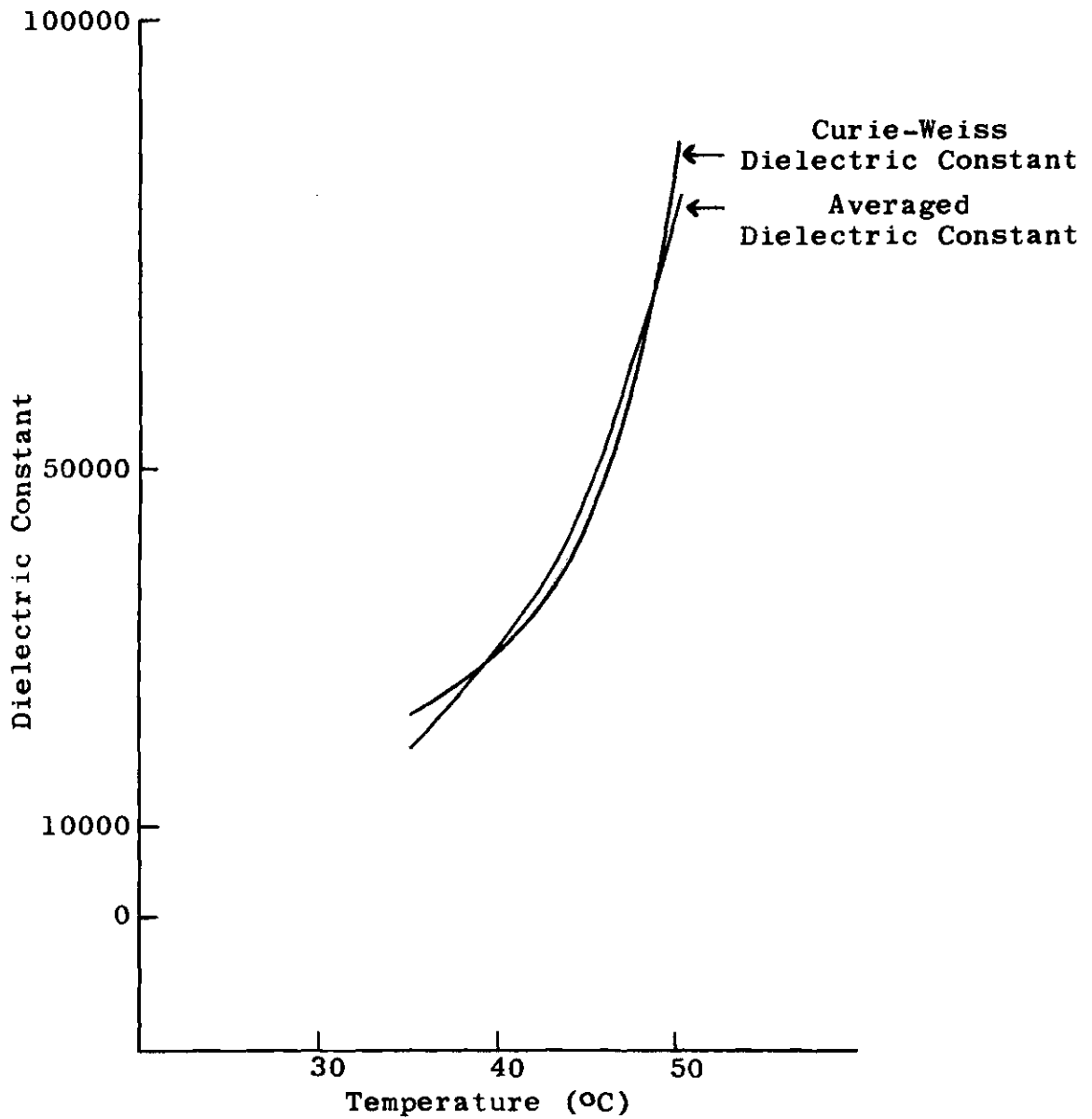
Figure 17. Curie-Weiss Law for Sodium RNA at 1000 cps
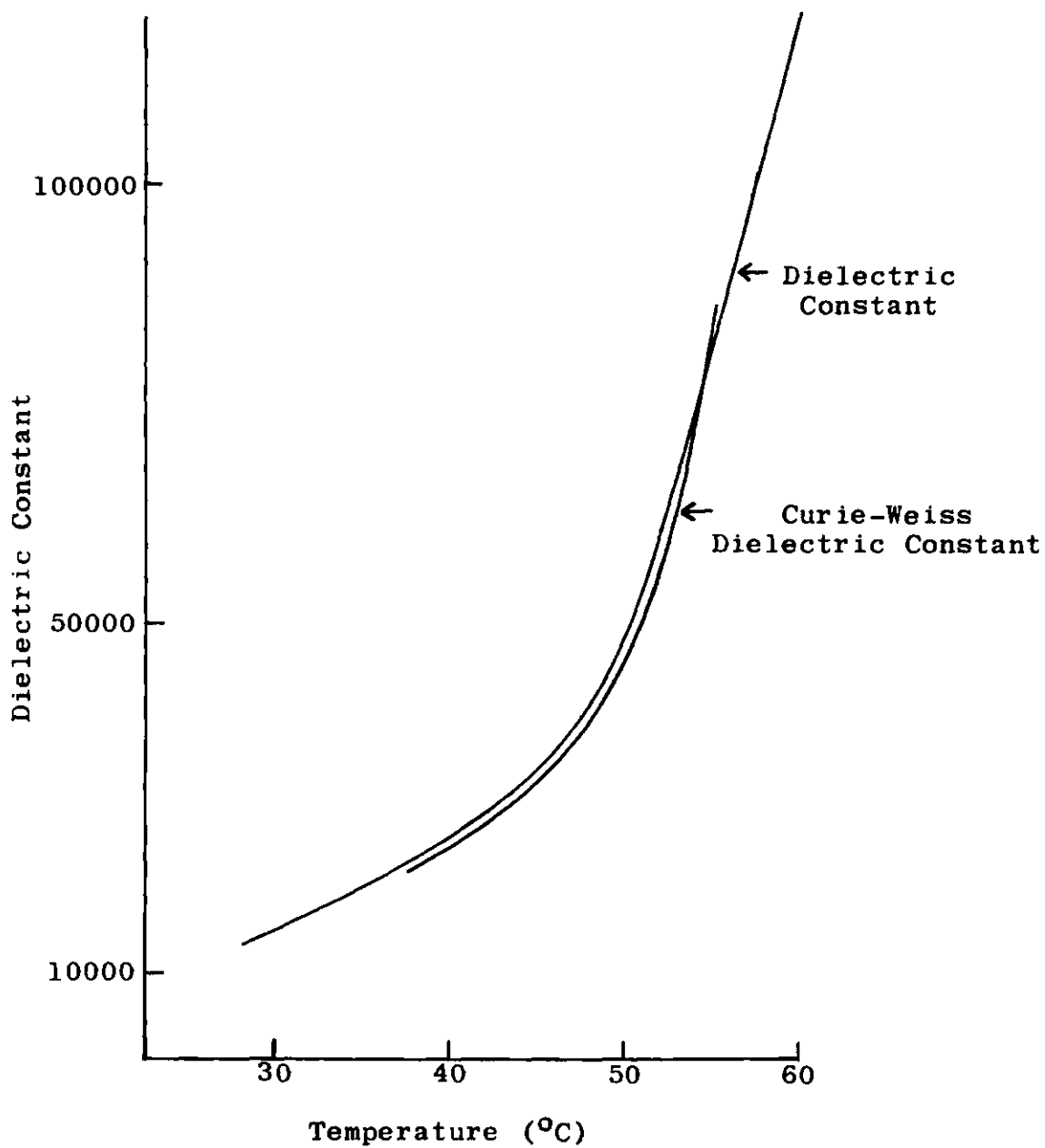
Figure 18. Curie-Weiss Law for Sodium RNA at 500 cps
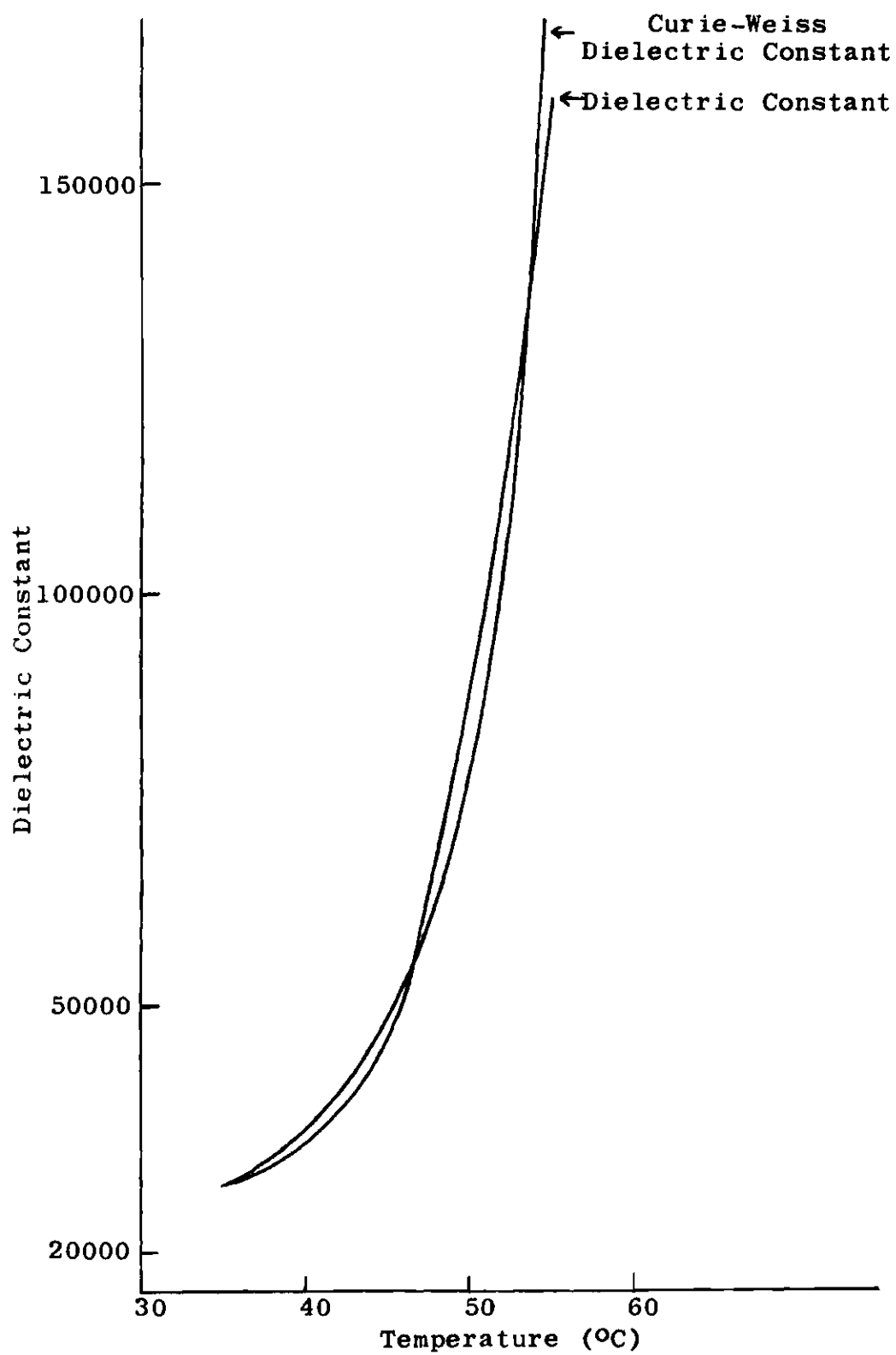
Figure 19. Curie-Weiss Law for Sodium RNA at 100 cps

100 cps obeys

$$\epsilon = 6.45 \times 10^{5}/(58.2 - T). \tag{18}$$

These dielectric constant equations are not to be taken as proof that a ferroelectric transition exists. However, structural changes do take place in the nucleic acids as discussed in Chapter I. In view of this, it is reasonable to assume some sort of transition in the temperature range up to about 50°C. Such a transition may take place relatively slowly and cause a gradual onset of ferroelectricity. On the other hand, what appears to be the onset of ferroelectricity may actually be merely a decrease in the coercive field strength.

Sodium DNA. The dielectric constant curves for sodium DNA exhibit a slight irregularity in the temperature range between 35°C and 45°C (see Figures 20,43 and 44). The hysteresis loops shown in Figure 21 are asymmetric below about 50°C and symmetric above about 70°C with a transition region between 50°C and 70°C. The asymmetry in DNA is much greater than in similar samples of RNA (compare Figures 15 and 20). Insofar as it is possible to compare the hysteresis loops and dielectric constant of DNA in view of the difference in measuring frequencies, only a very slight correlation can be made. The irregularity in the dielectric constant curve can be compared with the change in hysteresis loops from asymmetric to symmet-
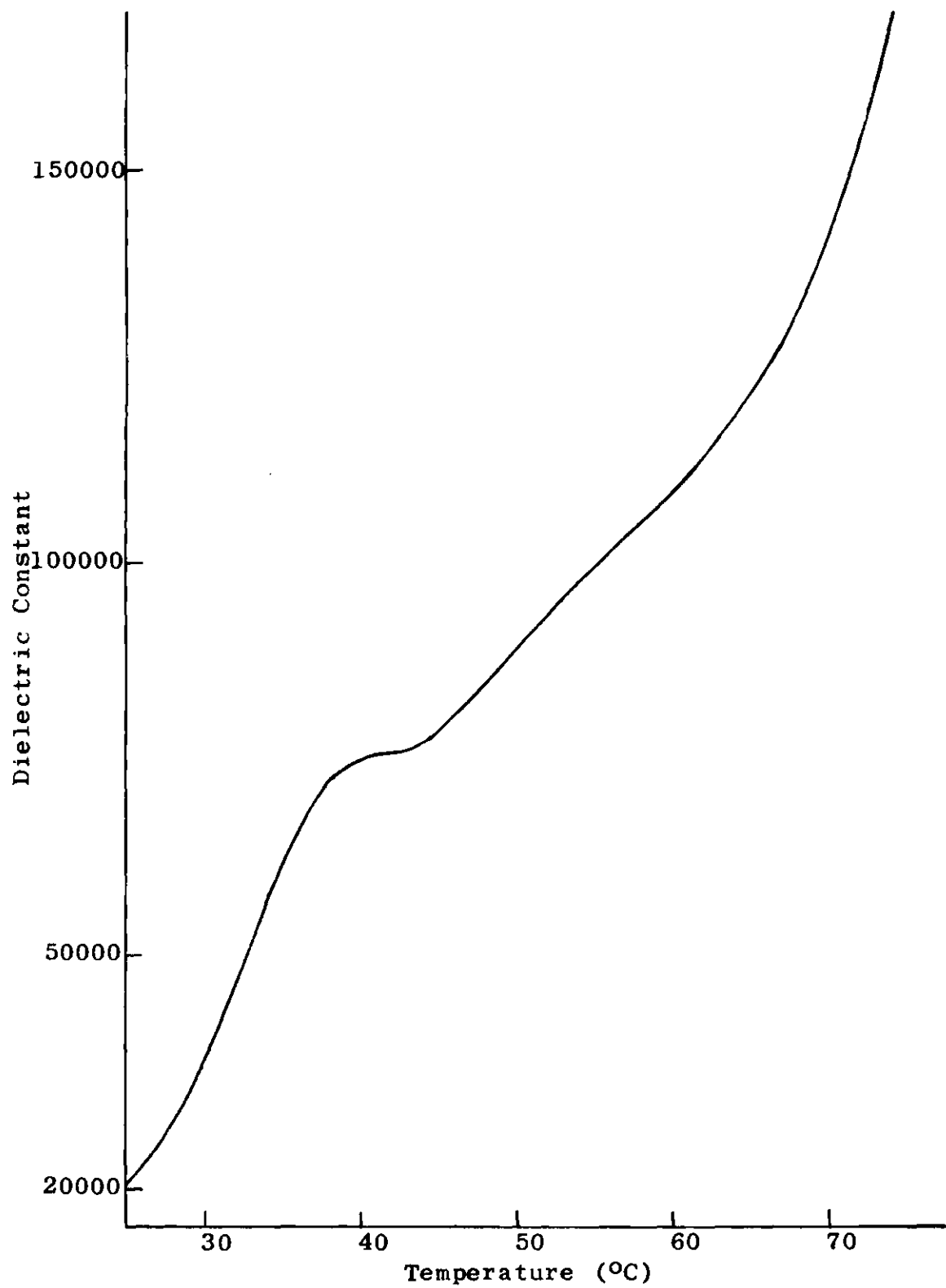
Figure 20.   Dielectric Constant of Sodium DNA

$D = 0.657 \quad d = 0.0569 \quad HC = III$

28 °C

30 °C

1 volt

2 volts

1 volt

2 volts

39 °C

54 °C

1 volt

2 volts

1 volt

2 volts

70 °C

84 °C

1 volt

2 volts

2 volt
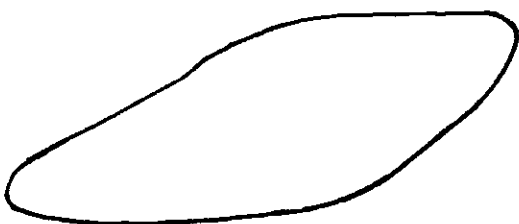
2 volts

Figure 21. Hysteresis Loops of Sodium DNA

ric even though the two temperature ranges do not overlap. Comparison of the dielectric constant curves of RNA at 1000 cps and 100 cps shows that the irregularity not only broadens but actually tends to shift to a slightly higher temperature. A similar shift here of only a few degrees centigrade would be sufficient to have the two temperature ranges overlap.

Polyadenylic Acid Potassium. Figure 22 shows the dielectric constant curve for polyadenylic acid potassium. It is possible to broadly divide this curve into three regions: (1) the slowly increasing portion up to $55^{\circ}C$ or $60^{\circ}C$, (2) the more rapidly increasing portion between $60^{\circ}C$ and $80^{\circ}C$, and (3) the decreasing portion above $80^{\circ}C$. It is to be noted that the dielectric constant maximum value is approximately one forth of the maximum value of most other materials used here in the same temperature range. This is probably due to the greater stability of the double helix caused by the purine-phosphate bonding. The region above $80^{\circ}C$ approximately corresponds to the helix-coil transition (denaturation) temperature. This portion of the curve was included here because the denaturing resulted in a smooth decrease in the dielectric constant. In all the other materials studied, when denaturing occurred, the dielectric constant change was rather abrupt and unsteady. Comparison of these temperature ranges with the hysteresis loops of Figure 23 shows some correlation. The middle temperature range of $60^{\circ}C$ to $80^{\circ}C$ corresponds to loops in the range between $45^{\circ}C$ and $75^{\circ}C$. Above and below

Figure 22. Dielectric Constant of Polyadenylic Acid Potassium

$$D = 0.487 \quad d = 0.0152 \quad HC = II$$
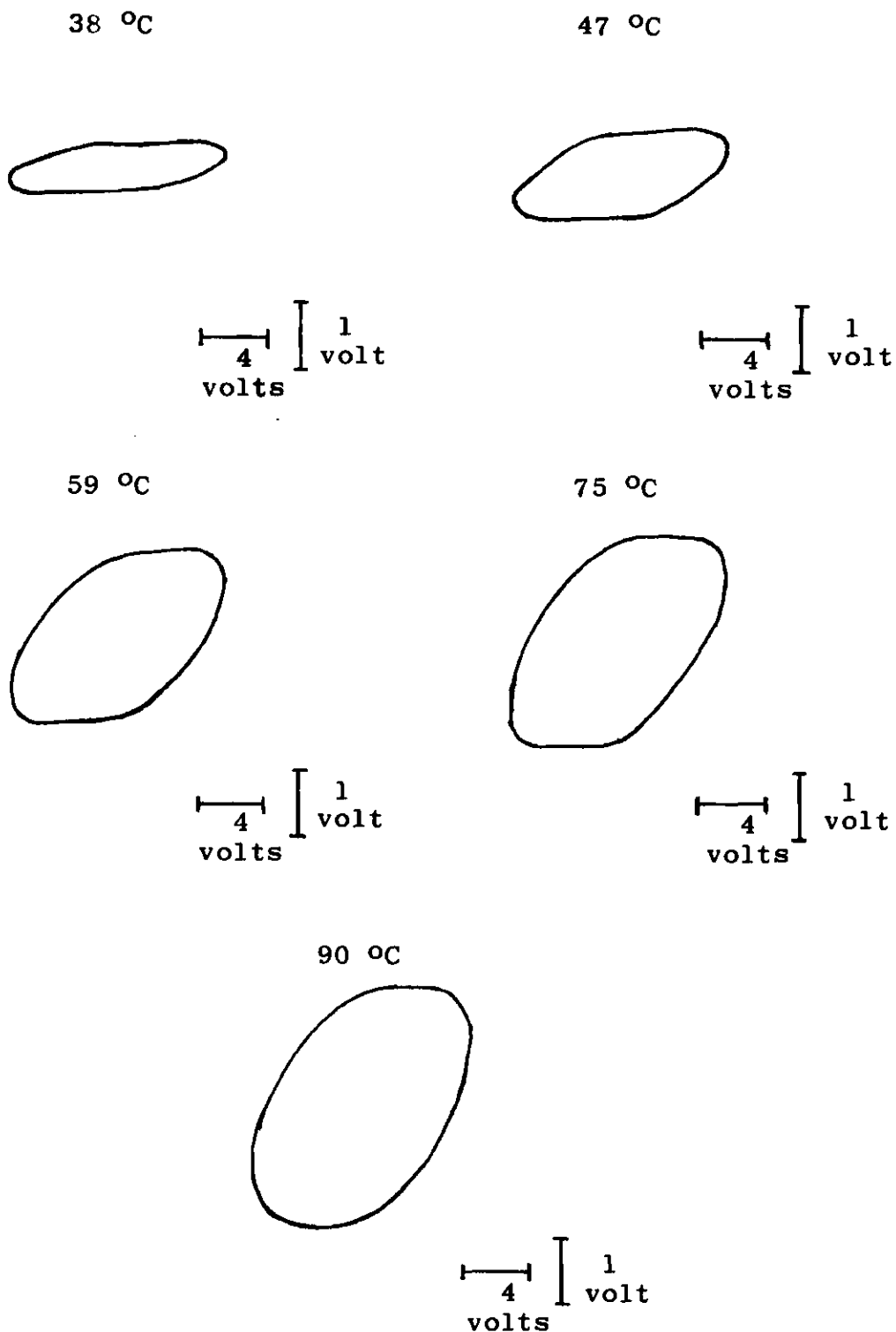
Figure 23.   Hysteresis Loops of Polyadenylic Acid Potassium

this range the loops have less definite hysteresis shape.

Polycytidylic Acid Potassium. A very slight bulge can be observed in the dielectric constant curve of polycytidylic acid in the temperature range of about $50^{\circ}C$ to $70^{\circ}C$ (see Figure 24). Figure 25 shows the hysteresis loops for this material. Below about $40^{\circ}C$ the loops are asymmetric, between $40^{\circ}C$ and $45^{\circ}C$ the loops become symmetric and above $45^{\circ}C$ the loops are again asymmetric but in the opposite direction. This latter region probably results from a combination of the onset of denaturation and increased conductivity of the sample. Any correlation of the change in the shape of the loops to the slight bulge in the dielectric constant curve must be superficial.

Adenylic Acid Sodium. The slight bulge in the dielectric constant curve of adenylic acid at approximately $40^{\circ}C$ as shown in Figure 26 may be related to the change in the hysteresis loops up to $50^{\circ}C$, as seen in Figure 27. The rapid increase in the dielectric constant curve above $55^{\circ}C$ corresponds to the change in the symmetry of the hysteresis loops. These latter changes are probably due again to conductivity and denaturation.

Guanylic Acid Disodium. The bulge in the dielectric constant curve of this purine containing salt, as shown in Figure 28, and the temperature region in which change occurs in the hysteresis loops shown in Figure 29, compare favorably with the similar changes in adenylic acid sodium. Here the
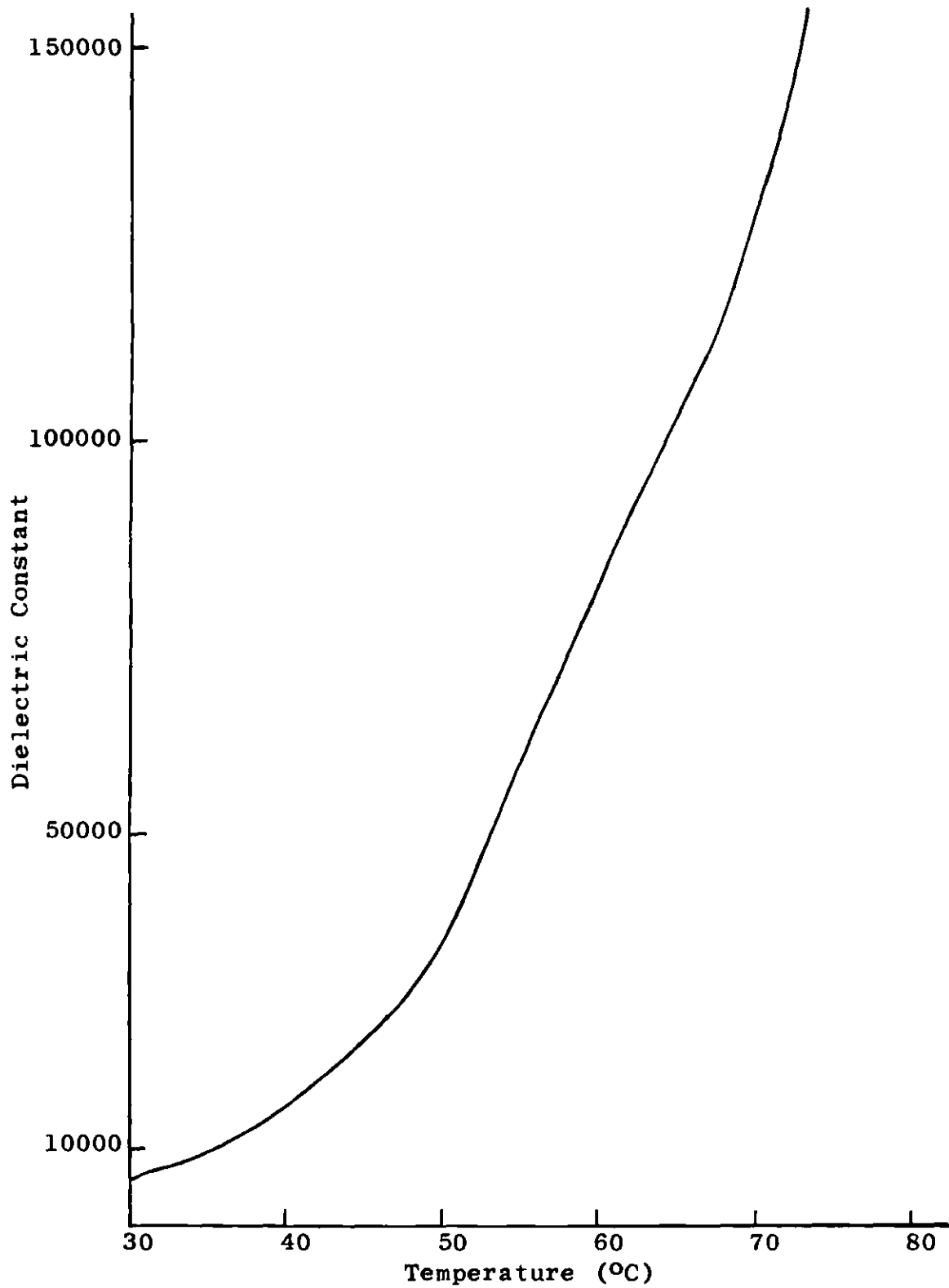
Figure 24. Dielectric Constant of Polycytidylic Acid Potassium

D= 0.657   d= 0.0140   HC= II

33 °C

                    2
    ⊢——⊣ ⌶ volts
      2
    volts

37 °C

                    2
    ⊢——⊣ ⌶ volts
      2
    volts

47 °C

                    2
    ⊢——⊣ ⌶ volts
      2
    volts

57 °C

                    2
    ⊢——⊣ ⌶ volts
      2
    volts

66 °C

                    2
    ⊢——⊣ ⌶ volts
      2
    volts

72 °C
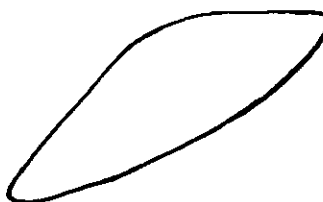
                    2
    ⊢——⊣ ⌶ volts
      2
    volts

Figure 25.   Hysteresis Loops of Polycytidylic Acid Potassium
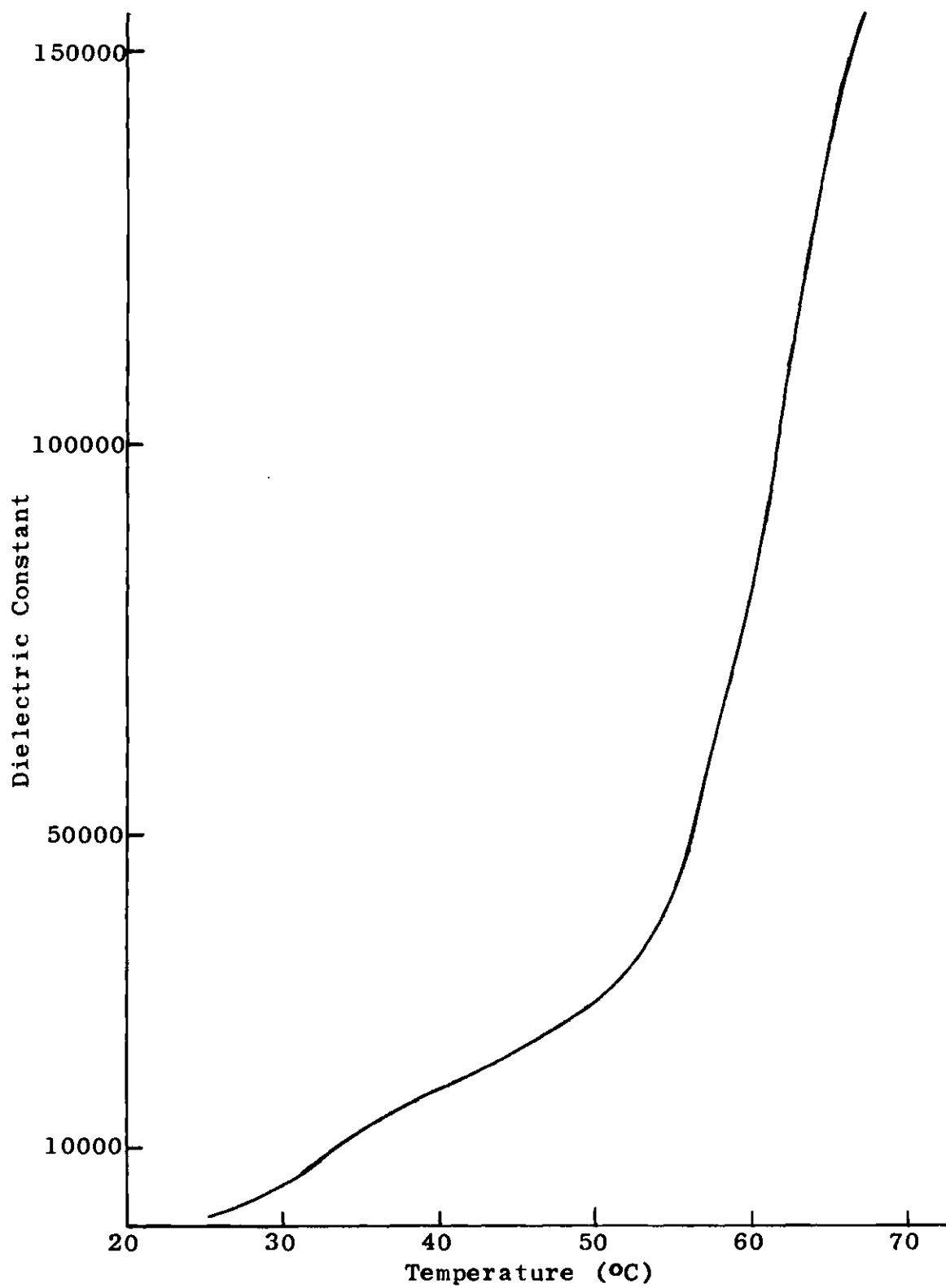
Figure 26. Dielectric Constant of Adenylic Acid Sodium

$$D = 1.03 \quad d = 0.0432 \quad HC = II$$

43 °C

50 °C

10
10
volts
volts

10
10
volts
volts

58 °C

71 °C

10
10
volts
volts

10
10
volts
volts

83 °C

90 °C

10
10
volts
volts
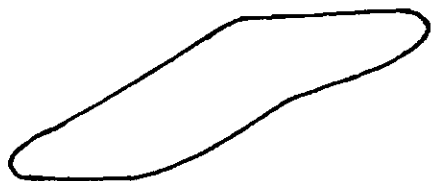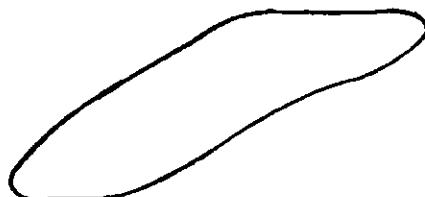
10
10
volts
volts

Figure 27. Hysteresis Loops of Adenylic Acid Sodium
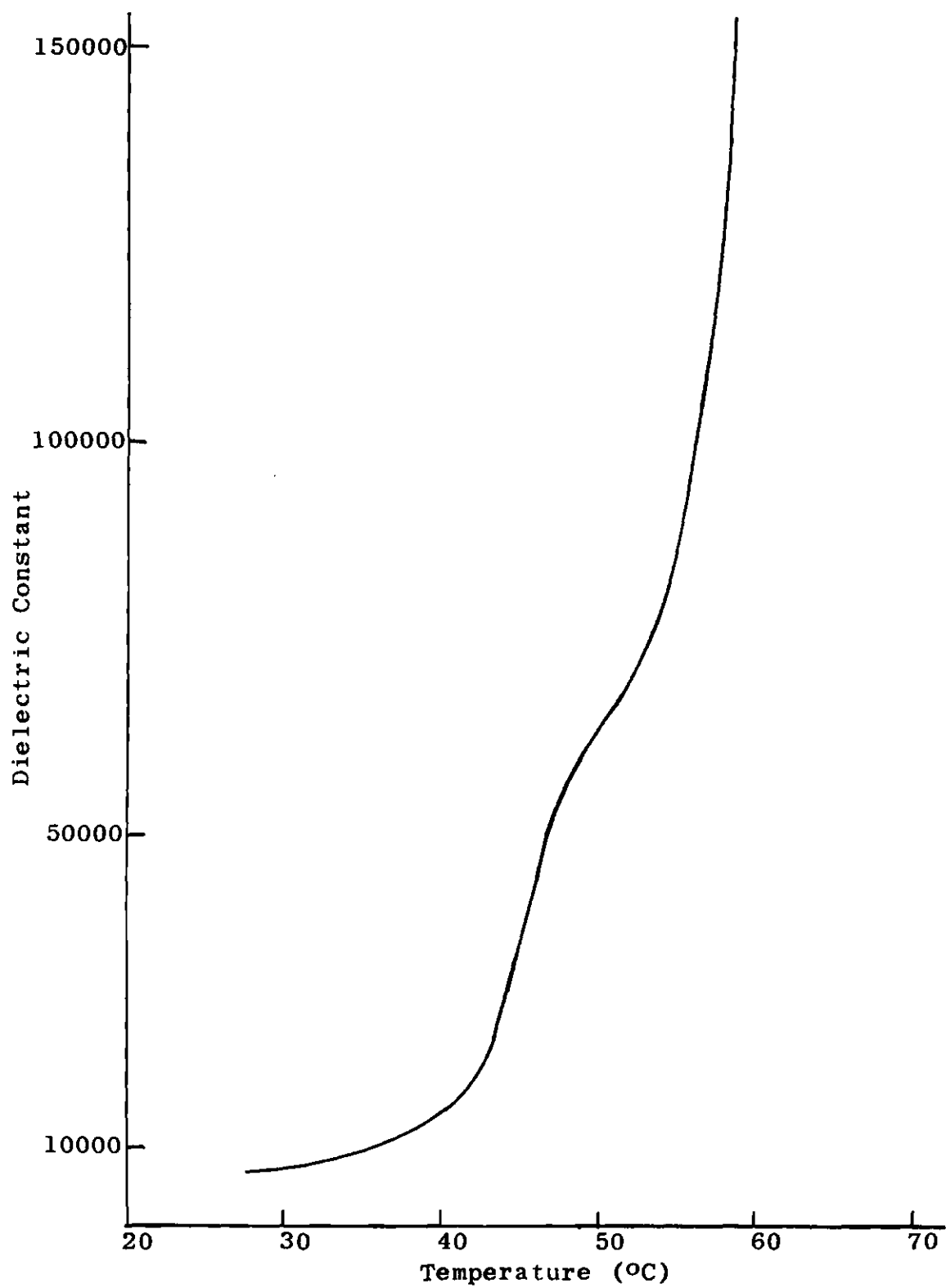
Figure 28. Dielectric Constant of Guanylic Acid Disodium

$$D = 0.228 \quad d = 0.0102 \quad HC = II$$

42 $^{\text{o}}$C
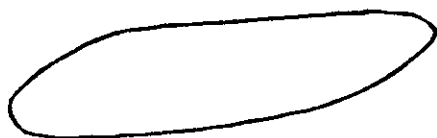
49 $^{\text{o}}$C

0.1
volts

4
volts

0.1
volts

4
volts

58 $^{\text{o}}$C

70 $^{\text{o}}$C

0.2
volts

4
volts

0.4
volts

4
volts

80 $^{\text{o}}$C

1
volt

4
volts
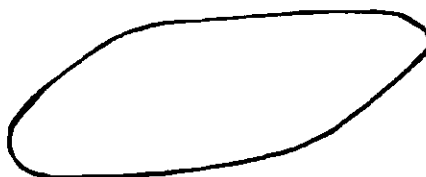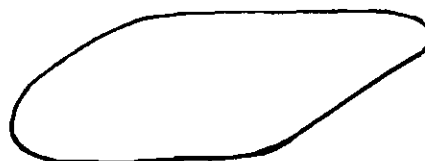
Figure 29. Hysteresis Loops of Guanylic Acid Disodium

bulge occurs closer to 45°C, the increase in the dielectric constant above the bulge is more rapid and the hysteresis loops become asymmetric rather than symmetric. However, in a general way guanylic acid disodium and adenylic acid sodium behave similarly.

Cytidylic Acid Disodium. The dielectric constant curve of cytidylic acid shown in Figure 30, shows a very smooth increase with no irregularities. The value of the dielectric constant does not become appreciable until approximately 65°C and then increases rapidly within a range of 15 degrees. This may be correlated to the hysteresis loops of Figure 31 which shows symmetric loops only in the range between 70°C and 80°C.

Thymidylic Acid Sodium. Figure 32 is the dielectric constant curve for this material and the curve has the same general shape as that for cytidylic acid disodium. The hysteresis loops of Figure 33 are of poor quality but can be related to the dielectric constant curve in the same manner as was done with cytidylic acid disodium. Hence the pyrimidine containing salts, like the purine containing salts, behave similarly.

Pressed Wafer Dielectric Constants. It was not possible to obtain hysteresis loops with any of the materials in the pressed wafer form. This was probably due to the extremely small crystallites and the masking effect of entrapped air. Figures 34 and 35 show the dielectric constant curves of adenylic acid sodium and uridylic acid disodium respectively. It was not possible to obtain similar curves for the pressed
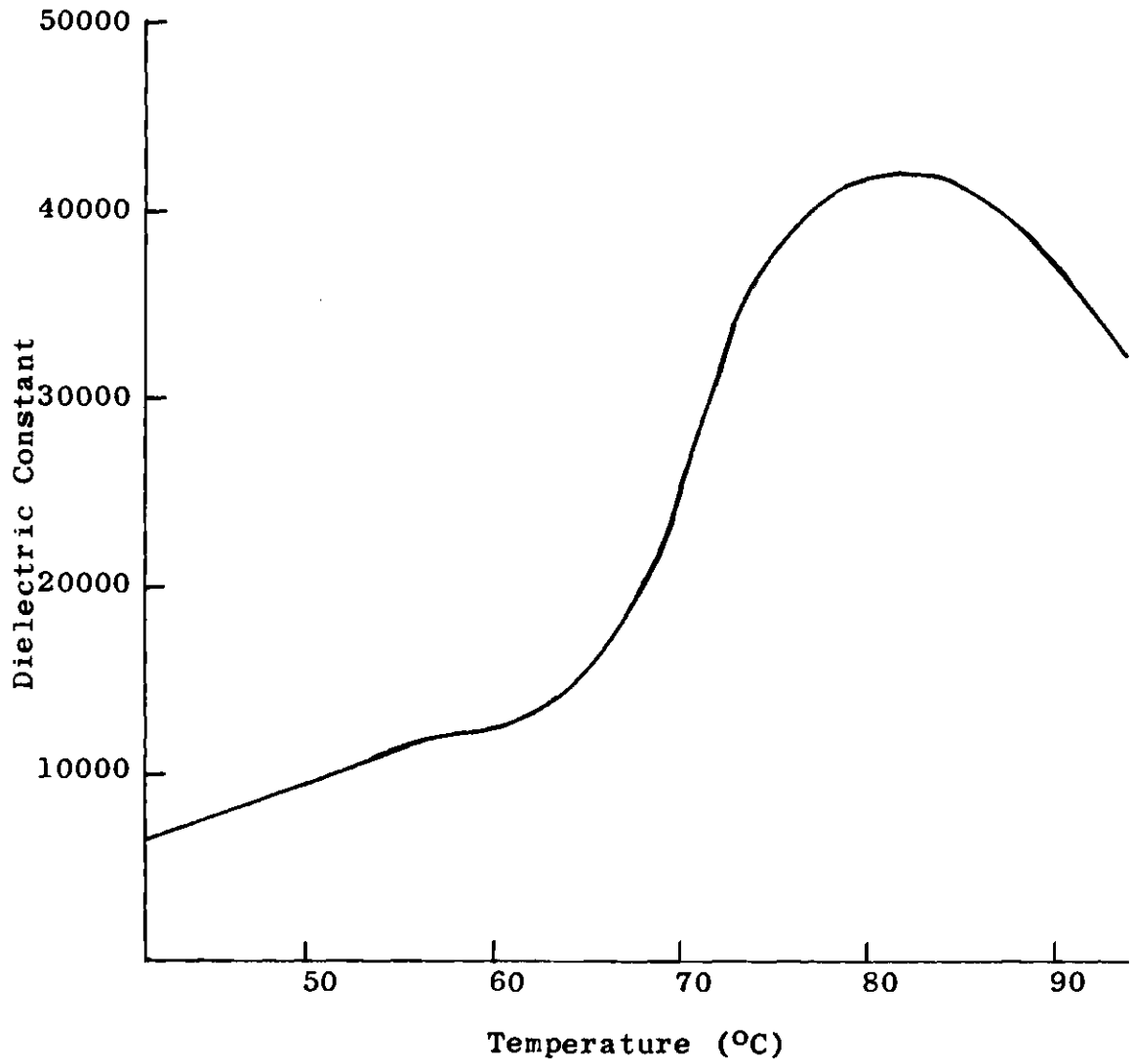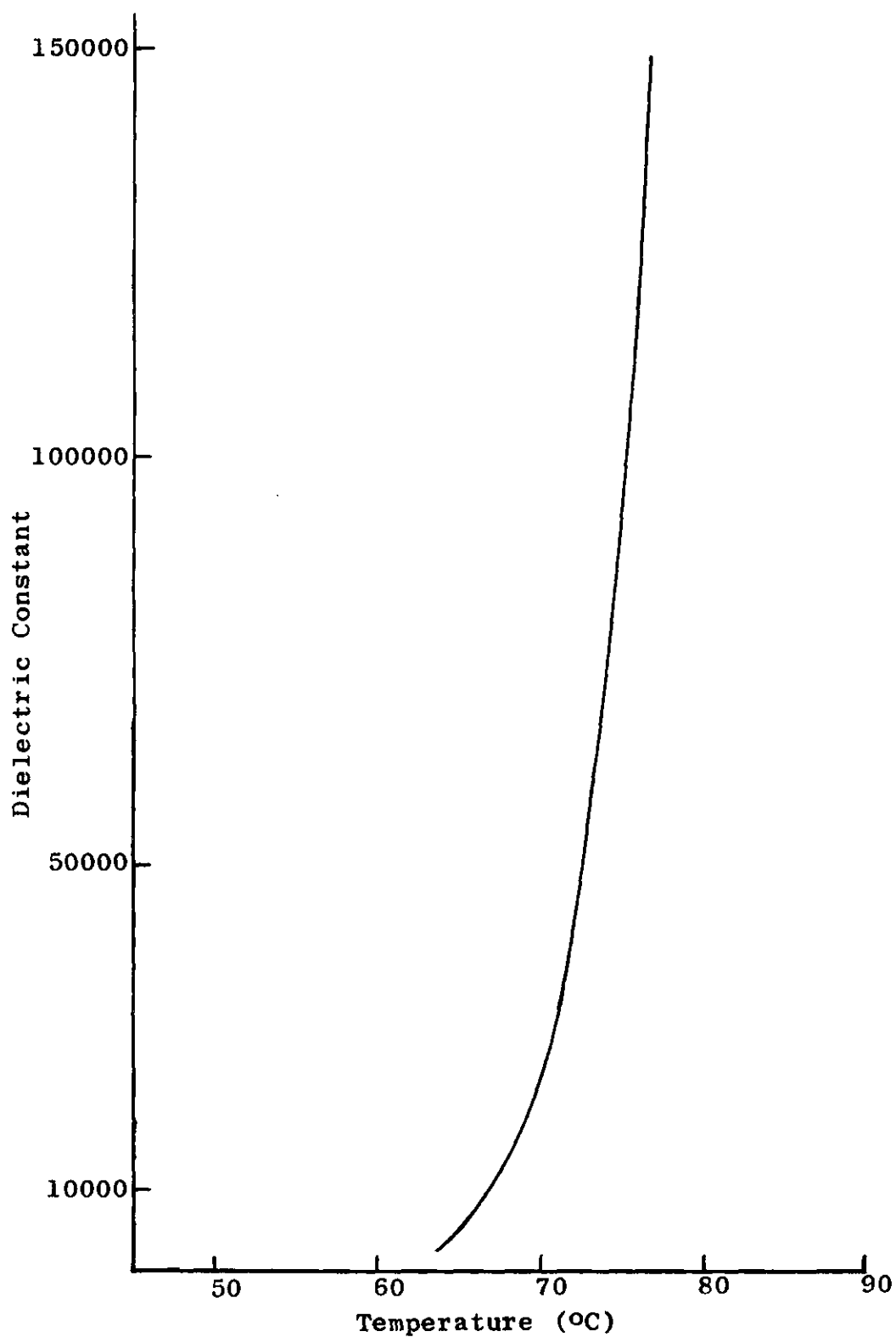
Figure 30. Dielectric Constant of Cytidylic Acid Disodium

$$D = 0.657 \quad d = 0.107 \quad HC = II$$
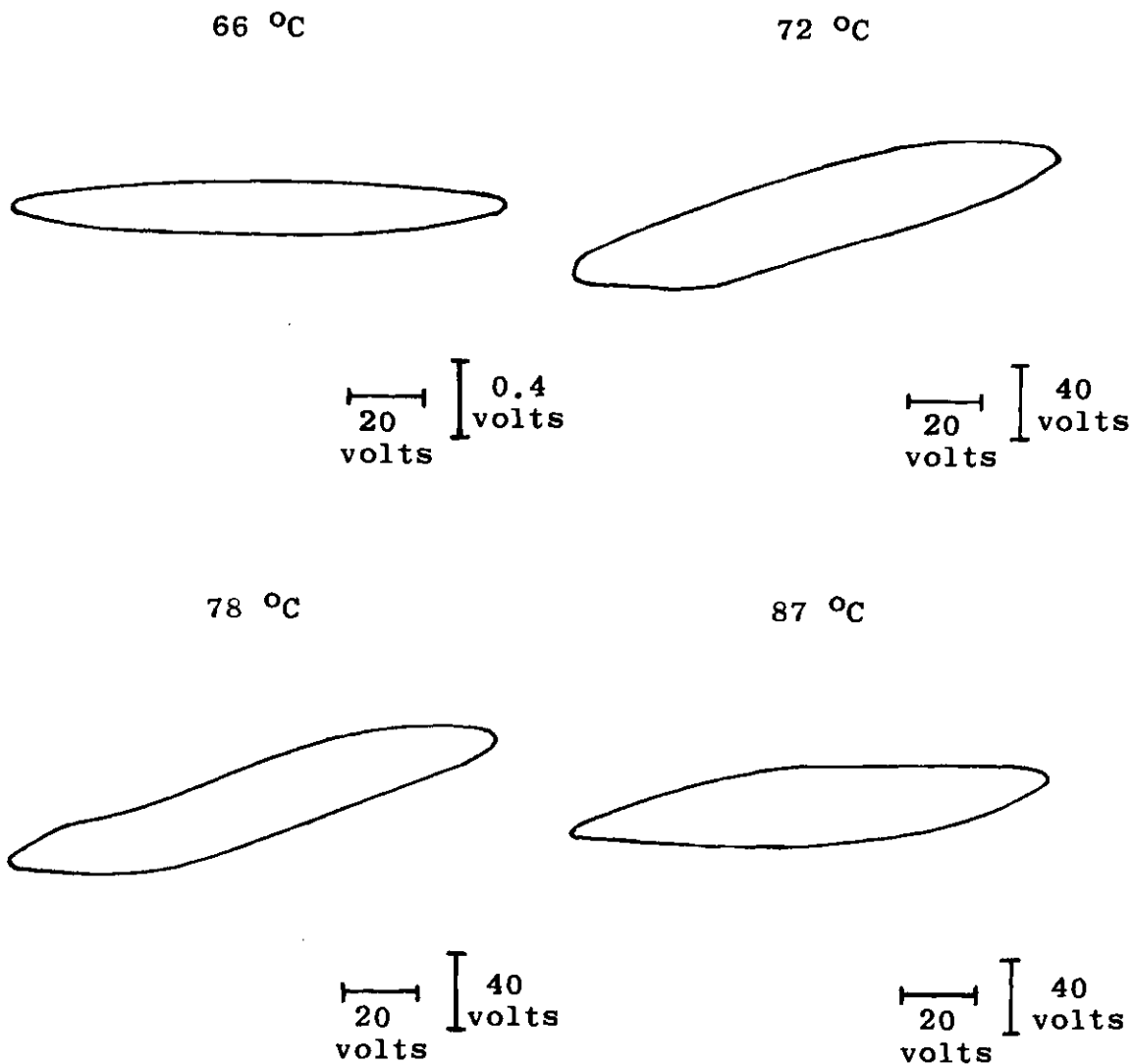
Figure 31. Hysteresis Loops of Cytidylic Acid Disodium
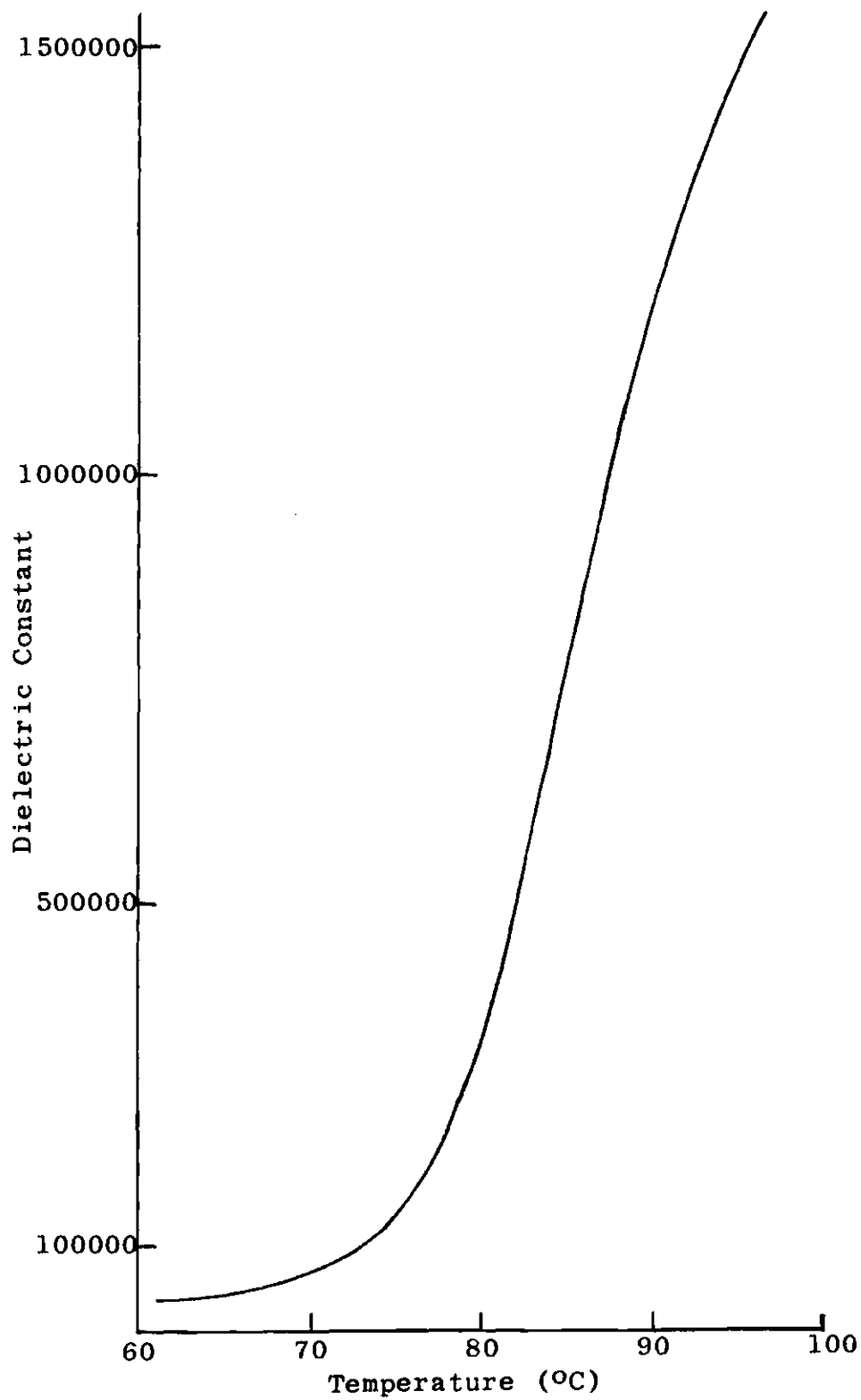
Figure 32. Dielectric Constant of Thymidylic Acid Sodium

D = 0.228   d = 0.0330   HC = II

55 °C

62 °C

┌─┐
├─┤] 2
  4   ] volts
volts

┌─┐
├─┤] 1
  4   ] volt
volts

67 °C

90 °C

┌─┐
├─┤] 0.4
  4   ] volts
volts

┌─┐
├─┤] 0.4
  4   ] volts
volts
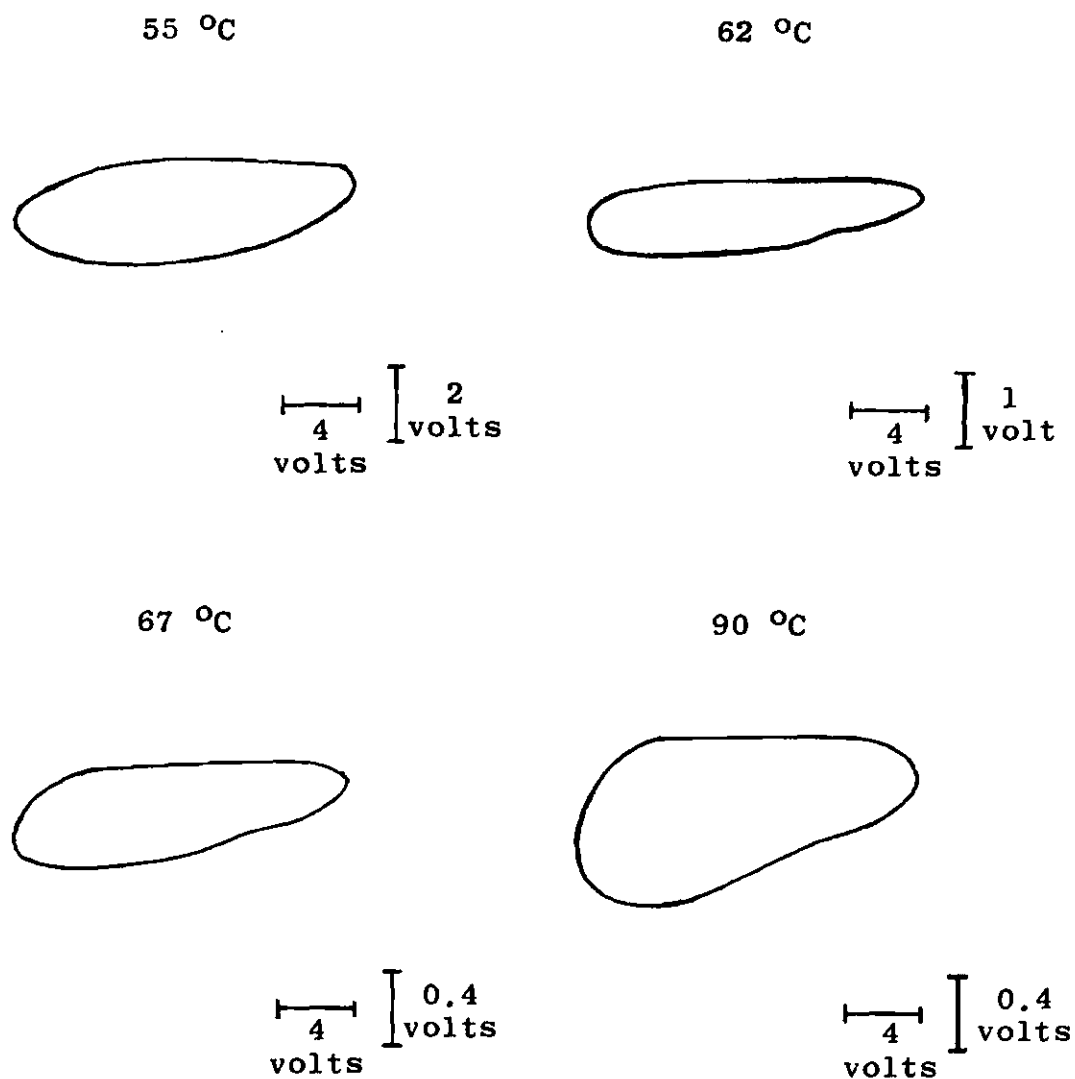
Figure 33.   Hysteresis Loops of Thymidylic Acid Sodium
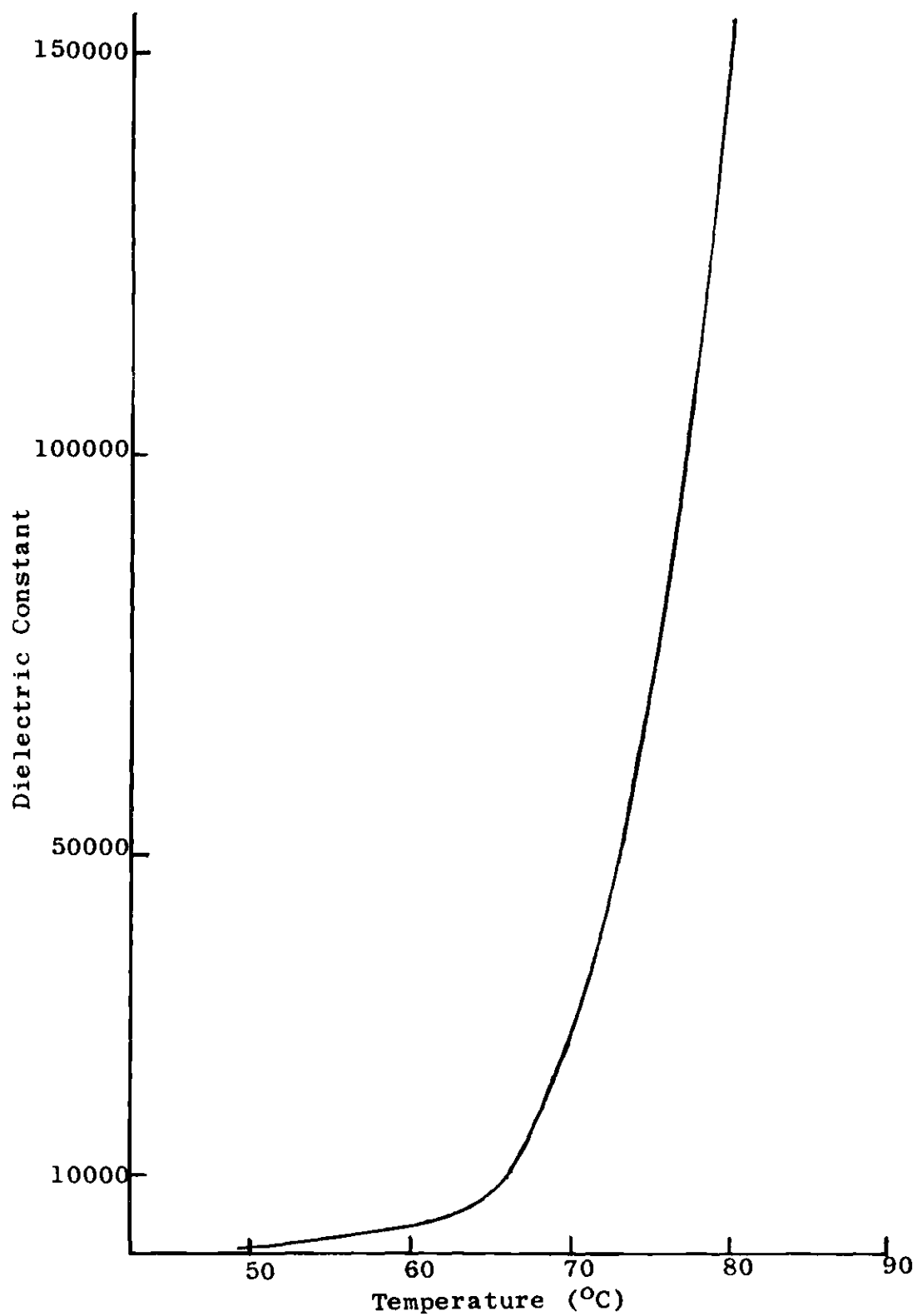
Figure 34. Dielectric Constant of Adenylic Acid Sodium Wafer
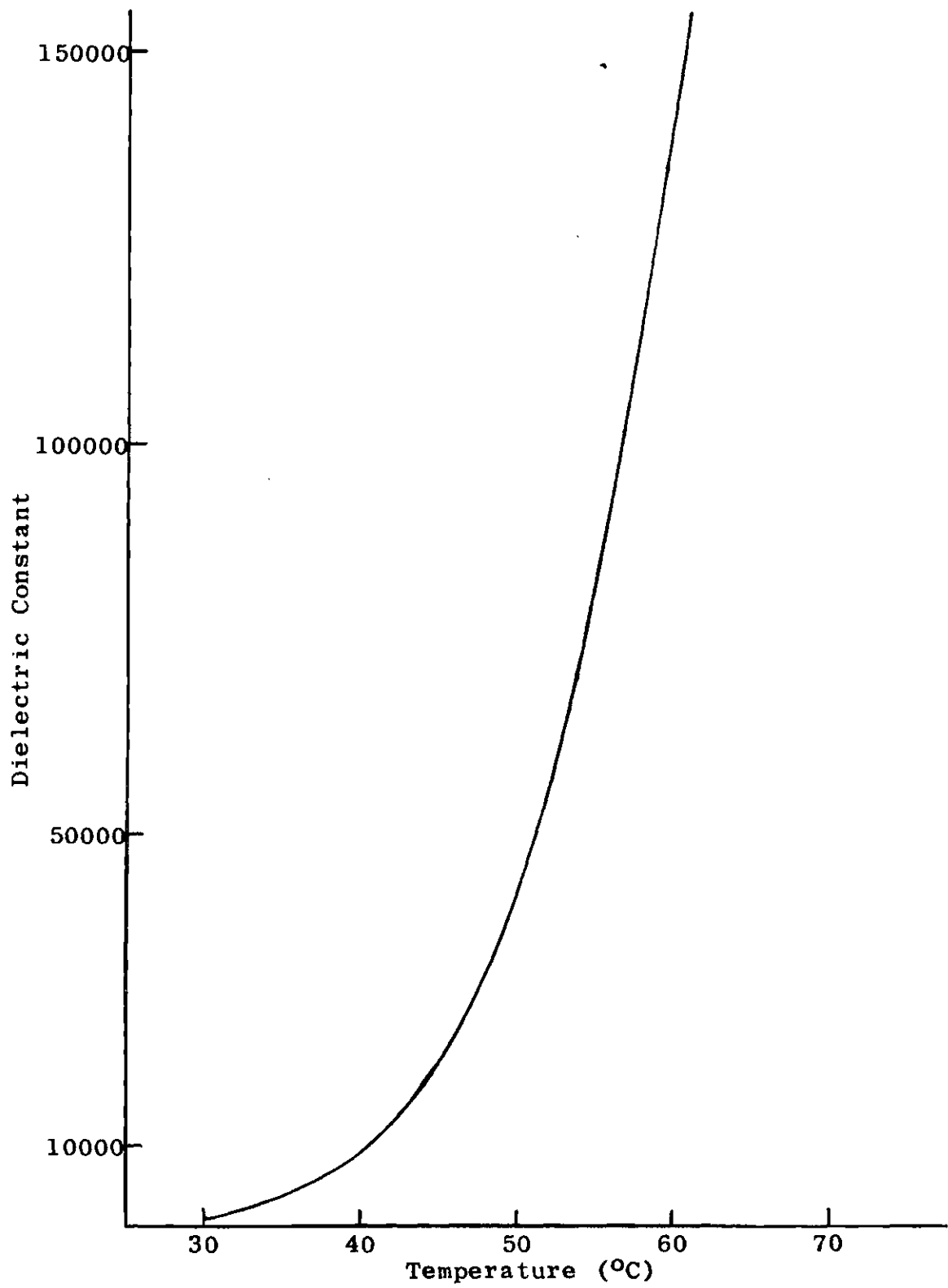
Figure 35. Dielectric Constant of Uridylic Acid Disodium Wafer

wafer of either adenosine or adenine. Over the temperature range used, approximately $25^{O}C$ to $100^{O}C$, the dielectric constants of adenosine and adenine remained extremely small.

The ferroelectric hysteresis of the materials studied here may arise from the permanent dipoles of the sugar, phosphate and bases, the various hydrogen bonds, or a combination of these sources. In the case of DNA the hydrogen bonds between the two strands may be responsible for the ferroelectricity, but if this is the sole source, single stranded RNA should not be ferroelectric (24). It has been proposed that the ferroelectric hysteresis of RNA is due to the stacking of bases but this explanation may not be adequate to explain the ferroelectricity of the smaller molecules such as adenylic acid (24). The ferroelectricity of the materials studied here probably arises from a combination of the permanent dipoles of the molecules and the hydrogen bonds. However, it is likely that the main contribution of the ferroelectricity originates in the phosphate group. This can be seen by considering the following: (1) the phosphate group is the most polar part of the sodium DNA molecule and hence also of the nucleotides (18), (2) the essential difference between adenosine and adenylic acid is the lack of a phosphate group in adenosine, as indicated by Figures 4 and 5, and (3) the dielectric constant of the pressed wafer of adenylic acid sodium is quite large and increases greatly with increasing temperature while the dielectric constant of the pressed wafer of adenosine

remains quite small in the same temperature range. Further-
more, it has been reported that the phosphate groups in these
biological molecules have a tetrahedral arrangement (20,21,25).
This information is pertinent since a partially successful
theory by Slater (1941) bases the ferroelectricity of KH_2PO_4
on the orientation of the $(H_2PO_4)^-$ dipoles, where the oxygen
atoms are located at the corners and the phosphorus atoms at
the centers of tetrahedra which are hydrogen bonded to one
another (26). The hydrogens do not lie midway between oxygen
atoms but rather may exist in crystallographically non-equiv-
alent positions with different energies. Thus an explanation
of the ferroelectricity of these biological molecules based
on the orientation of phosphate group dipoles is entirely
plausible.

CHAPTER V

CONCLUSIONS AND RECOMMENDATIONS

It is advisable to briefly review the nature of the molecules studied here. The five nucleic acid bases consist of two purines, adenine and guanine, and three pyrimidines, cytosine, thymine and uracil. A nucleoside is the combination of any base and a pentose sugar. The nucleoside is a riboside or a deoxyriboside depending on whether the sugar is ribose or deoxyribose respectively. The nucleosides are adenosine, guanosine, cytidine, thymidine and uridine. The molecule formed from a bonding of a phosphoric acid molecule to the sugar molecule of a nucleoside is a nucleotide. The pentose sugar determines if these are ribonucleotides or deoxyribonucleotides. The nucleotides are adenylic acid, guanylic acid, cytidylic acid, thymidylic acid and uridylic acid. Of the nucleotides used here, only thymidylic acid is a deoxyribonucleotide. The bonding of nucleotides, phosphate group to sugar group, into chains result in either RNA or DNA. If only one type of nucleotide forms a chain, the result is a polyribonucleotide or a polydeoxyribonucleotide. In this work the sodium or potassium salts of the various acids were utilized.

Samples of a crystal nature were obtained for the salts of RNA, DNA, adenylic acid, guanylic acid, cytidylic acid

thymidylic acid, polyadenylic acid and polycytidylic acid. Evaporation of aqueous solutions of the salts produced these samples. Unsaturated hysteresis loops were observed for all these materials. Furthermore, they displayed increasing dielectric constants with increasing temperature which is characteristic of many ferroelectric materials.

A lower transition point seems to exist for sodium RNA although this effect may be due to a lowering of the value of the coercive field. Irrespective of this, the ferroelectric character of RNA has been demonstrated for the first time. The sequence of the nucleotides in the macromolecules does not affect their dielectric properties since RNA, DNA, poly-adenylic acid and polycytidylic acid all exhibit this ferro-electric character. Ferroelectric behavior was observed in specimens containing: (1) ribose sugar, RNA, polyadenylic acid, polycytidylic acid, adenylic acid, guanylic acid and cytidylic acid, and (2) deoxyribose sugar, DNA and thymidylic acid. Hence, the type of pentose sugar present does not sig-nificantly affect the ferroelectricity of these materials. Since the purine nucleotides and pyrimidine nucleotides all appear to be ferroelectric, and since the dielectric proper-ties of the purine nucleotides are similar and the pyrimidine nucleotides are similar, this property is independent of the type of base present. Comparison of the ferroelectric prop-erties of adenylic acid and polyadenylic acid, and cytidylic acid and polycytidylic acid, indicates that the length of the

molecule is not a determining factor of the ferroelectricity of the molecule. In summary, the existance of ferroelectricity in the nucleic acids appears to be independent of the type of pentose sugar present, the types of bases present, the sequence of bases and the length of the molecule. Hence, one might speculate that in a living system, the ferroelectricity of the nucleic acids is not confined to any particular type of nucleic acid.

It was not possible to obtain samples of a crystal nature for adenine, adenosine or uridylic acid disodium. Wafers were made of the powdered material using a hydraulic press. For comparison purposes, wafers were also made of adenylic acid sodium. Hysteresis was not observed for any of these materials in the wafer form. The dielectric constants of the wafers of adenylic acid sodium and uridylic acid disodium both exhibit the characteristic behavior of many ferroelectric materials. However, it is not possible to say that uridylic acid disodium is ferroelectric. The dielectric constants of the wafers of adenine and adenosine did not show any characteristic ferroelectric behavior and were quite small. The results of the dielectric constant measurements of adenine and the adenine containing nucleoside and nucleotide, suggest that the phosphate group is the origin of the ferroelectricity of the materials studied here.

From the results of this work and from the conclusions reached, the following recommendations are made: (1) Ferro-

electric and pyroelectric studies should be made on the fiber form of the nucleic acids and polynucleotides, and on single crystals of the nucleotides and salts of these materials. These forms of the materials should result in better defined hysteresis loops which indicate saturation. (2) Studies should be made of the nucleosides and nucleotides to test whether or not the phosphate group is the origin of the ferroelectricity. Furthermore, deuterated nucleotides should be studied to determine the effect of the hydrogen bonds on the ferroelectricity. (3) Controlled humidity and temperature experiments should be performed to determine the effect of these on the electrical properties and on the crystal structure. Any observed effects may be useful in determining the nature of any transition which might occur.

APPENDIX A

DIPOLES AND FERROELECTRICITY

In attempting to describe or determine the origin of the ferroelectricity of some material it is desirable to associate dipoles with the molecules of the material. This is true since many theoretical works on ferroelectricity have dipole orientation as their basis. However, it is not always possible to select pairs of equal and opposite charges with associated dipole moment given by the product of charge and separation. In the case of non-molecular crystals where atoms are linked in a three dimensional array it may be unreasonable to ascribe special associations between specific pairs of atoms. These pairs may not retain any special relationship with respect to their neighbors since all atoms may be symmetrically related. An example of this is sodium chloride where each atom of sodium is associated with six atoms of chlorine and each chlorine atom is associated with six sodium atoms.

Dipole identification in many instances is not only possible but also quite reasonable. Two cases where it might be possible to ascribe dipoles to a particular substance, not necessarily ferroelectric, are: (1) in an ionic crystal when application of an electric field causes separa-

tion of charges within each ion and (2) in a crystal which contains molecules which may be dipoles and are free to rotate with respect to the rest of the structure. In the case of some ferroelectrics, it may be possible to assign dipoles on the basis of both electrical and crystallographical information. Such an assignment is possible in the case of KH_2PO_4. The phosphorus and oxygen atoms form a tetrahedron with the oxygen atoms at the corners and the phosphorus atom at the center. Each tetrahedra is hydrogen bonded to four others. An assumption is made that each tetrahedra has only two hydrogens near it, the other two hydrogens being nearer other tetrahedra. This assumption makes the $(H_2PO_4)^-$ group an electric dipole (12). Finally, in the case of $BaTiO_3$ the dipole is assigned to the octahedron formed with oxygen at its corners and the off centered positioned titanium atom (12).

APPENDIX B

SAWYER-TOWER CIRCUIT WITH LINEAR ELEMENTS

Figure 36 shows three Sawyer-Tower circuits containing ideal linear elements. C_x and C_o are capacitances, R_x is a resistance, V_o is the voltage across C_o and V_{in} is the input voltage which is assumed to be sinusoidal and given by

$$V_{in} = E_o \sin \omega t \ , \tag{19}$$

where E_o is a magnitude, ω is the angular frequency and t is the time.

An oscilloscope is usually employed to display voltage when using the Sawyer-Tower circuit. The input voltage V_{in} of the circuit is the horizontal input to the oscilloscope. Thus, the x coordinate of the trace on the oscilloscope is just the value V_{in} and is given by the equation

$$x = E_o \sin \omega t \ . \tag{20}$$

The vertical input to the oscilloscope is the voltage V_o, which is the y coordinate of the trace on the oscilloscope. The equation of the oscilloscope trace may be obtained by relating x and y. The voltage V_o is just the product of the input voltage V_{in} and the ratio of the impedance of C_o
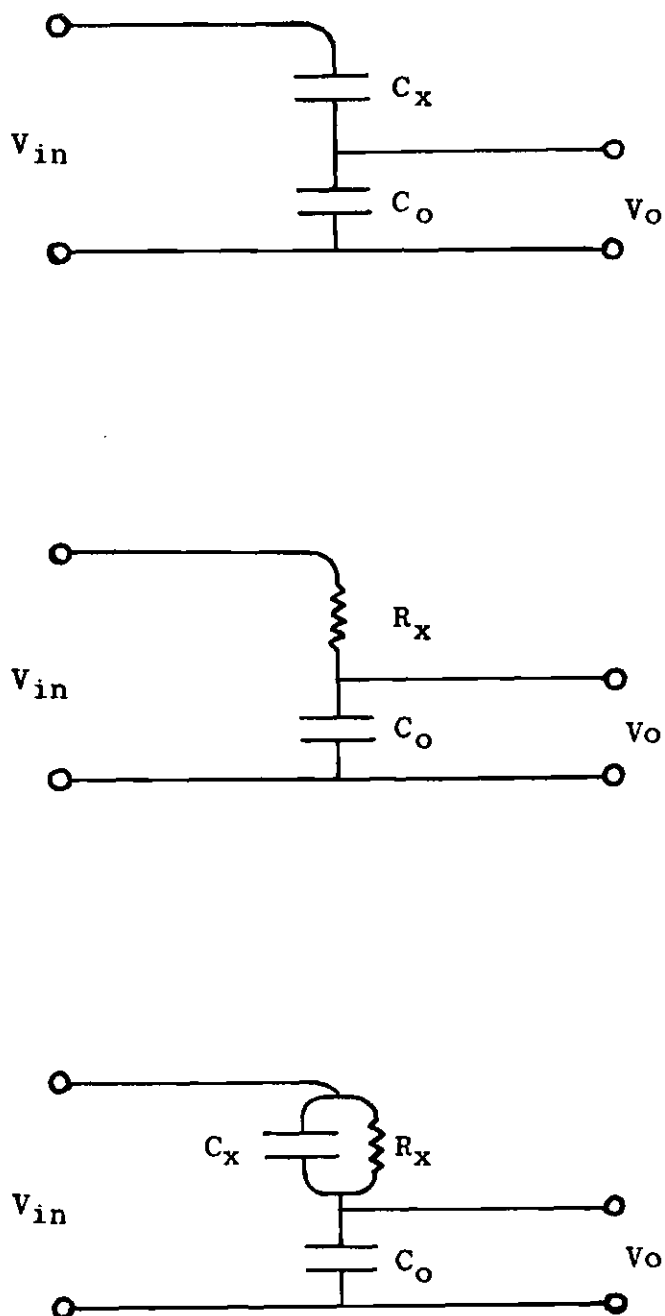
Figure 36. Sawyer-Tower Circuit with Linear Elements

to the total impedance.

Impedances may be written as complex exponentials and this practice will be followed here. In the following, the letter Z stands for impedance. The impedance of C_O may be written as

$$Z_O = (1/\omega C_O)\exp(-i\pi/2) \ . \tag{21}$$

The impedance of C_X is

$$Z_X = (1/\omega C_X)\exp(-i\pi/2) \ . \tag{22}$$

The impedance of R_X is just the value of the resistance, and the impedance of R_X in parallel with C_X is

$$Z_X = (1/R_X^2 + \omega^2 C^2)^{-\frac{1}{2}}\exp(-i\theta) \ , \tag{23}$$

where θ is related to ω, R_X and C_X by the equation

$$\tan\theta = \omega R_X C_X \ . \tag{24}$$

For the circuit containing the two capacitances C_O and C_X, the total impedance is

$$Z = ((C_O + C_X)/\omega C_O C_X)\exp(-i\pi/2) \ . \tag{25}$$

The voltage V_O, and hence coordinate y, is then given by

$$V_O = (C_x/(C_O + C_x))E_O \sin \omega t . \tag{26}$$

Equation (20) may be used to eliminate $\sin \omega t$ from Equation (26) and the result, relating y and x, is

$$y = (C_x/(C_O + C_x))x \tag{27}$$

which is the equation of a straight line.

For the circuit containing R_x and C_O, the total impedance is

$$Z = (R_x^2 + 1/\omega^2 C_O^2)^{\frac{1}{2}} \exp(-i\phi) , \tag{28}$$

where ϕ is related to ω, R_x and C_O by the equation

$$\tan \phi = 1/\omega R_x C_O . \tag{29}$$

The voltage V_O is then given by the equation

$$V_O = KE_O(\sin \omega t \cdot \sin \phi - \cos \omega t \cdot \cos \phi) , \tag{30}$$

where K is a constant given by the equation

$$K = (1/\omega C_O)/(R_x^2 + 1/\omega^2 C_O^2)^{\frac{1}{2}} . \tag{31}$$

Use of Equation (20) and the substitution of y for V_O yields the following expression

$$K^2x^2 - 2K\sin\phi\, xy + y^2 - K^2\cos^2\phi\, E_O^2 = 0 \ . \tag{32}$$

Equation (32) is of the form

$$Ax^2 + Bxy + Cy^2 + Dx + Ey + F = 0 \ , \tag{33}$$

which is an equation of an ellipse or its degenerate case if the inequality

$$B^2 - 4AC < 0 \tag{34}$$

is satisfied (27). Substitutions from Equation (32) yields

$$B^2 - 4AC = 4K^2\sin^2\phi - 4K^2 = 4K^2(\sin^2\phi - 1) \ . \tag{35}$$

From Equation (29), $\sin\phi$ may be expressed as

$$\sin\phi = (1/\omega C_O)/(R_X^2 + 1/\omega^2 C_O^2)^{\frac{1}{2}} \ . \tag{36}$$

Since the resistance is non zero by assumption, $\sin\phi$ can not be equal to one. Hence, since K is positive, the inequality is satisfied and the oscilloscope trace is an ellipse or its degenerate case.

For the circuit containing R_x, C_x and C_o, the resulting equation relating x and y is identical in form to Equation (32) but with K given by

$$K = (1/\omega C_o)/(a^2 + b^2)^{\frac{1}{2}} \qquad (37)$$

and with ϕ expressed by the relation

$$\tan \phi = b/a , \qquad (38)$$

where b is given by

$$b = (1 + \omega^2 R_x^2 C_x^2 + \omega^2 R_x^2 C_x C_o)/\omega C_o(1 + \omega^2 R_x^2 C_x^2) \qquad (39)$$

and a is given by

$$a = R_x/(1 + \omega^2 R_x^2 C_x^2) . \qquad (40)$$

The inequality given above is satisfied here just as in the case of the circuit containing only R_x and C_o. In this case the equation analogous to Equation (36) would require either ω , R_x or C_o to be zero in order that $\sin \phi$ would equal one. Since none of these are zero by assumption, the resulting trace is an ellipse or its degenerate case.

APPENDIX C

SAMPLE CHARACTERISTICS

This appendix consists of tables describing the characteristics of the samples used in this research. It is to be noted here that the drying of cytidylic acid disodium occurred at room temperature, not at five degrees centigrade. The water content refers to the amount of water initially added to obtain the solution and not the final water content of the samples. In the cases of the polyribonucleotides and guanylic acid disodium, as water from the sample cup evaporated more solution was added in order to obtain samples of sufficient thickness.

Table 2. Sample Characteristics

Material	Mass grams	Water Content cc	Drying Time days	Physical Appearance After Drying
Adenylic Acid Sodium	2.0	2.0	7-8	Transparent, colorless, multi-cracked, single piece
Cytidylic Acid Disodium	2.0	2.0	5-6	Transparent, colorless, single aggregate of needle shaped fibers
Guanylic Acid Disodium	2.0	36.0	1-2	Translucent, white, single piece, brittle, uncracked
Thymidylic Acid Sodium	1.0	1.0	7-8	Transparent, slightly yellow, cracked into many small pieces
Sodium DNA	5.0	7.0	1-2	Transparent, brown, cracked into irregular sizes and shapes
Sodium RNA	5.0	8.0	1-2	Transparent, brown cracked into irregular sizes and shapes
Poly-adenylic Acid Potassium Lyophilized	1.0	100	4-5	Translucent, white single piece, not brittle, uncracked
Poly-cytidylic Acid Potassium Lyophilized	0.50	35	4-5	Transparent, colorless, single piece, not brittle, uncracked

Table 3. Wafer Characteristics

Material	Mass grams	Pressure Applied to Form Wafers psi
Adenine	1.0	45000
Adenosine	1.0	45000
Adenylic Acid Sodium	1.0	45000
Uridylic Acid Sodium	1.0	45000

APPENDIX D

DIELECTRIC CONSTANT COMPILATION

The tables in this appendix contain the data of the dielectric constant curves appearing both in this appendix and in Chapter IV. The heading in the tables labled "Figure Number" correlates each dielectric constant curve to a particular listing in the tables. The heading, "Heating Curve", refers to the curves of Figure 14. The measuring voltage V is the voltage applied across the series combination of C_0 and the sample capacitance. The maximum electric field is the approximate field applied to the sample during the time when the sample capacitance is much less than the capacitance of C_0. Unless otherwise stated the measuring frequency is 1000 cycles per second.

Table 4. Dielectric Constant of Sodium Ribonucleate

Figure Number	15		37		38	
Heating Curve	II		II		II	
Electrode Area A cm^2	0.340		0.340		0.186	
Area Diameter D cm	0.657		0.657		0.487	
Sample Thickness d cm	0.0456		0.0438		0.0394	
Ratio D/d	14.1		15.0		16.7	
Measuring Voltage V volts	0.63		0.63		0.63	
Maximum Electric Field V/d volts/cm	13.5		14.4		16.0	

Temperature $^{\circ}$C	ϵ	Percent Error $\pm$	ϵ	Percent Error $\pm$	ϵ	Percent Error $\pm$
25	8800	20	11000	20		
30	14500	17	16700	17	12600	17
35	23000	15	27000	15	22000	15
40	38700	15	43000	15	35000	15
45	61800	15	68000	15	55500	15
50	99000	12	108000	12	89400	14
51	107000	12	113000	12	95300	12
52	112000	12	115000	12	100000	12
53	114000	12	114000	12	103000	12
54	114000	12	111000	12	102000	12
56	107000	12	104000	12	94800	12
58	103000	12	101000	12	90000	12
60	101000	12	101000	12	87500	14
62	106000	12	105000	12	87300	14
65	119000	12	118000	12	93000	12
70	165000	12	164000	12	118000	12
72.5	200000	12	200000	12		
79			336000	12		
80	355000	12				
85			487000	12		
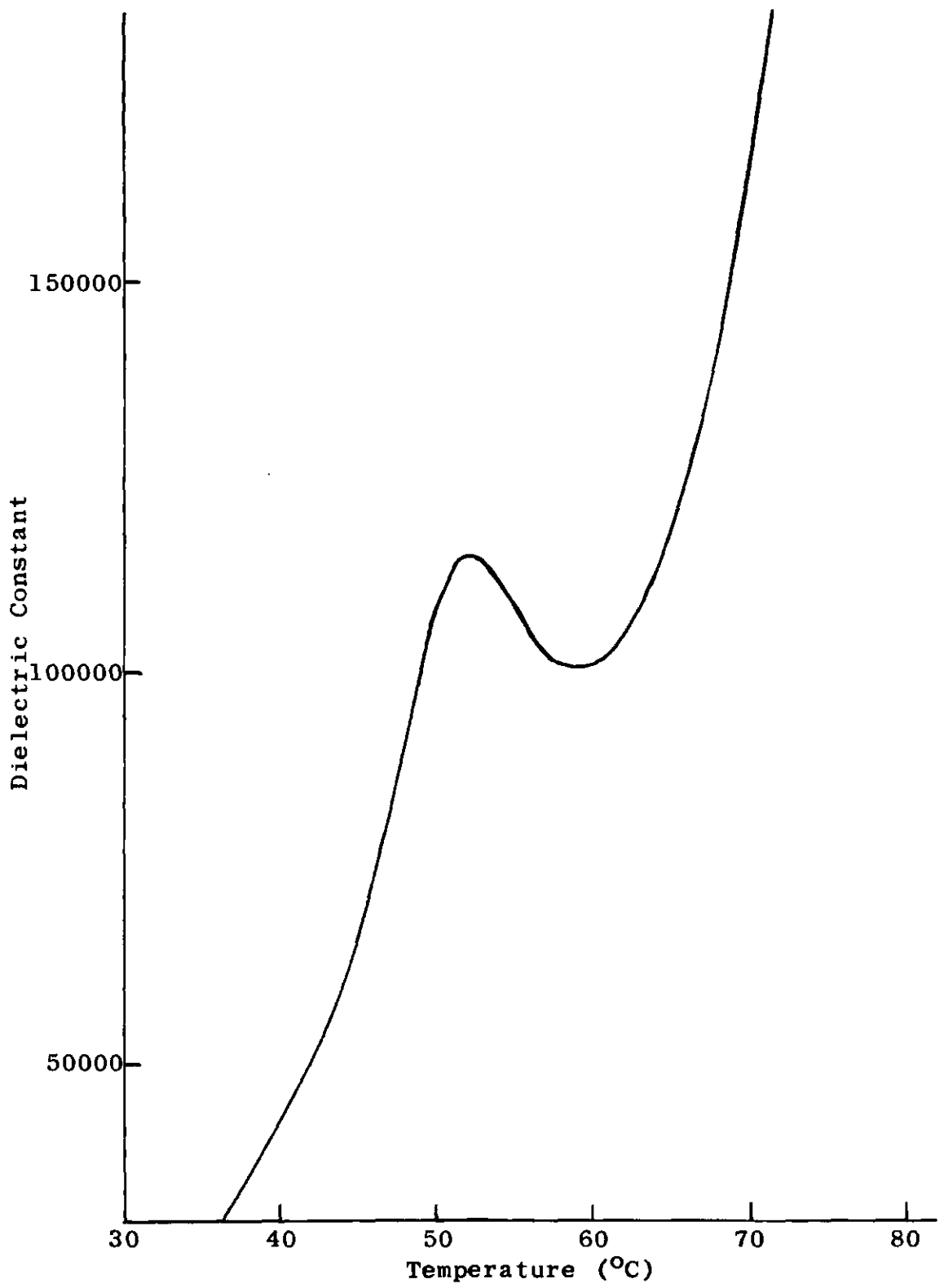
Figure 37. Dielectric Constant of Sodium RNA
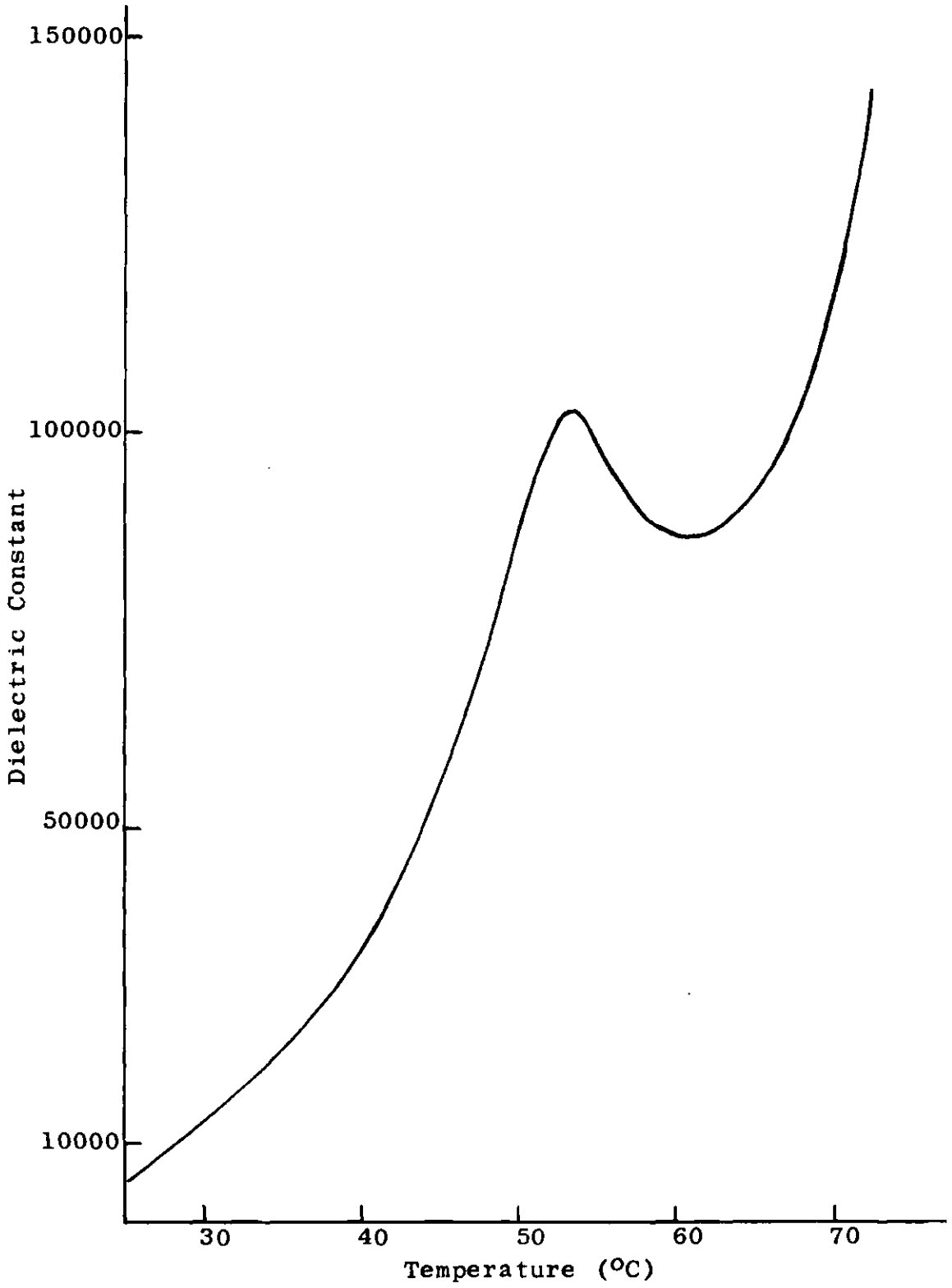
Figure 38. Dielectric Constant of Sodium RNA

Table 5.   Dielectric Constant of Sodium Ribonucleate

Figure Number	39	40
Heating Curve	II	II
Electrode Area A cm^2	0.186	0.340
Area Diameter D cm	0.487	0.657
Sample Thickness d cm	0.0533	0.0483
Ratio D/d	9.14	13.6
Measuring Voltage V volts	0.60	0.60
Maximum Electric Field V/d volts/cm	11.3	12.4

Temperature $^{\circ}$C	ϵ	Percent Error ±	ϵ	Percent Error ±
30	10700	25		
35	17100	25	13600	25
40	25300	20	22600	20
45	37000	20	35200	20
50	59000	20	62200	20
52	67000	20	70400	20
54	73700	20	75000	20
56	75300	20	77000	20
58	76600	20	77500	20
60	78600	20	78000	20
65	89000	20	85400	20
70	108000	15	104000	15
75	147000	15	141000	15
80	200000	15	200000	15
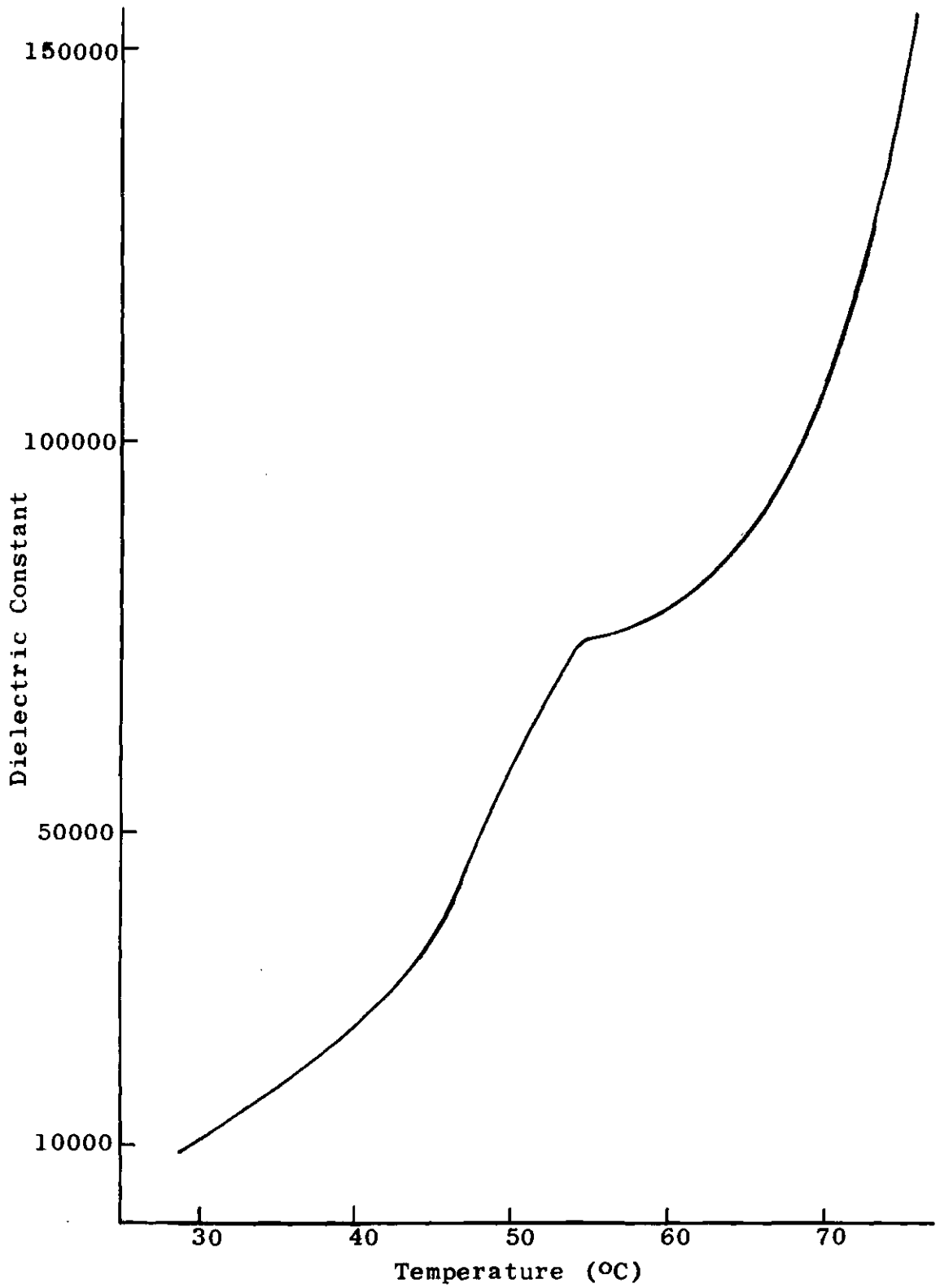
Figure 39. Dielectric Constant of Sodium RNA
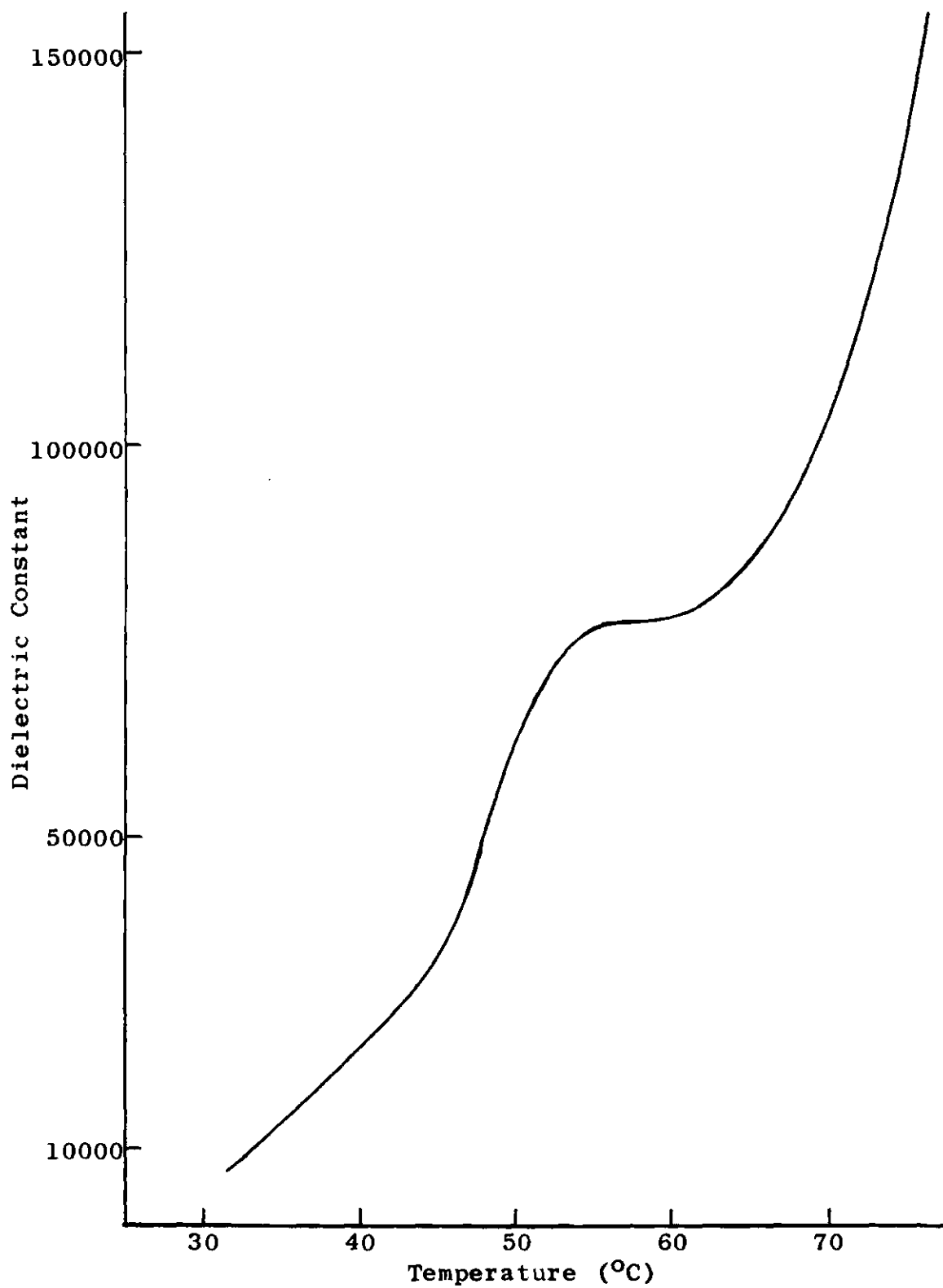
Figure 40. Dielectric Constant of Sodium RNA

Table 6. Dielectric Constant of Sodium Ribonucleate

Figure Number	41		42	
Heating Curve	II		II	
Electrode Area A cm^2	0.186		0.186	
Area Diameter D cm	0.487		0.487	
Sample Thickness d cm	0.0445		0.0508	
Ratio D/d	10.9		9.58	
Measuring Voltage V volts	0.60		0.60	
Maximum Electric Field V/d volts/cm	13.5		11.8	
Frequency cps	100		500	
Temperature $^\circ$C	ϵ	Percent Error ±	ϵ	Percent Error ±
30			14700	20
35	28000	18	19600	18
40	33000	15	25400	15
45	46000	15	33000	15
50	88000	12	47900	12
55	160000	12	82000	12
60	221000	12	120000	12
65	289000	12	147000	12
69	382000	12		
70			175000	12
71	463000	12		
72.5	523000	12	200000	12
75	626000	12	235000	12
80			324000	12
82			371000	12
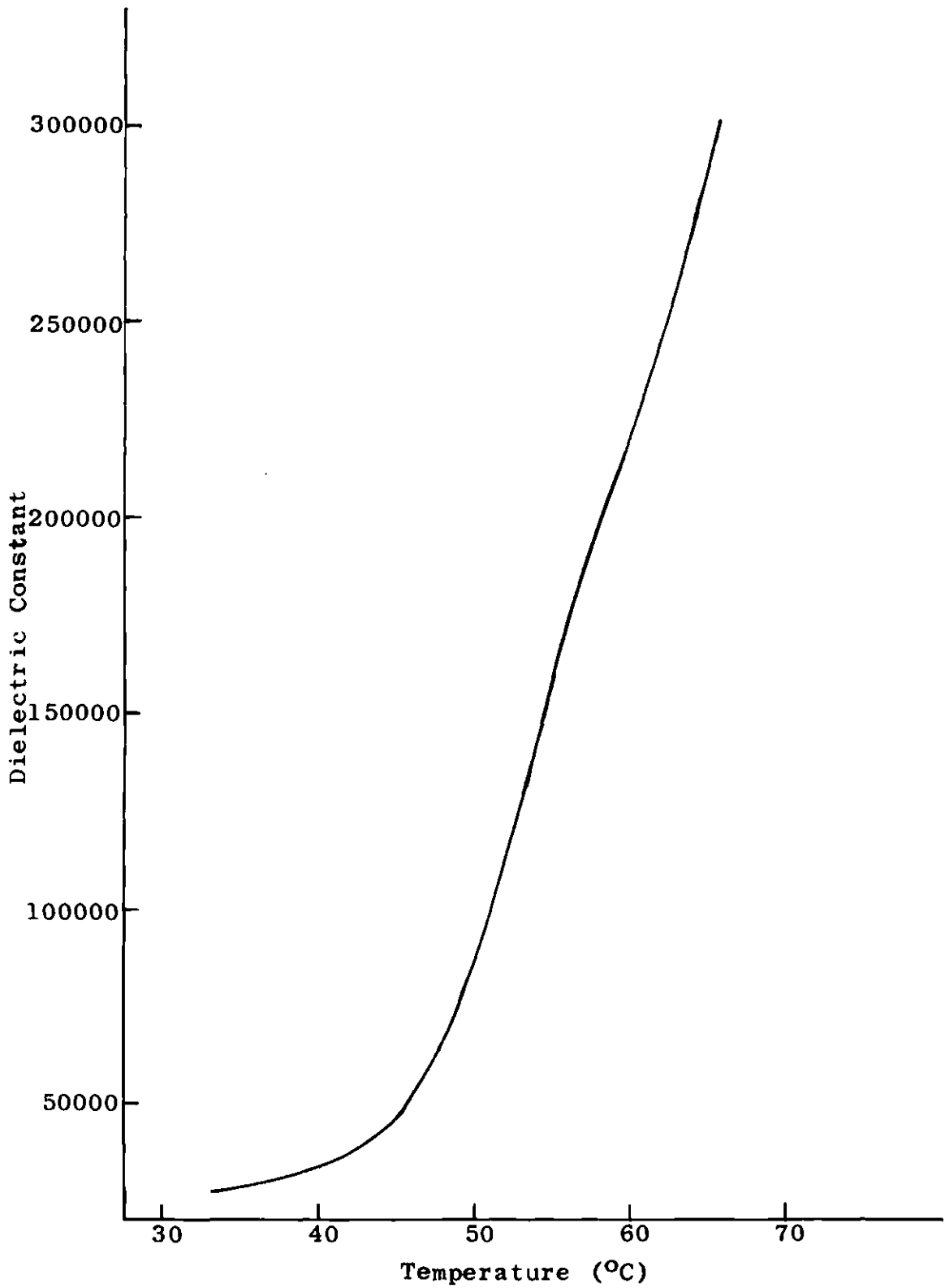
Figure 41. Dielectric Constant of Sodium RNA at 100 cps
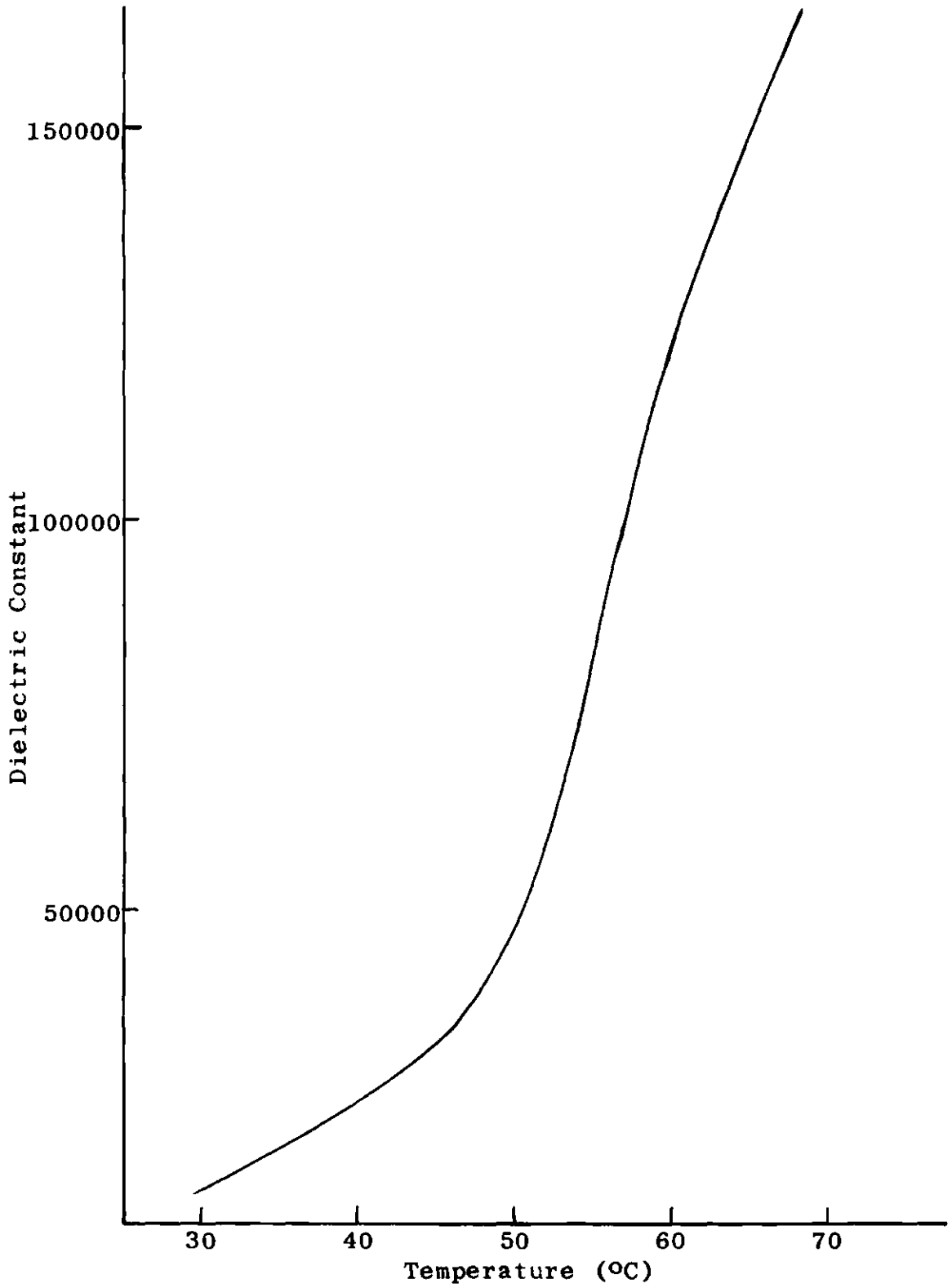
Figure 42. Dielectric Constant of Sodium RNA at 500 cps

Table 7.   Dielectric Constant of Sodium Deoxyribonucleate

Figure Number	20	**43**	**44**
Heating Curve	IV	IV	II
Electrode Area A cm^2	0.340	0.340	0.186
Area Diameter D cm	0.657	0.657	0.487
Sample Thickness d cm	0.0533	0.0724	0.0546
Ratio D/d	12.3	9.08	8.92
Measuring Voltage V volts	0.63	0.63	0.63
Maximum Electric Field V/d volts/cm	11.8	8.71	11.5

| Temperature ^{o}C	ϵ	Percent Error ±	ϵ	Percent Error ±	ϵ	Percent Error ±
25	20600	12	30000	12		
30	37000	12	46800	12	33000	12
35	61500	10	75800	10	56500	12
37.5	71000	10	83600	10	71300	10
40	74800	10	88700	10	80700	10
42.5	75700	10	91900	10	85500	10
45	78700	10	96600	10	89000	10
50	89200	10	109000	10	103000	10
55	99800	10	124000	10	117000	10
60	109000	10	140000	10	134000	10
65	122000	10	157000	10	154000	10
70	143000	10	178000	10	175000	10
72.5	159000	10	200000	10	189000	10
74.5	176000	10			200000	10
76.5			250000	10		
77	200000	10				
78					238000	10
80	233000	10	320000	10		
83			363000	10		
85					345000	10
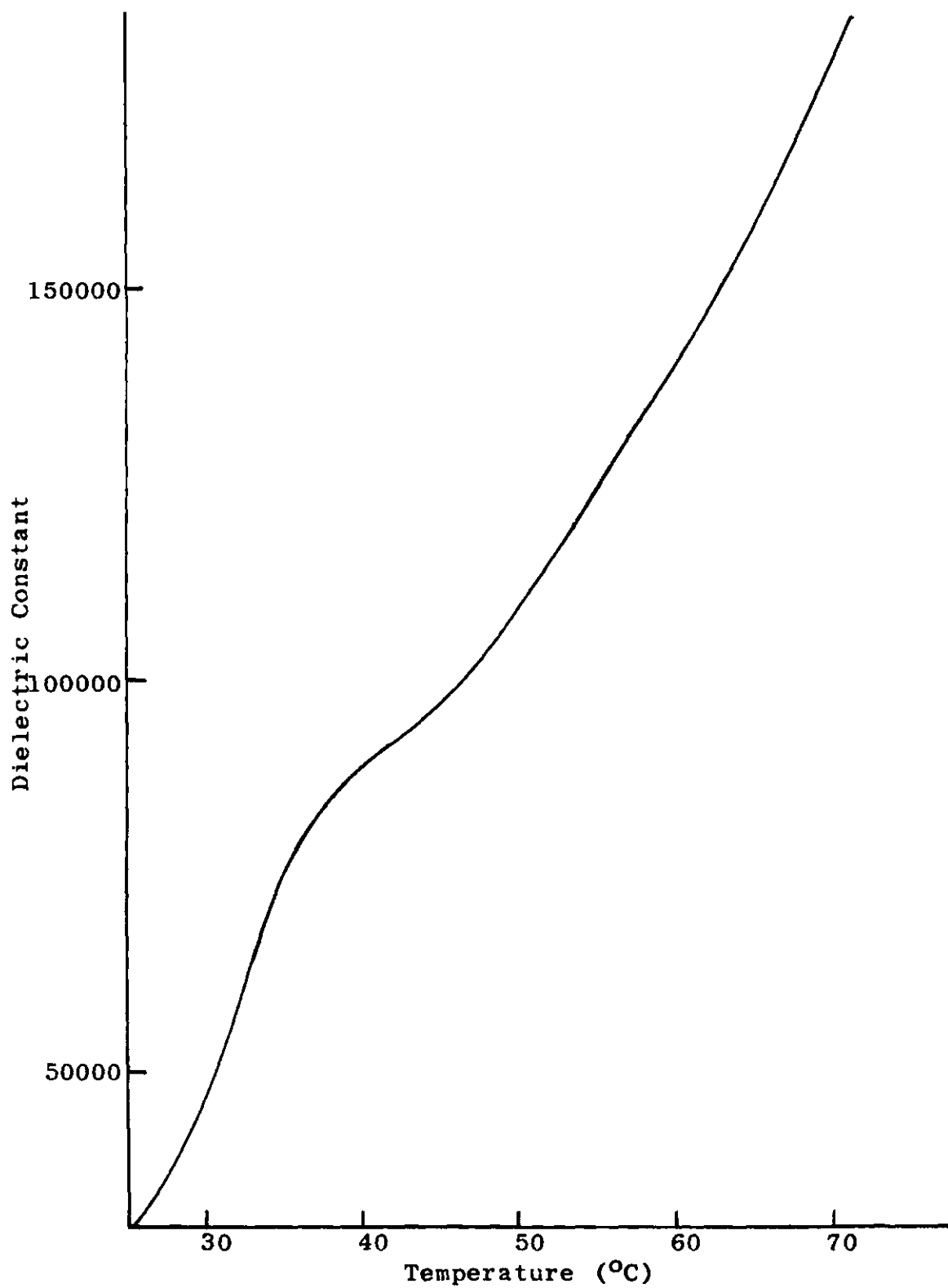
Figure 43. Dielectric Constant of Sodium DNA
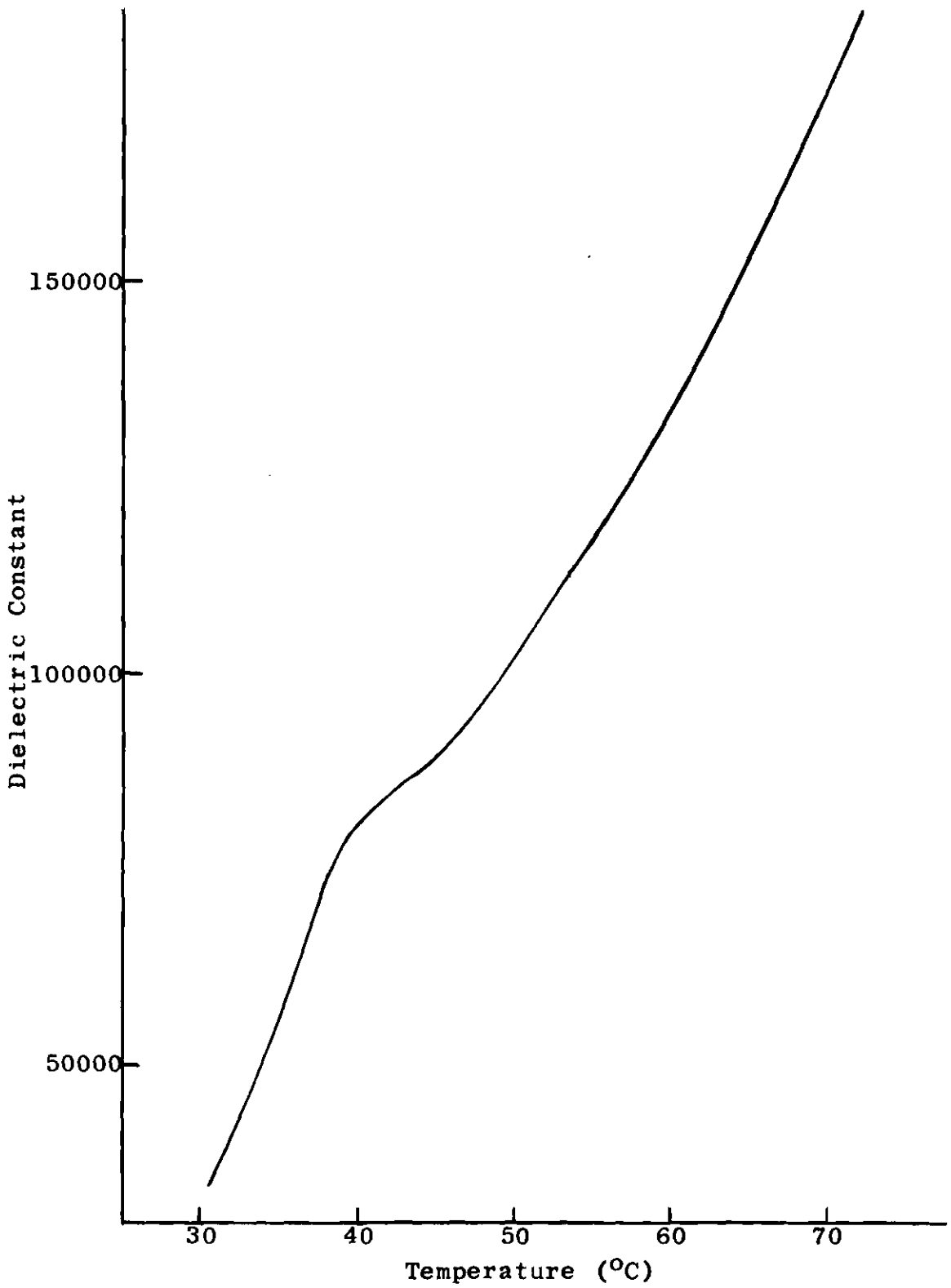
Figure 44. Dielectric Constant of Sodium DNA

Table 8. Dielectric Constant of Polyadenylic Acid Potassium

Figure Number	22	45	46
Heating Curve	II	II	II
Electrode Area A cm^2	0.340	0.340	0.340
Area Diameter D cm	0.657	0.657	0.657
Sample Thickness d cm	0.0013	0.0013	0.0013
Ratio D/d	506	506	506
Measuring Voltage V volts	0.25	0.25	0.25
Maximum Electric Field V/d volts/cm	192	192	192

Temperature $^{\circ}C$	ϵ	Percent Error $\pm$	ϵ	Percent Error $\pm$	ϵ	Percent Error $\pm$
30	2000	20	3600	20	4500	18
35	4300	18	5200	15	5800	15
40	6100	15	6400	15	6900	15
45	7700	15	7500	15	7800	15
50	9500	15	8700	15	9000	15
55	11300	15	10300	15	10700	15
60	12500	15	12300	15	12500	15
62.5	13600	15	15300	15	15000	15
65	15600	15	20200	12	19400	12
67.5	19200	12	26000	12	26400	12
70	25300	12	34900	12	35400	12
75	37800	12	44200	12	47300	12
80	41700	12	47400	12	51800	12
82.5	42000	12	49000	12	51300	12
85	41300	12	48500	12	49600	12
90	37100	12	45000	12	44400	12
95	30600	12	38800	12	36400	12
100	20000	12	31000	12	23000	12
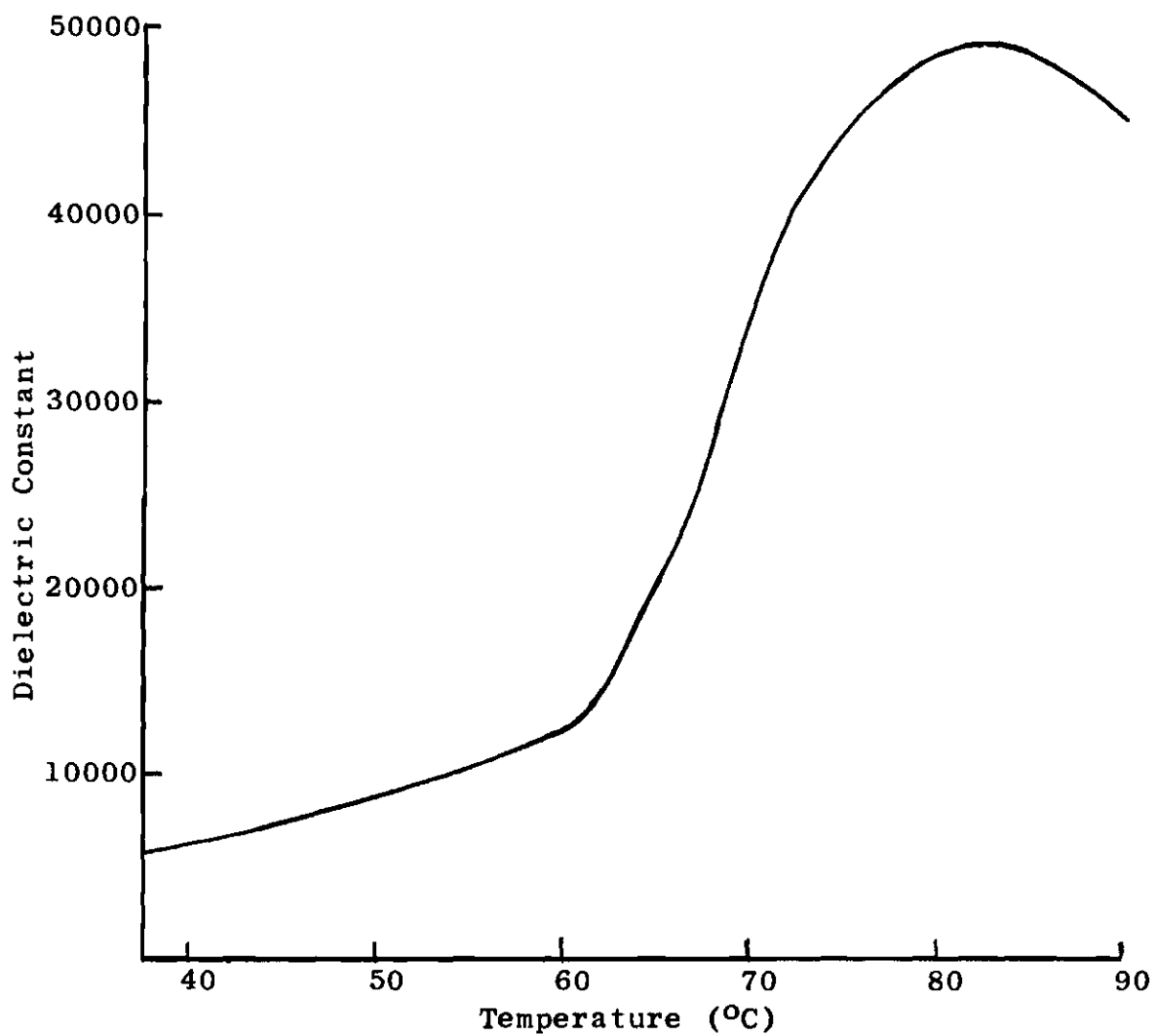
Figure 45. Dielectric Constant of Polyadenylic Acid Potassium
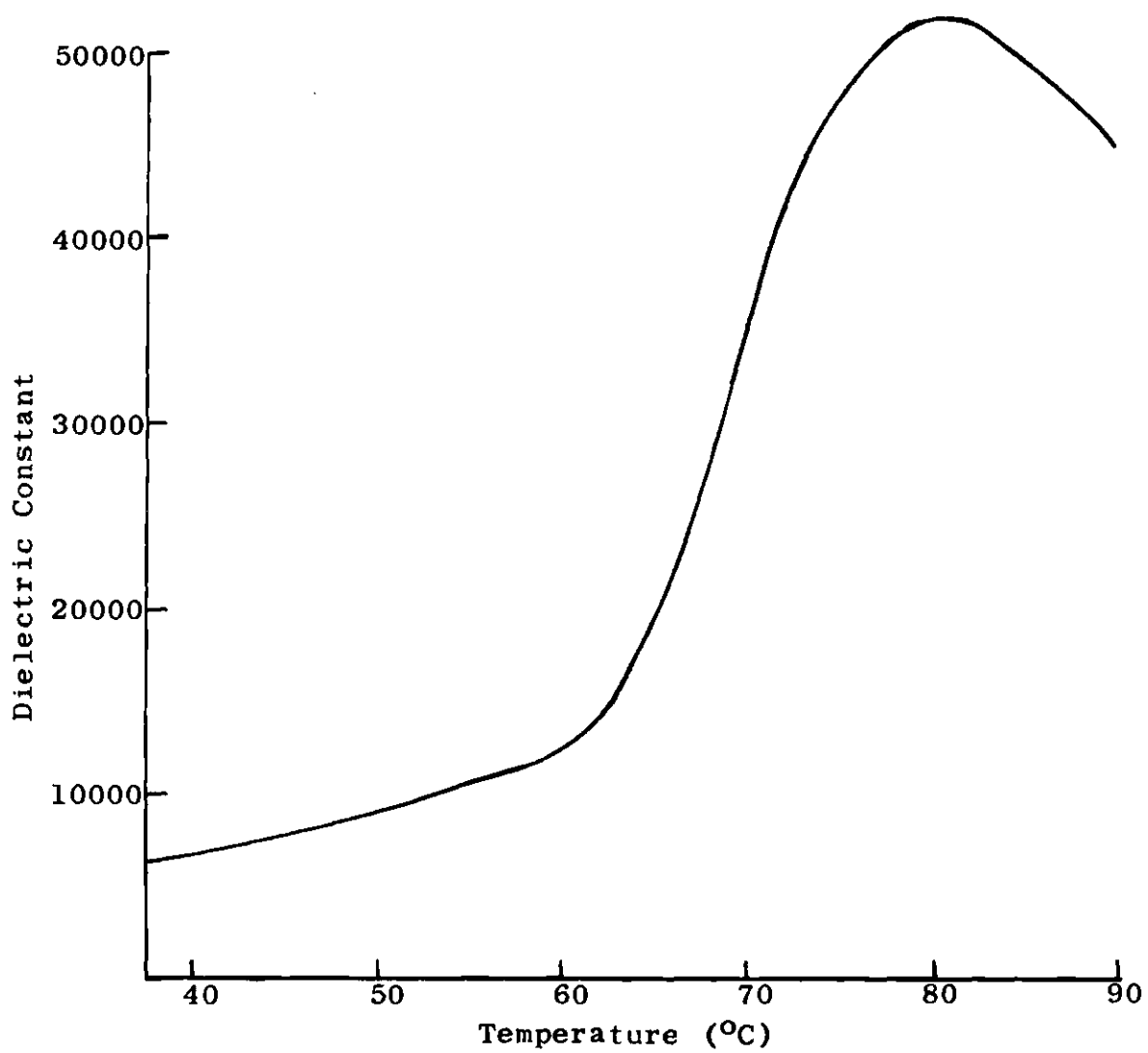
Figure 46. Dielectric Constant of Polyadenylic Acid Potassium

Table 9. Dielectric Constant of Polycytidylic Acid Potassium

	24	47	48
Figure Number	24	47	48
Heating Curve	II	II	II
Electrode Area A cm^2	0.340	0.340	0.340
Area Diameter D cm	0.657	0.657	0.657
Sample Thickness d cm	0.0140	0.0140	0.0140
Ratio D/d	46.9	46.9	46.9
Measuring Voltage V volts	0.25	0.25	0.25
Maximum Electric Field V/d volts/cm	17.8	17.8	17.8

Temperature ^oC	ϵ	Percent Error ±	ϵ	Percent Error ±	ϵ	Percent Error ±
25	3000	20	3800	20	3400	20
30	6000	18	7100	18	6000	18
35	9700	15	11800	15	9000	15
40	15700	15	19000	15	13000	15
45	23700	15	28200	15	19400	15
50	36700	15	40800	15	31000	15
55	54500	15	55700	15	50500	15
60	76500	15	77500	15	72000	15
65	102000	15	105000	15	89800	15
70	129000	15	128000	15	111000	15
75	172000	15	148000	15	137000	15
77.5	200000	15	160000	15	153000	15
80			173000	15	172000	15
82.5			188000	15	192000	15
83.5					200000	15
84.5			200000	15		
85	251000	15				
92			251000	15	251000	15
97			260000	15		
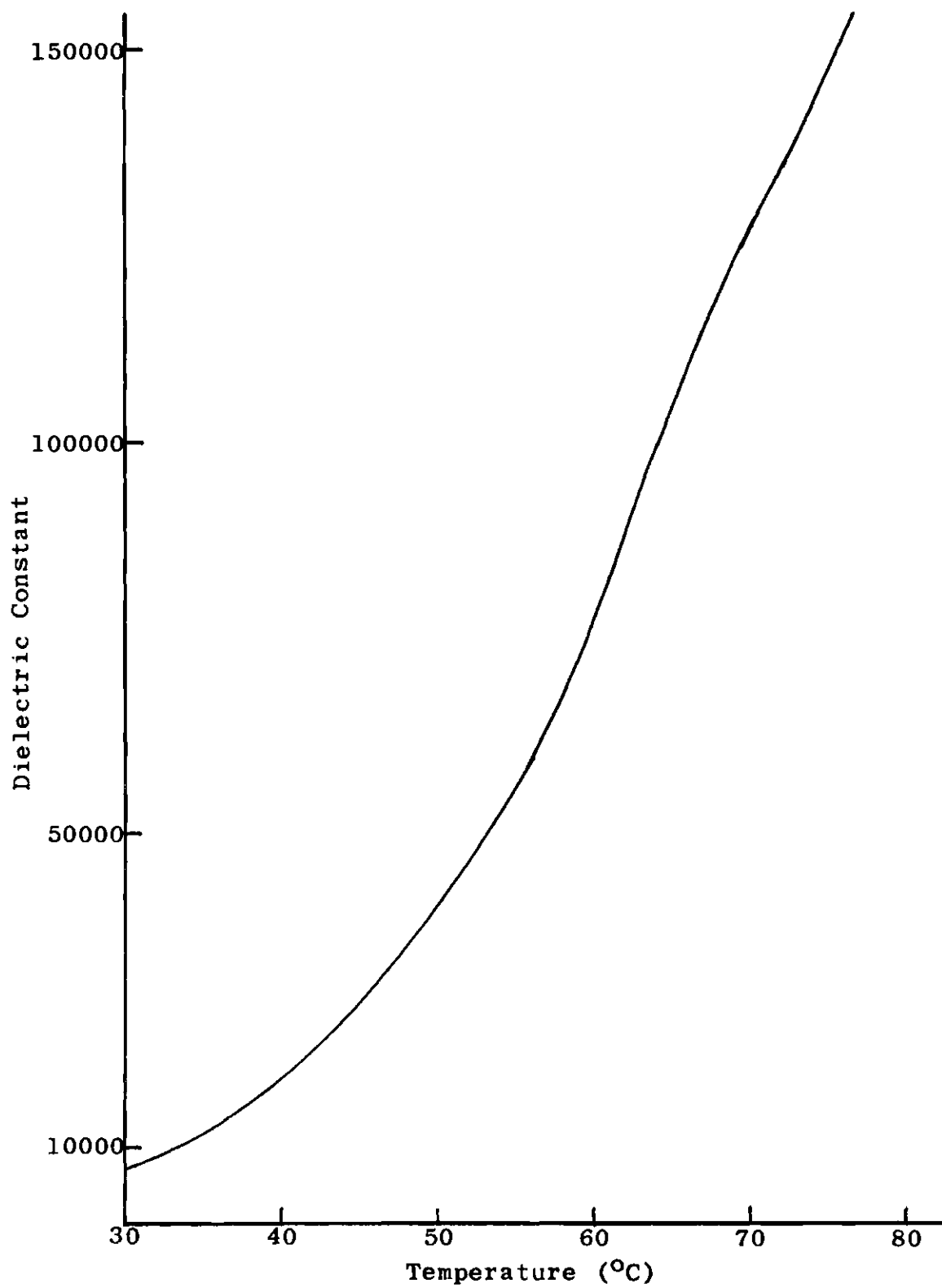
Figure 47. Dielectric Constant of Polycytidylic Acid Potassium
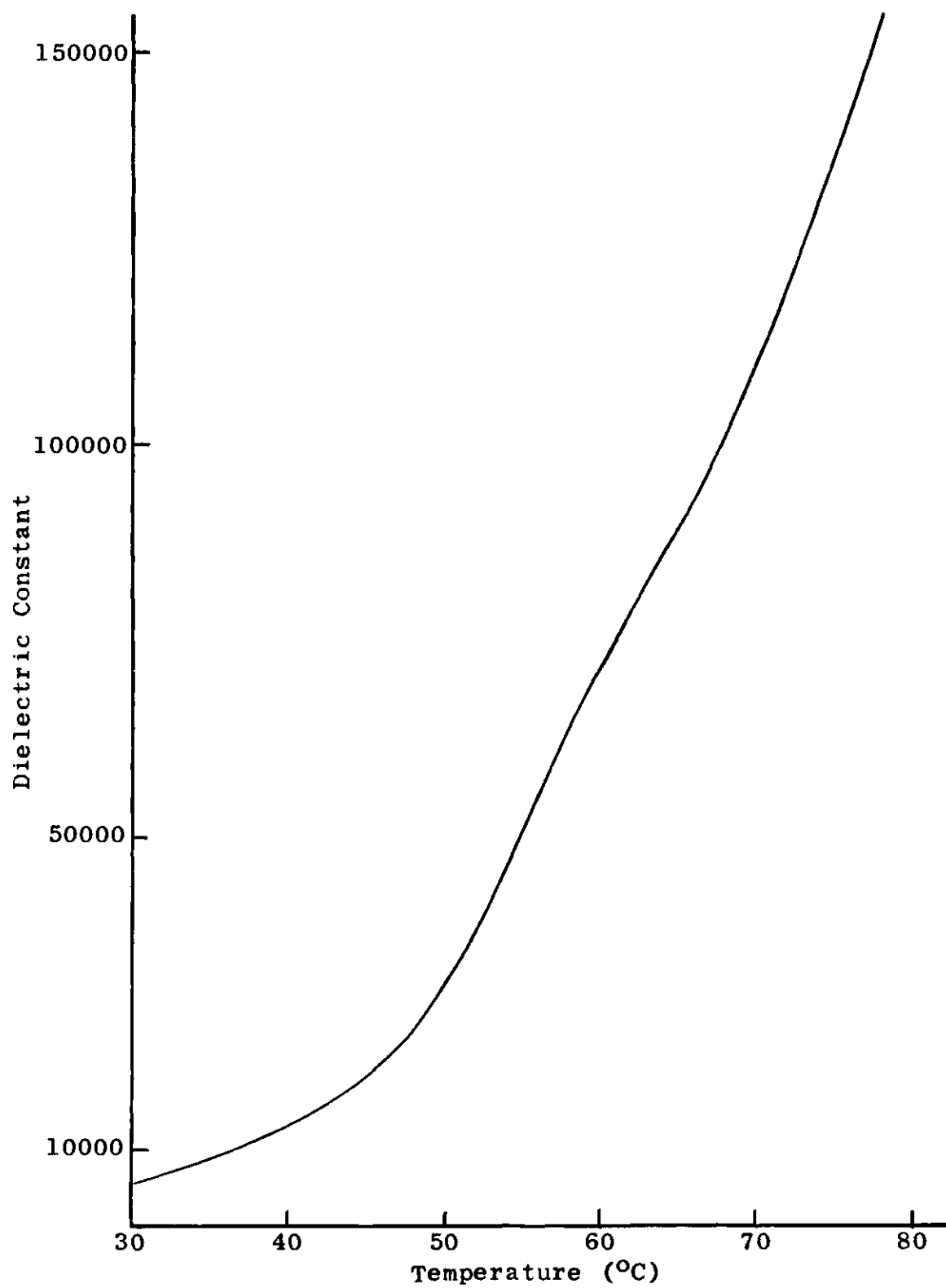
Figure 48.   Dielectric Constant of Polycytidylic Acid Potassium

Table 10. Dielectric Constant of Adenylic Acid Sodium

	26	49	50
Figure Number	26	49	50
Heating Curve	I	I	II
Electrode Area A cm^2	0.840	0.840	0.840
Area Diameter D cm	1.03	1.03	1.03
Sample Thickness d cm	0.0406	0.0457	0.0488
Ratio D/d	25.4	22.6	21.1
Measuring Voltage V volts	0.63	0.63	0.63
Maximum Electric Field V/d volts/cm	15.5	13.8	12.9

| Temperature °C	ϵ	Percent Error ±	ϵ	Percent Error ±	ϵ	Percent Error ±
28	3000	18	1800	20		
30	5300	15	3400	18		
35	12000	12	10000	12	4600	15
40	17500	12	16200	12	12700	12
45	22500	12	21800	12	19700	12
50	29000	12	26400	12	24300	12
52.5	34000	12	31500	12	27100	12
55	44500	12	41000	12	31400	12
57.5	62000	12	54500	12	39000	12
60	82000	12	77500	12	55500	12
65	140000	12	134000	12	110000	12
67.5	158000	12	162000	12	140000	12
70			200000	12	169000	12
72.5					200000	12
74					221000	12
80			297000	12		
82					319000	12
85			329000	12		
86					354000	12

Figure 49. Dielectric Constant of Adenylic Acid Sodium
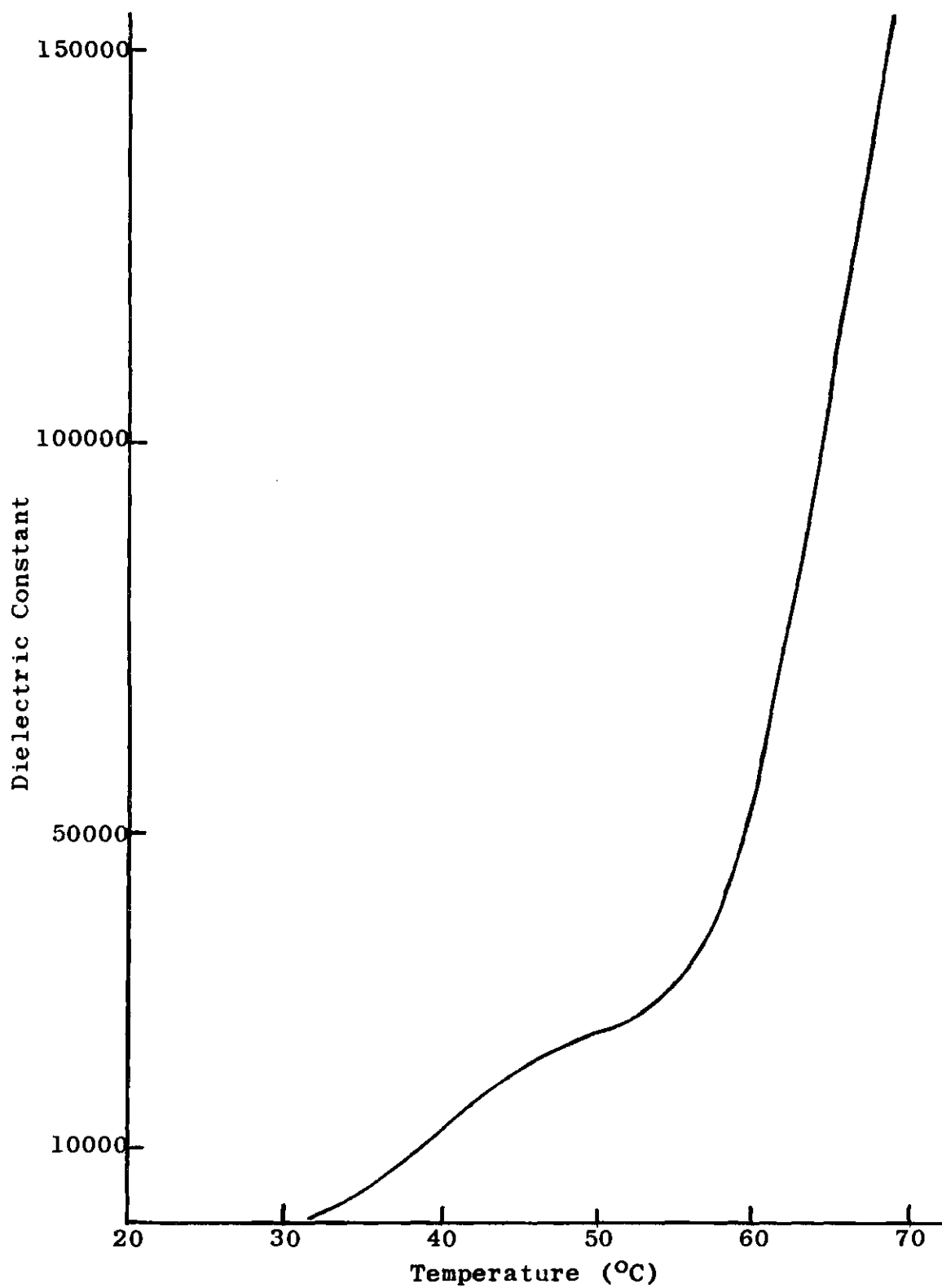
Figure 50. Dielectric Constant of Adenylic Acid Sodium

Table 11.   Dielectric Constant of Guanylic Acid Disodium

	28	51	52
Figure Number	28	51	52
Heating Curve	II	II	II
Electrode Area A cm^2	0.186	0.186	0.186
Area Diameter D cm	0.487	0.487	0.487
Sample Thickness d cm	0.0203	0.0223	0.0254
Ratio D/d	24.0	21.8	19.2
Measuring Voltage V volts	0.40	0.40	0.40
Maximum Electric Field V/d volts/cm	19.7	17.9	15.7

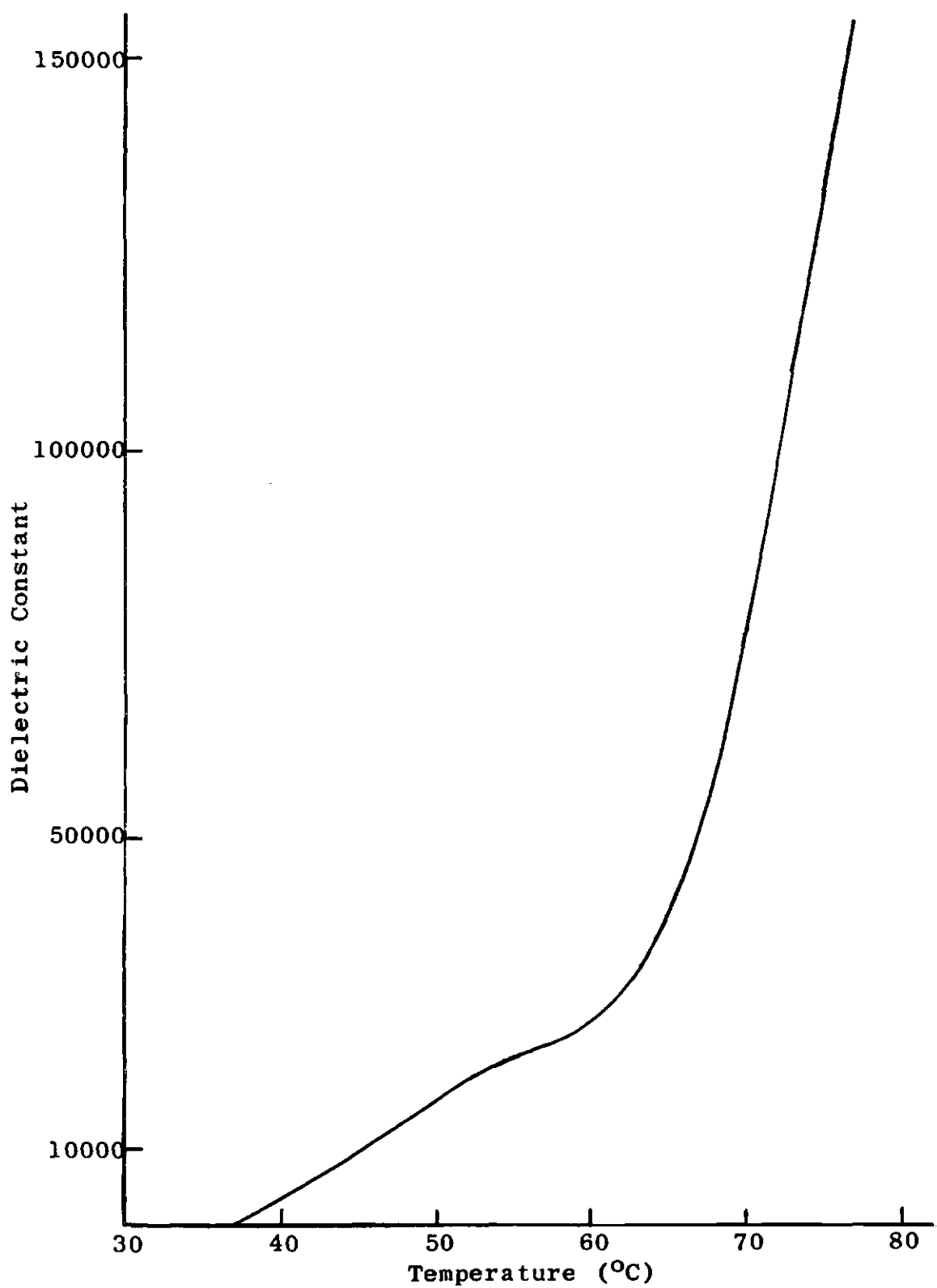| Temperature ^{o}C	ϵ	Percent Error $\pm$	ϵ	Percent Error $\pm$	ϵ	Percent Error $\pm$
30	7300	22	8800	22	8900	22
34	9000	22	13600	22	12000	22
36	10300	22	18400	22	14800	22
38	12000	22	31000	20	19300	22
40	14000	22	51400	20	28000	20
42	18700	22	69000	20	46000	20
44	29000	20	85200	20	67300	20
46	45500	20	103000	20	84000	20
48	60000	20	143000	20	98400	20
49.5			200000	20		
50	63300	20	207000	20	111000	20
52.5	72400	20			136000	20
55	88200	20	378000	20	200000	20
57.5	120000	20				
58					334000	20
59.5	200000	20				
60	268000	20	658000	20		
61					428000	20
62	344000	20				
64			976000	20		
69	599000	20			909000	20
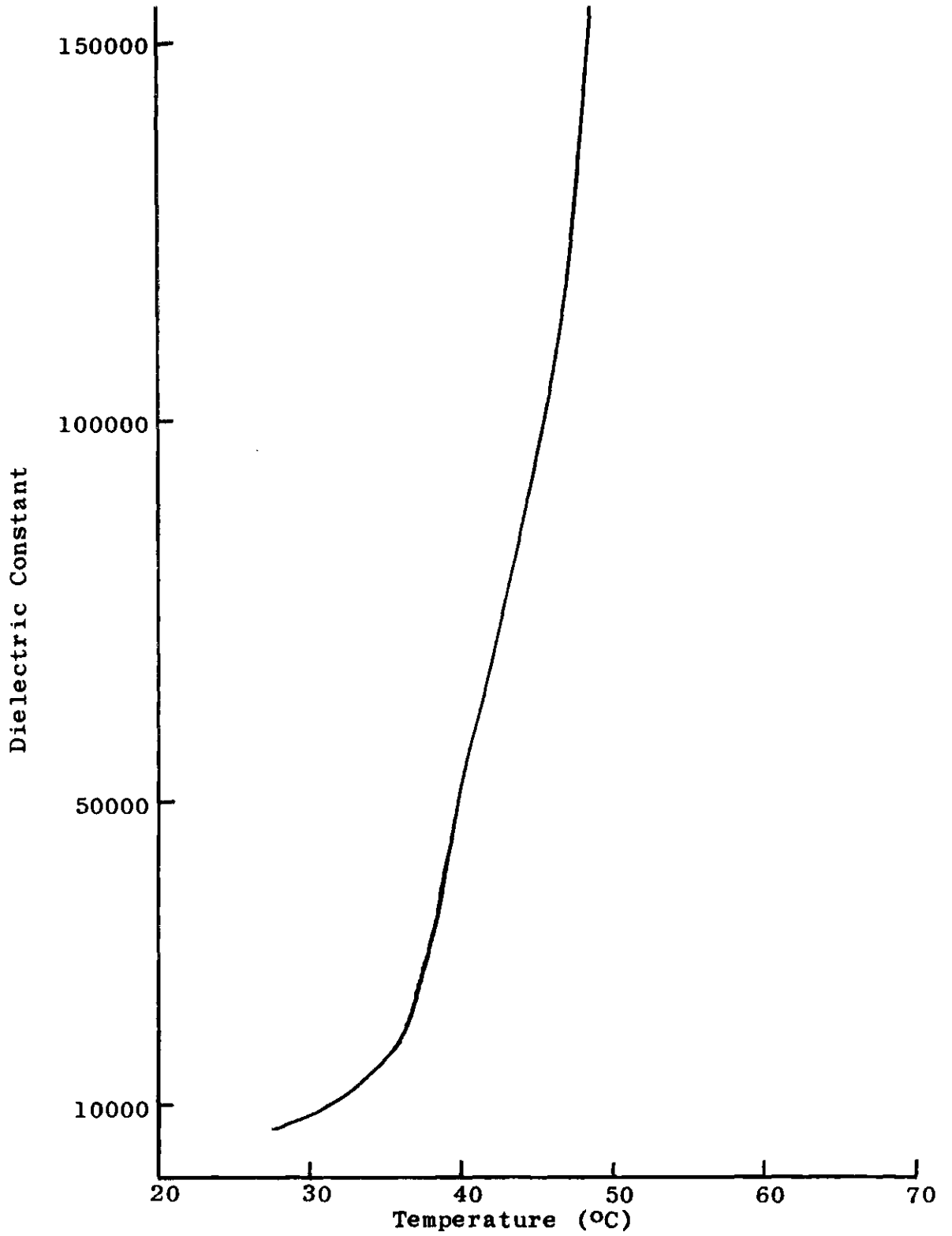
Figure 51. Dielectric Constant of Guanylic Acid Disodium
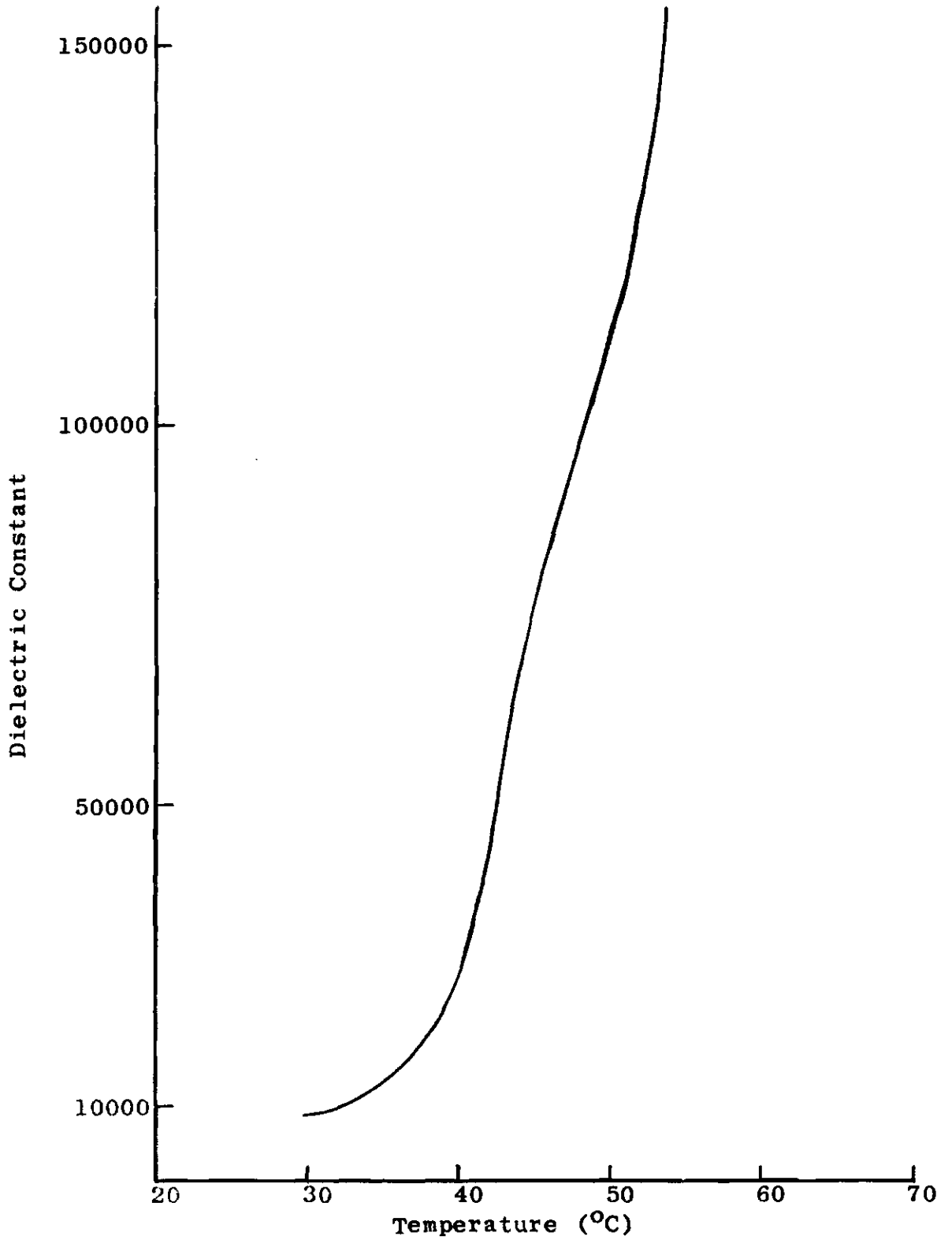
Figure 52. Dielectric Constant of Guanylic Acid Disodium

Table 12. Dielectric Constant of Cytidylic Acid Disodium

Figure Number	30		53	
Heating Curve	II		II	
Electrode Area A cm^2	0.186		0.340	
Area Diameter D cm	0.487		0.657	
Sample Thickness d cm	0.0635		0.0762	
Ratio D/d	7.67		8.63	
Measuring Voltage V volts	0.60		0.60	
Maximum Electric Field V/d volts/cm	9.45		7.88	

Temperature $^{\circ}$C	ϵ	Percent Error ±	ϵ	Percent Error ±
65	5600	22	2500	22
67.5	12800	20	5700	22
70	24500	20	11000	20
72	45300	20	17800	20
74	75000	20	30000	20
76	125000	20	50000	20
77	170000	20	64500	20
78	200000	20	82500	20
80	295000	20	127000	20
82	405000	20	179000	20
82.5			200000	20
84	494000	20	226000	20
87	587000	20	283000	20
91	745000	20	359000	20
98	915000	20	385000	20
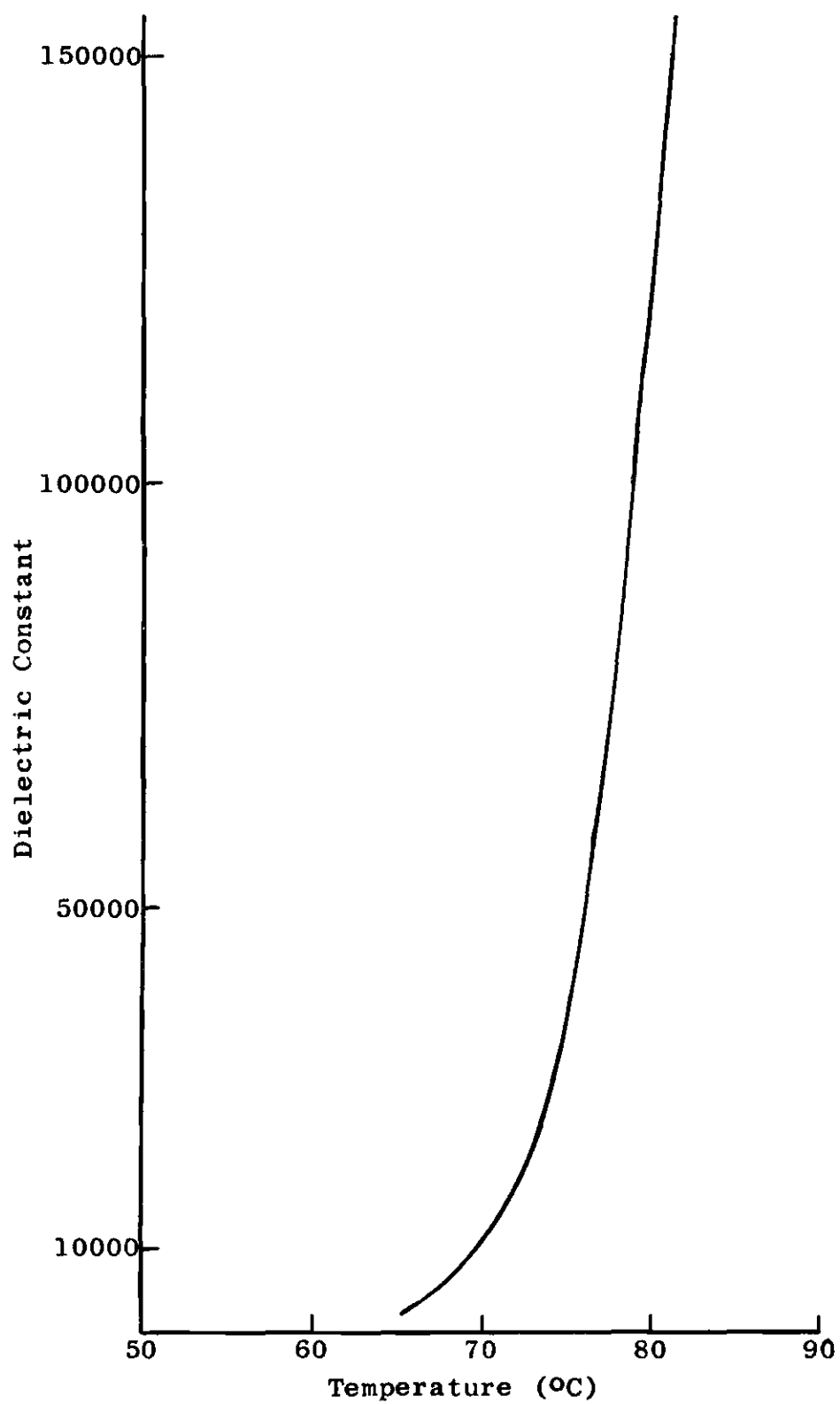
Figure 53. Dielectric Constant of Cytidylic Acid Disodium

Table 13.   Dielectric Constant of Thymidylic Acid Sodium

	32	54
Figure Number	32	**54**
Heating Curve	II	II
Electrode Area A cm^2	0.0410	0.0410
Area Diameter D cm	0.228	0.228
Sample Thickness d cm	0.0305	0.0267
Ratio D/d	7.48	8.54
Measuring Voltage V volts	0.30	0.30
Maximum Electric Field V/d volts/cm	9.84	11.2

Temperature $^{\circ}C$	ϵ	Percent Error ±	ϵ	Percent Error ±
65	44000	28	70000	25
67.5	53000	25	89000	25
70	70000	25	127000	22
75	138000	22	300000	22
80	344000	22	700000	22
85	765000	22	1170000	22
90	1190000	22	1520000	22
95	1470000	22		
100	1630000	22		
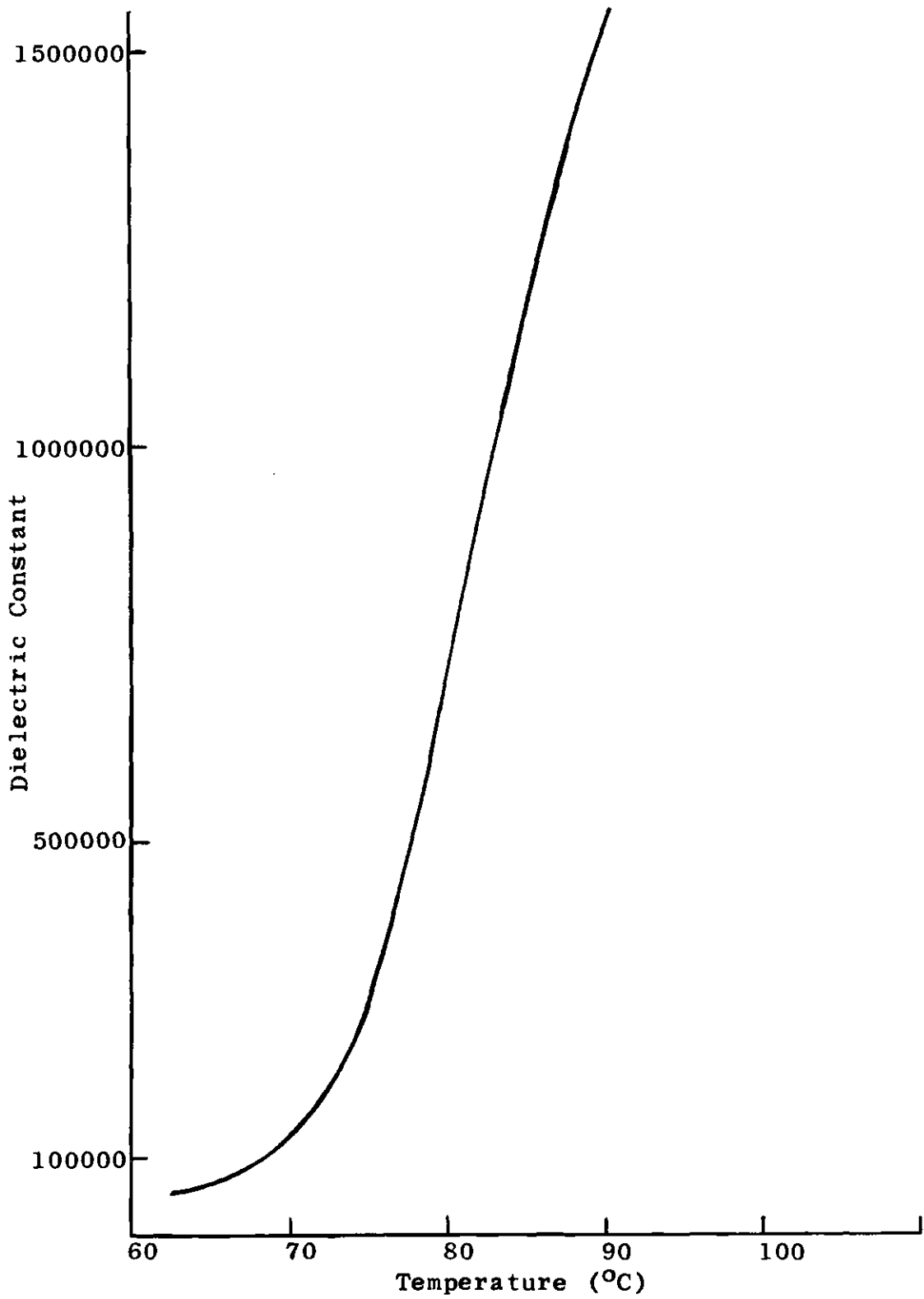
Figure 54. Dielectric Constant of Thymidylic Acid Sodium

Table 14. Dielectric Constant of Adenylic Acid Sodium Wafer

Figure Number	34		55	
Heating Curve	III		III	
Electrode Area A cm^2	2.85		2.85	
Area Diameter D cm	1.91		1.91	
Sample Thickness d cm	0.216		0.212	
Ratio D/d	8.85		9.02	
Measuring Voltage V volts	7.0		7.0	
Maximum Electric Field V/d volts/cm	32.4		33.0	

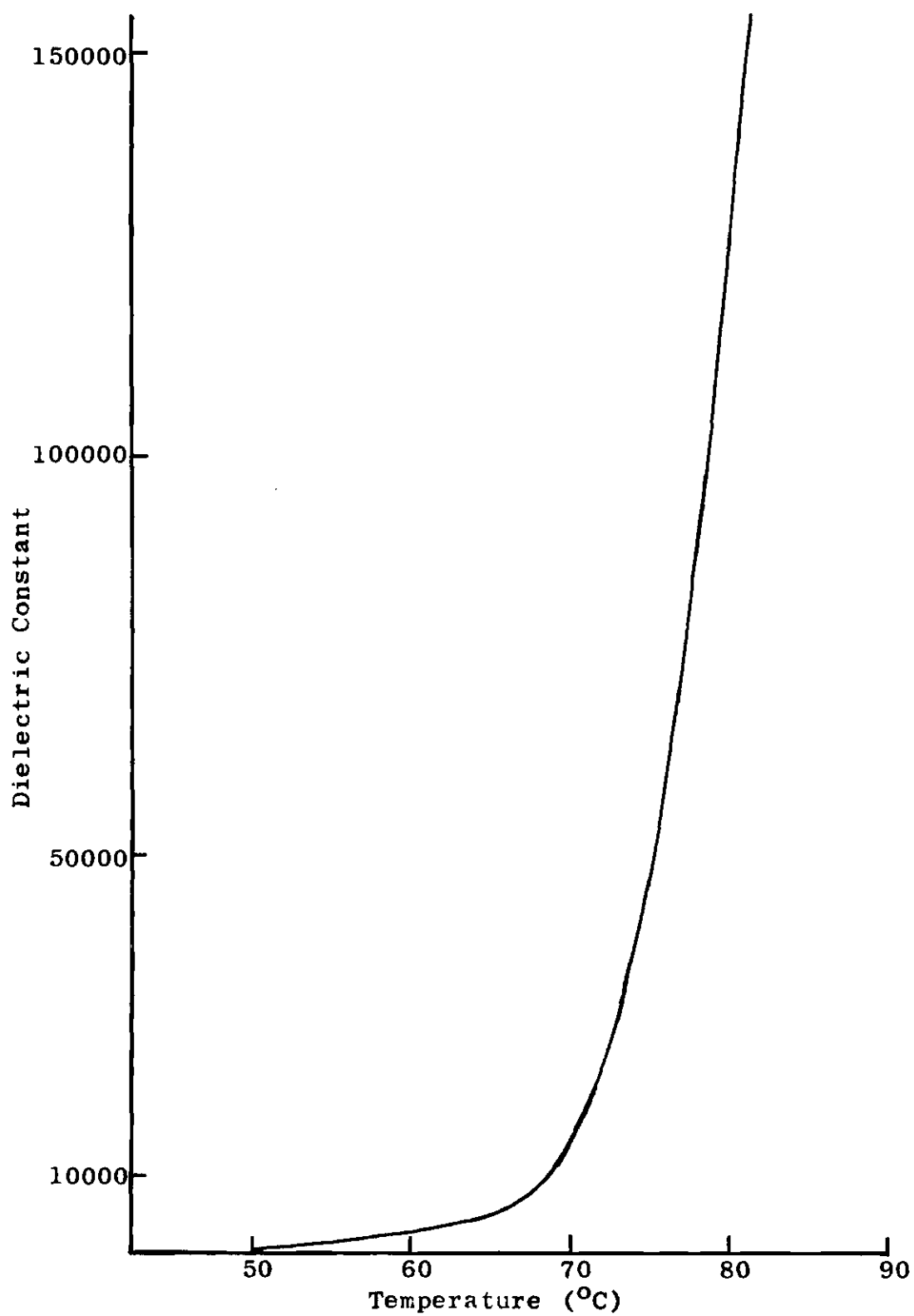| Temperature $^{\circ}C$	ϵ	Percent Error $\pm$	ϵ	Percent Error $\pm$
50	1000	12	1000	12
55	2000	12	1700	12
60	3200	9	2700	9
65	7800	8	4800	9
70	28000	7	14000	7
75	71000	7	46200	7
80	153000	7	130000	7
82	200000	7	172000	7
83			200000	7
86	280000	7	275000	7
87			355000	7
87.5	362000	7		
90			441000	7
91	450000	7		
99	766000	7	752000	7

Figure 55. Dielectric Constant of Adenylic Acid Sodium Wafer

Table 15. Dielectric Constant of Uridylic Acid Disodium Wafer

	35		56	
Figure Number	35		**56**	
Heating Curve	III		III	
Electrode Area A cm^2	2.85		2.85	
Area Diameter D cm	1.91		1.91	
Sample Thickness d cm	0.216		0.216	
Ratio D/d	8.85		8.85	
Measuring Voltage V volts	7.0		7.0	
Maximum Electric Field V/d volts/cm	32.4		32.4	

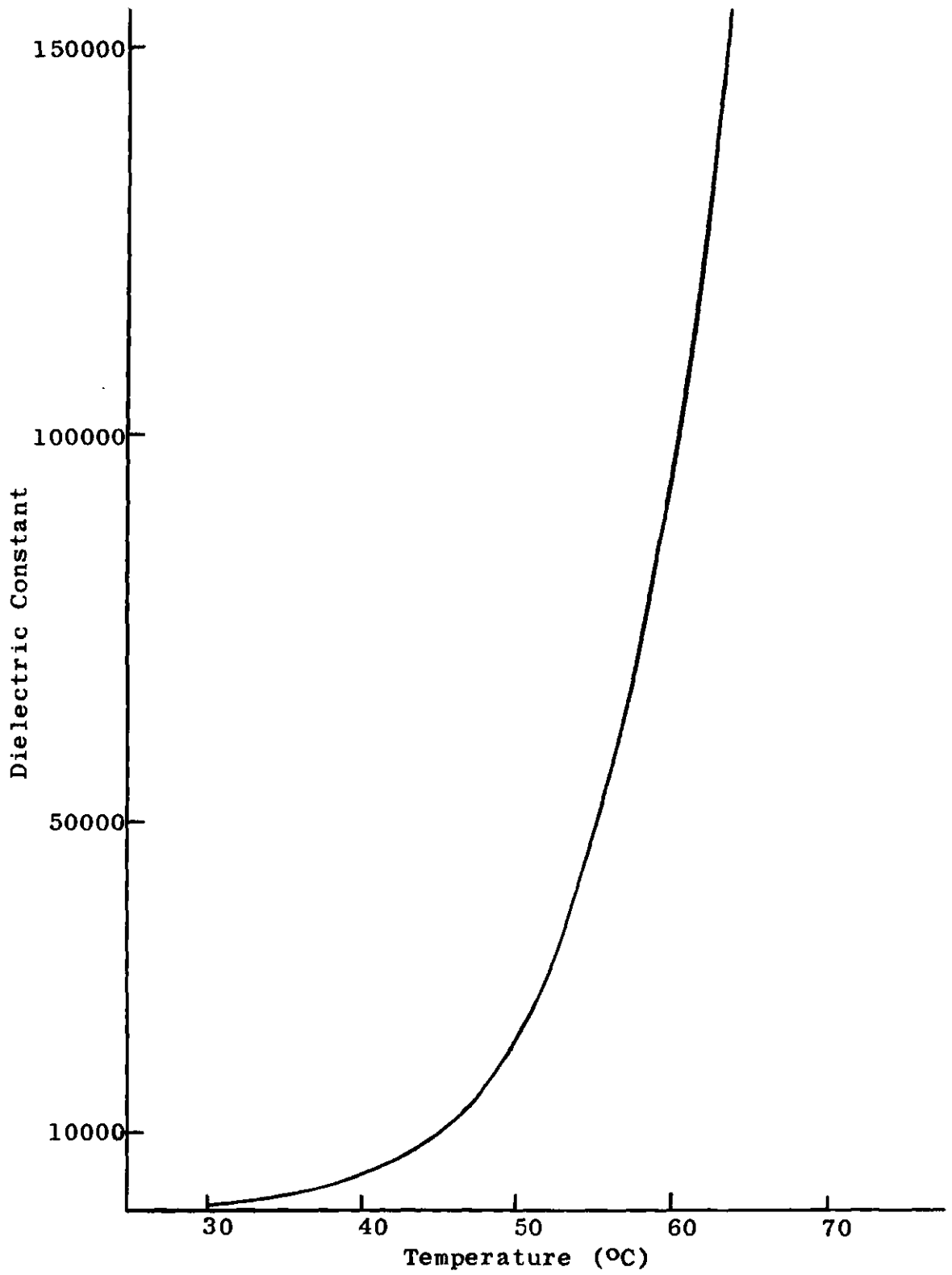| Temperature ^oC	ϵ	Percent Error ±	ϵ	Percent Error ±
30	1000	14	1000	14
35	4000	11	1800	13
40	10000	10	4300	11
45	21000	9	10000	10
50	43000	9	22000	9
55	83000	9	48000	9
60	144000	9	93000	9
63.5	200000	9	148000	9
67			200000	9
70	386000	9		
71			288000	9
75	514000	9		
77			463000	9
80	703000	9		
85	891000	9	788000	9
89	1220000	9		
90			1220000	9

Figure 56. Dielectric Constant of Uridylic Acid Disodium Wafer

LITERATURE CITED

(1)   D. O. Jordan, The Chemistry of the Nucleic Acids,
      Butterworth & Co., Ltd., London, 1961.

(2)   W. C. Corning and R. E. John, Science, 134, pp. 1363-
      1365 (1961).

(3)   John W. Zemp, Proceedings of the United States National
      Academy of Science, 55, pp. 1423-1431 (1966).

(4)   H. Hyden and E. Egyhazi, Proc. U. S. Nat. Acad. Sci.,
      52, pp. 1030-1035 (1964).

(5)   Walter G. Cady, Piezoelectricity, McGraw-Hill Book
      Company, Inc., New York, 1946.

(6)   G. Shirane, F. Jona and R. Pepinsky, Proceedings of the
      Institute of Radio Engineers, 43, pp. 1738-1793 (1955).

(7)   Helen D. Megaw, Ferroelectricity in Crystals, Methuen
      & Co., Ltd., London, 1957.

(8)   A. F. Devonshire, Philosophical Magazine, 40, pp. 1040-
      1063 (1949)

(9)   A. F. Devonshire, Phil. Mag., 42, pp. 1065-1079 (1951).

(10) W. Cochran, Advances in Physics, 9, pp. 387-423 (1960).

(11) H. Diamant, K. Drenck and R. Pepinsky, The Review of
      Scientific Instruments, 28, pp. 30-33 (1957).

(12) E. Fatuzzo and W. J. Merz, Selected Topics in Solid
      State Physics, Editor, E. P. Wohlfarth, 7, John Wiley
      & Sons, Inc., New York, 1967.

(13) David Cohen, The Biological Role of the Nucleic Acids,
      American Elsevier Publishing Co., Inc., New York, 1965.

(14) Max E. Rafelson, Jr. and Stephen B. Binkley, Basic
      Biochemistry, The Macmillan Company, New York, 1968.

(15) Rosalind E. Franklin and R. G. Gosling, Acta Crystal-
      lographica, 6, pp. 673-677 (1953).

LITERATURE CITED (Continued)

(16) Rosalind E. Franklin and R. G. Gosling, Acta Cryst., 6, pp. 678-685 (1953).

(17) Alexander Rich, David R. Davies, F. H. C. Crick and J. D. Watson, Journal of Molecular Biology, 3, pp. 71-86 (1961).

(18) F. H. C. Crick and J. D. Watson, Proceedings of the Royal Society of London, A223, pp. 80-96 (1954).

(19) Alexander Rich, Reviews of Modern Physics, 31, pp. 191-199 (1959).

(20) T. M. Birshtein and O. B. Ptitsyn, Conformations of Macromolecules. Interscience Publishers, New York, 1966.

(21) Joseph Polonsky, Pierre Douzou and Charles Sodron, Comptes Rendus, 250, pp. 3412-3416 (1960).

(22) A. L. Stanford, jun. and R. A. Lorey, Nature, 219, pp. 1250-1251 (1968).

(23) C. B. Sawyer and C. H. Tower, Physical Review, 35, pp. 269-273 (1930).

(24) Peter Fong, American Physical Society Bulletin, 13, p. 617 (1968).

(25) J. Kraut and L. H. Jensen, Acta Cryst., 16, pp. 79-88 (1963).

(26) J. C. Slater, Journal of Chemical Physics, 9, pp. 16-33 (1941).

(27) Ross R. Middlemiss, Analytic Geometry, McGraw Hill Book Co., Inc., New York, 1955.

OTHER REFERENCES

(1) Buerger, M. J., _Elementary Crystallography_, John Wiley & Sons, Inc., New York, 1956.

(2) Dekker, Adrianus J., _Solid State Physics_, Prentice-Hall Inc., Englewood Cliffs, New Jersey, 1957.

(3) _Handbook of Chemistry and Physics_, Editor in Chief, Charles D. Hodgman, 43rd Edition, Chemical Rubber Publishing Co., Cleveland, pp. 2358-2359, 2654 (1961).

(4) Jefimenko, Oleg D., _Electricity and Magnetism_, Appleton-Century-Crofts, New York, 1965.

(5) Känzig, Werner, _Solid State Physics_, Editors, Fredrick Seitz and David Turnbull, 4, Academic Press, Inc., New York, 1957.

(6) Kimball, John W., _Biology_, Addison Wesley Publishing Co., Inc., Reading, Massachusetts, 1965.

(7) Kittel, Charles, _Introduction to Solid State Physics_, John Wiley & Sons, Inc., New York, 1956.

(8) Smyth, Charles P., _Physics and Chemistry of the Organic Solid State_, Editors, David Fox, Mortimer M. Labes and Arnold Weissberger, 1, Interscience Publishers, New York, 1963.

(9) Watson, J. D., _Molecular Biology of the Gene_, W. A. Benjamin, Inc., New York, 1965.

VITA

Richard Anthony Lorey was born in Pittsburgh, Pennsylvania on December 28, 1939. He received his elementary and secondary education in the Pittsburgh public school system and graduated from Allegheny High School in 1957. He attended the University of Pittsburgh and received the degree Bachelor of Science in Physics in 1962. He served in the United States Army as a first lieutenant assigned to the Nuclear Defense Laboratory in Edgewood Arsenal, Maryland until 1965. It was during this time that he married Virginia Joan Longo on December 5, 1964. Their only son, Brandon Craig Lorey, was born in Atlanta, Georgia on November 10, 1968. Upon completion of his tour of active duty he entered graduate school in the School of Physics at the Georgia Institute of Technology. He received the degree Master of Science in Physics from the Georgia Institute of Technology in 1967. He was the recipient of a National Science Foundation Traineeship during 1967-1968 and a United States Steel Fellowship during 1968-1969.